

Project File Number _____
 EDF Serial Number *W* ER-WAG7-56
 Functional File Number _____
 INEL Number INEL-95/012

ENGINEERING DESIGN FILE

Project/Task _____
 Subtask _____

EDF Page ____ of ____

TITLE: <u>Large-Scale Aquifer Pumping Test Results</u>			
SUMMARY The summary briefly defines the problem or activity to be addressed in the EDF, gives a summary of the activities performed in addressing the problem and states the conclusions, recommendations, or results arrived at from this task.			
<p>A 36-day 3000 gpm multiple well aquifer test was conducted on a Test Well at the Idaho National Engineering Laboratory to calculate aquifer transmissivity, specific yield, determine whether or not the aquifer is locally confined or unconfined, and supply water for an infiltration test, a complementary field experiment.</p> <p>The barometric efficiency of the aquifer is about 90% for short-term fluctuations and 60% for long-term fluctuations, suggesting that the aquifer is confined. Analysis of data from the aquifer pumping tests indicates that the aquifer acts as an unconfined aquifer in this locality since the aquifer test data best fit type curves based on an unconfined aquifer analytical model. Perhaps the units isolating the aquifer from barometric pressure fluctuations are not acting as aquitards, or are above the potentiometric surface of the aquifer.</p> <p>Even though the Test Well was completed as an open hole, the well efficiency is about 6%. This may indicate that preferential flow paths exist and that permeability is not evenly distributed throughout flow groups comprising the aquifer, and water is entering the well in only a few isolated horizons.</p> <p>Pumping test results were also analyzed using a finite difference model with automatic parameter estimation capabilities. The drawdown data follow a pattern that can be approximated by the simulation model with two transmissivity zones, an inner high transmissivity zone around the Test Well and observation wells and an outer lower transmissivity zone. Although there was not a unique transmissivity value identified, the value is probably within a factor of three of 1×10^8 ft²/day. The specific yield estimate provided by the numerical modeling is uncertain because specific yield and transmissivity are strongly correlated.</p>			
Distribution (complete package):		K.J. Dooley (3920), E.C. Miller (3953), L.N. Peterson (2110), T.M. Stoops (3921) W.H. Sullivan (3920)	
Distribution (summary page only):			
Author A.H. Wylie J.M. McCarthy E. Meher B.D. Higgs	Dept. Integrated Earth Sciences	Reviewed Date <i>Deborah McElroy</i> 2/22/95 <i>for Joel Hubbell</i> <i>James O. Maymoun</i> 2/22/95	Approved Date <i>G. Starming</i> 2/22/95
		EG&G Review Date <i>J.P. Silca</i> 2/22/95	LIFE EG&G Approval Date <i>K.J. Dooley</i> 2/22/95

Introduction

The Snake River Plain aquifer consists of a series of basalt flows and interlayered pyroclastic and sedimentary materials that contain ground water and underlies the Eastern Snake River Plain east of Bliss. It extends from Bliss on the west to Ashton on the northeast (Figure 1). Its lateral boundaries are formed by contacts with less permeable rocks at the margins of the plain (Mundorff et al., 1964). The Idaho National Engineering Laboratory and the Radioactive Waste Management Complex (RWMC) overlies the north-central portion of the Snake River Plain aquifer.

This report discuss a 36 day 3,000 gpm aquifer pumping test conducted at the RWMC. This aquifer test was conducted in conjunction with the large scale infiltration test during the summer of 1994. Overview of the experiments are described in Porro et al. (1994) and Wylie et al. (1994). This report includes a brief discussion of test objectives, the geo-hydrological conceptual model, and aquifer test design followed by data analysis/data reduction, analytical evaluation, and numerical modeling of the aquifer test.

Objectives of Test

Sensitivity analysis of fate and transport modeling performed to evaluate risk from waste stored at the RWMC has shown that inadequately defined or assumed hydrological and geochemical parameters result in unacceptable risk uncertainty. These data gaps have been previously identified in Department of Energy (DOE) contractor reports (SAIC, 1990; Wood and Wylie, 1991). The tests described here are part of a comprehensive plan for characterizing the aquifer in the vicinity of the RWMC to aid environmental decision makers.

The objectives of the large-scale aquifer test as reported in Wylie (1994a), are to generate data for:

- Calculating transmissivity representative of the aquifer,
- Calculating a storage coefficient representative of the aquifer,
- Determining if the aquifer is confined or unconfined, and
- Supplying sufficient water to conduct the infiltration test about one mile from the Test Well.

Geology

Volcanism on the Snake River Plain is intermediate between flood basalt volcanism of the Columbia Plateau, and basaltic shield volcanism of the Hawaiian

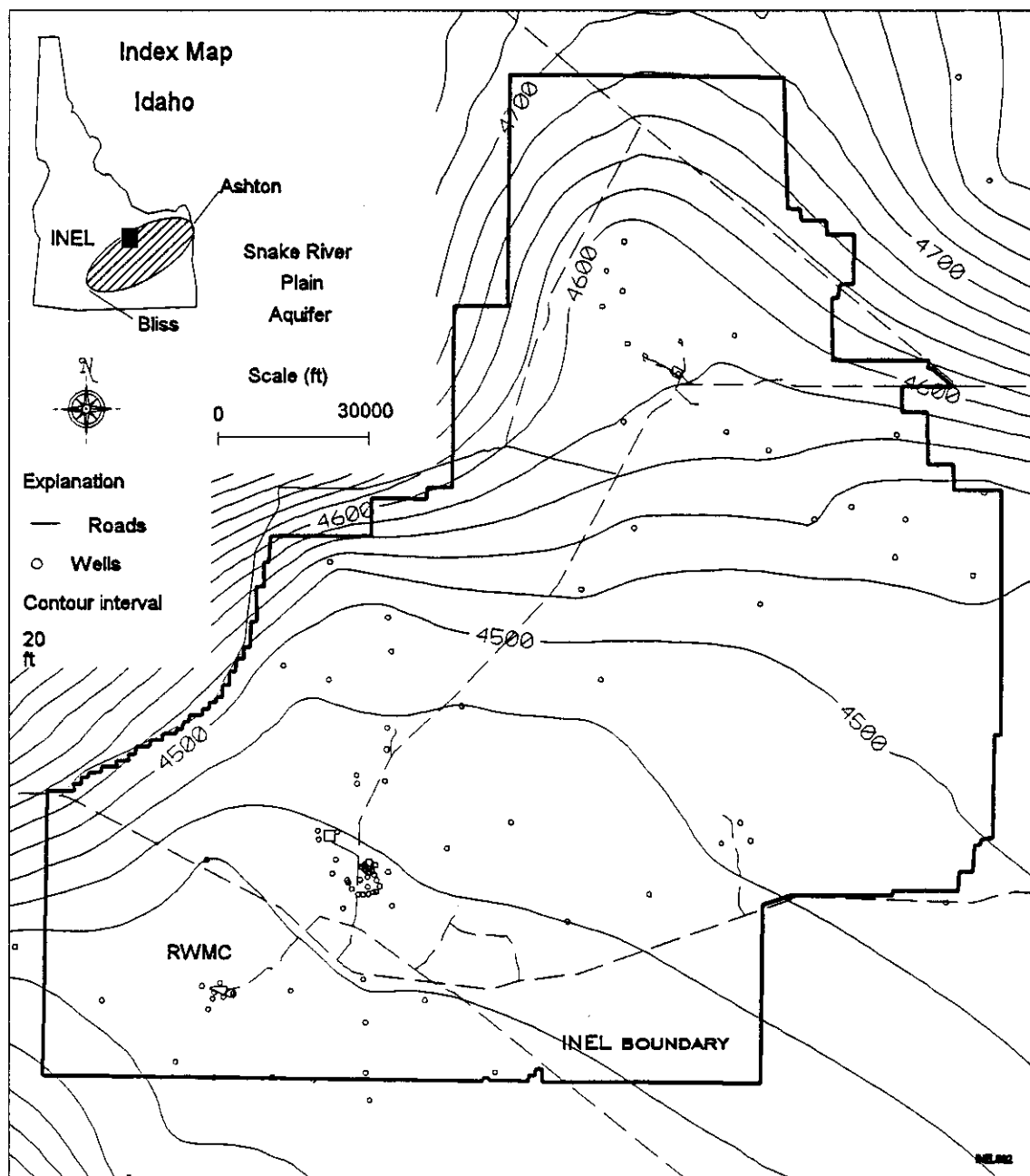


Figure 1. April 1992 water table map for the Snake River Plain Aquifer.

Islands (Greeley, 1982). The Snake River Plain basalts differ from the Greeley plains-style volcanism in two general ways that have important hydrological implications. First, volcanic vents are not randomly distributed over the plain, but are primarily restricted to volcanic rift zones (Figure 2). Most vents in the INEL region are located in the Hell's Half Acre Rift Zone and the Arco Rift Zone. The rift zones are characterized by fissuring and minor faulting associated with emplacement of dikes feeding the vents. The Arco Rift zone is situated just south of the RWMC as shown in Figure 2. Dikes and sills may act to locally reduce aquifer transmissivity in the rift zones. Second, deposition of sediments that fill in low-lying areas between shields and rift zones can reduce the vertical transmissivity in the aquifer. These sediments are of several types: loess, alluvial silts, sands, gravels, and lacustrine clays and silts.

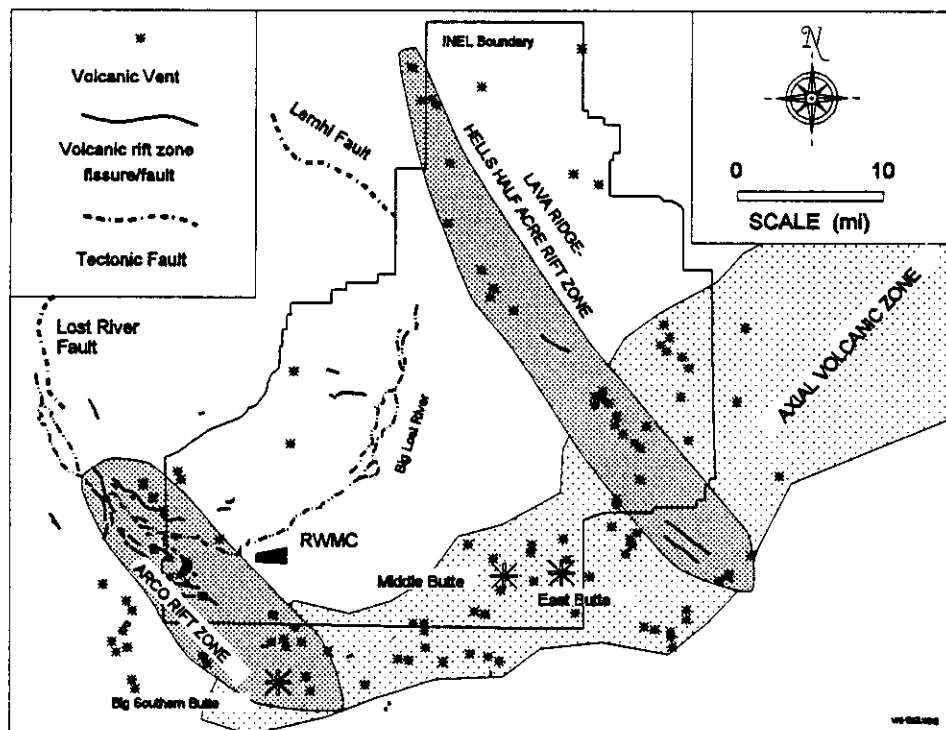


Figure 2. Volcanic rift zones near the INEL.

Anderson and Lewis (1989) correlated stratigraphy at the RWMC based on 40 wells, including eight aquifer wells. Geophysical well logs, well cuttings, cores, K-Ar (potassium-argon) ages, and geomagnetic properties were used to establish the correlations. Cross sections, maps and tables of the stratigraphy for the RWMC are found in this report. Figure 3, based on their correlations, show the general stratigraphy in the vicinity of the RWMC and Figure 4, based on correlations by Anderson (1994), shows the stratigraphy in the vicinity of the aquifer pumping test. These cross sections show that the stratigraphic units are relatively continuous in the vicinity of the RWMC and folding and/or faulting are not apparent. These cross sections represent straight-line correlations between wells based on identification of basalt flow groups and sedimentary interbeds. Basalt flow groups may be associated with single or multiple eruptive events of lava with similar chemical and physical characteristics. Individual flows or flow units within groups are more difficult to distinguish using geophysical well logs. Although there is considerable lateral continuity in the flow groups, the horizontal continuity of individual flows within flow groups may be limited. The sedimentary interbeds are probably not as laterally continuous as depicted in Figure 3. However, the fact that they are readily correlated suggests the interbeds act, in general, as aquitards.

Based on the indicated stratigraphic correlations, the wells utilized for the cross-section in Figure 3 are thought to also be in hydraulic connection with the same basalt flow units G(1) and H(1) in which the Test Well and observation wells are open to the aquifer. This suggests that aquifer parameters calculated from this test will also be representative of the aquifer at the RWMC.

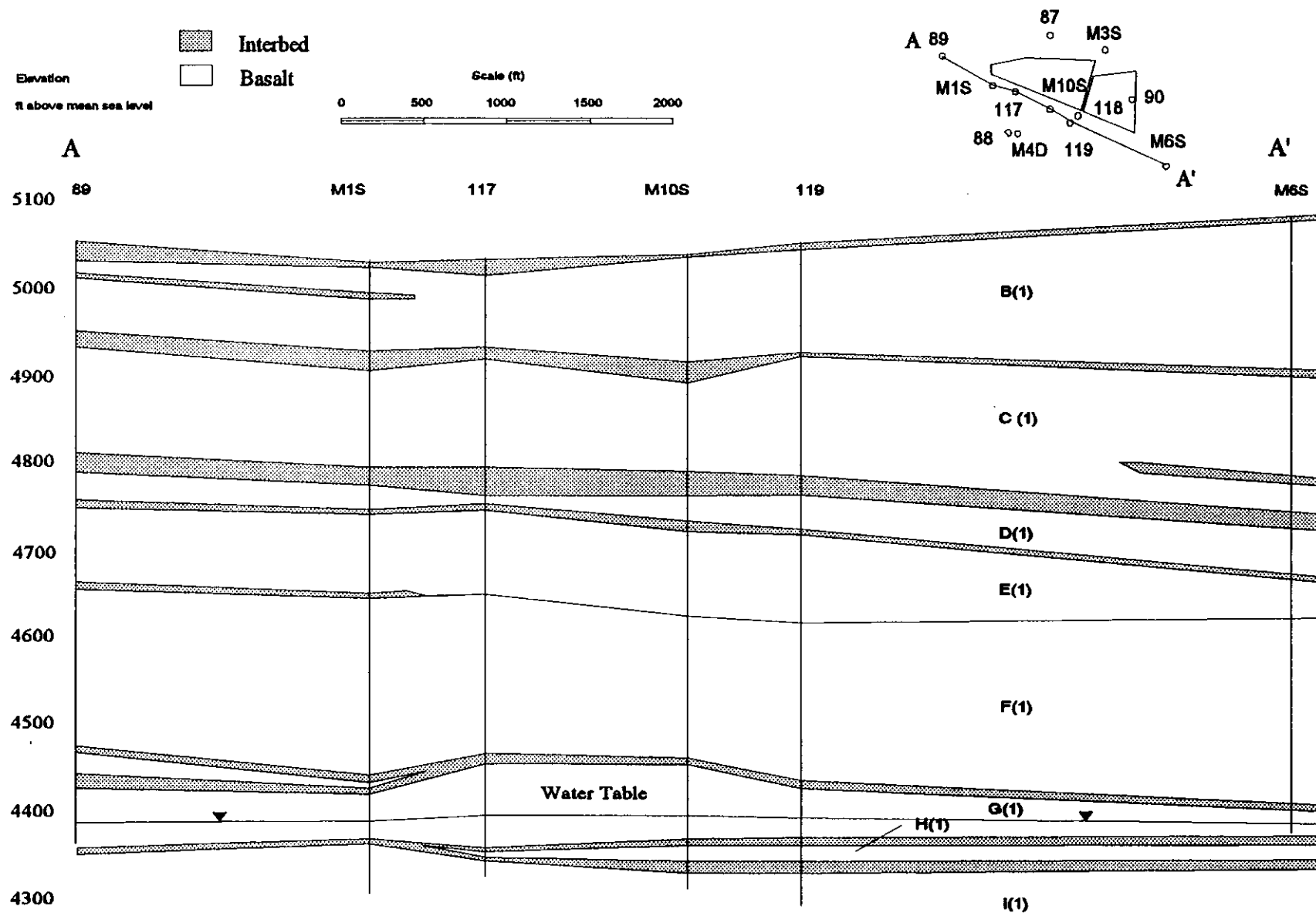


Figure 3. Geologic cross-section along A-A'.

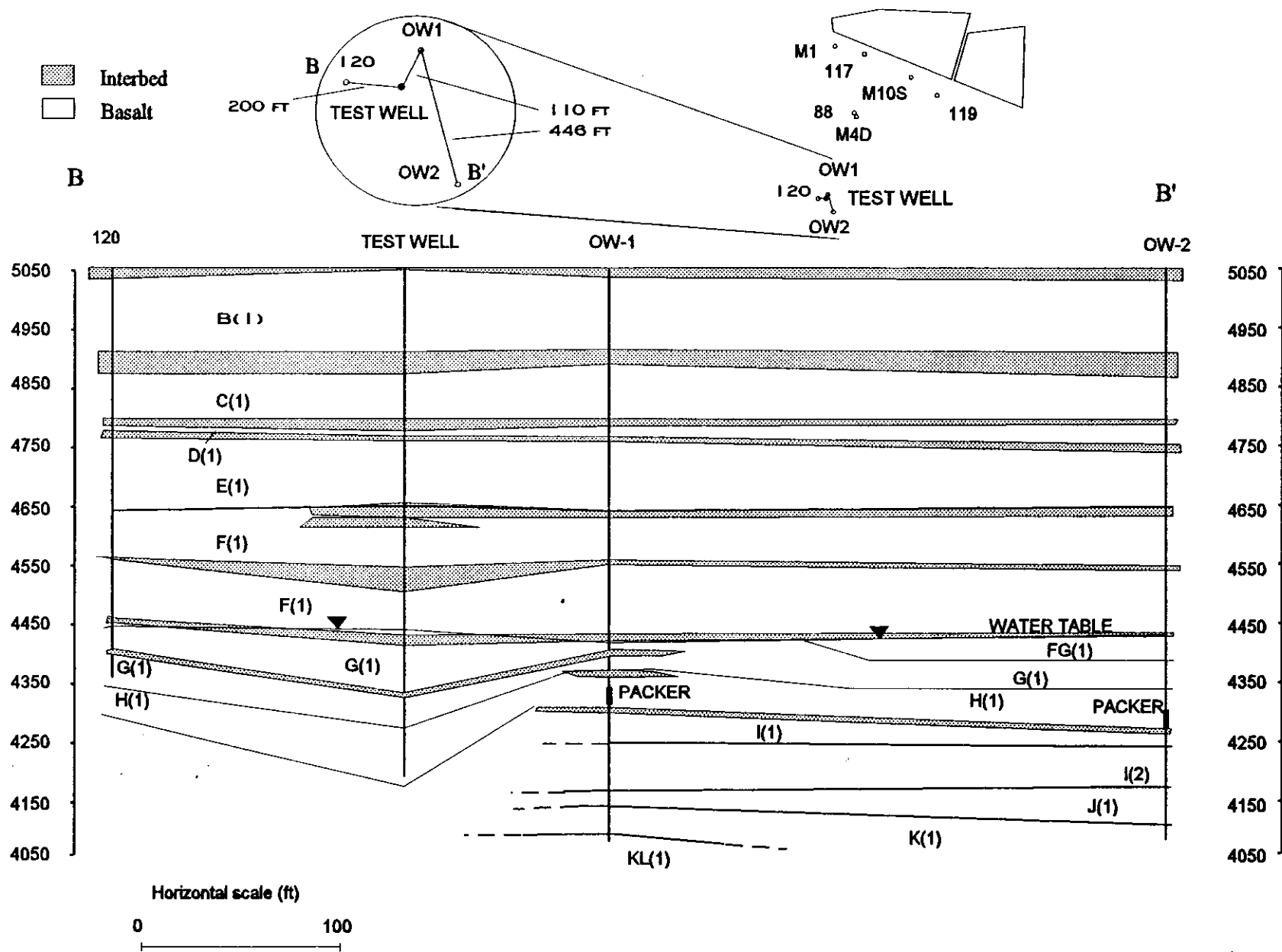


Figure 4. Geologic cross section along B-B'.

Hydrology

Construction data for wells near the RWMC are summarized in Table 1, with the well locations shown in Figure 5. The total depth of the wells ranges from 626 to 1,000 ft, and the depth to water is about 600 ft. Well construction varies from wells open to the formation through perforated casing or open hole, to wells completed with wire-wrapped, stainless-steel screen. Most of the wells are open in the upper 20 to 50 ft of the aquifer.

The elevation of the potentiometric surface for the Snake River Plain aquifer in the vicinity of the INEL is depicted in Figure 1. The regional flow is to the south-southwest, although, locally, the direction of ground water flow is affected by recharge from intermittent rivers, surface water spreading areas, and heterogeneity in the aquifer. The average hydraulic gradient is about 4 ft/mi across the INEL. Depth to water varies from about 200 ft in the northeast corner of the INEL to more than 900 ft in the southwest corner (Barraclough and Jensen, 1973).

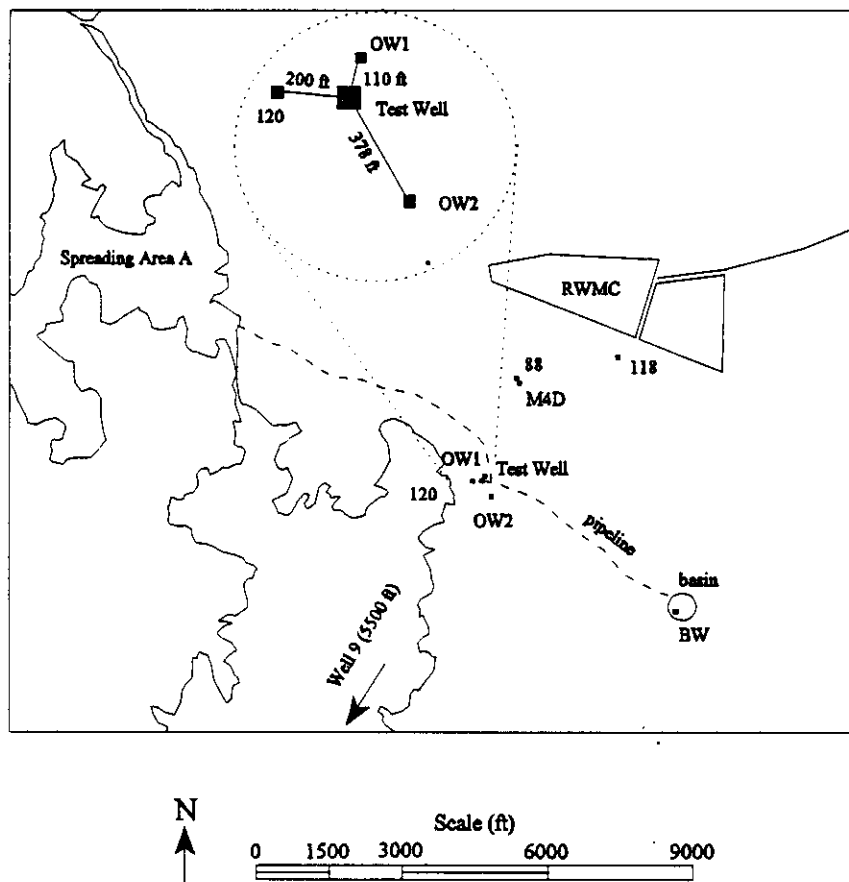


Figure 5. Location of Test Well and observation wells.

Table 1 Summary of well construction data for wells in the RWMC area (Wood and Wylie, 1991).

Well Name	year drilled	Total Depth	casing material	Cased interval	Screened/Open Interval(s)	Screen Type	Geophysical Logs	Flow Group at completion zone	Depth to water when drilled
RWMC Production Well	1974	683	Steel	0 - 660	590 - 610 625 - 635	Perforated Perforated	Yes	G(1)	571.00
USGS-86	1966	691	Steel	0 - 48	48 - 691	Open	Yes	J(1)	643.70
USGS-87	1971	640	Steel	0 - 585	585 - 607 Caved to 607	Open	Yes	G(1)	582.70
USGS-88	1971	635	Steel	0 - 587	587 - 635	Open	Yes	G(1), H(1)	583.65
USGS-89	1972	646	Steel	0 - 576	576 - 646	Open	Yes	G(1), H(1)	590.64
USGS-90	1972	626	Steel	0 - 580	580 - 609 Caved to 609	Open	Yes	F(1), FG(1)	674.62
USGS-117	1987	655	Steel/SS	0 - 555	555 - 653	Perforated	Yes	G(1), - H(1)	581.30
USGS-119	1987	705	Steel	0 - 639	639 - 705	Perforated	Yes	G(1), - H(1)	600.80
USGS-120	1987	750	Steel/SS	0 - 638	638 - 705	Perforated	Yes	G(1), H(1)	611.45
Test Well	1993	857	Steel	0 - 440	615 - 857	Open	Yes	G(1), H(1)	615
OW1	1993	1000	Steel	0 - 623	623 - 1000	Open	Yes	G(1) - KL(1)	614
OW2	1993	1000	Steel	0 - 600	621 - 1000	Open	Yes	FG(1) - K(1)	620.87
M1-SA	1992	678	SS Steel	0 - 608	608 - 638	Wire Wrapped	Yes	H(1)	585
M3-S	1992	660	SS Steel	0 - 602.8	602.8 - 632.8	Wire Wrapped	Yes	NA	588
M4D	1992	836	SS Steel	0 - 798	798 - 828	Wire Wrapped	Yes	NA	594
M6S	1992	696	SS Steel	0 - 638	638 - 668	Wire Wrapped	Yes	G(1)	637
M7S	1992	638	SS Steel	0 - 598	598 - 628	Wire Wrapped	Yes	NA	575
M10-S	1992	678	SS Steel	0 - 617	617 - 647	Wire Wrapped	Yes	G(1)	593

Figure 6 contains a potentiometric surface map of the area near the RWMC. Note that there is a mound in the potentiometric surface near Well 88. Burgess et al. (1993) attributed the mound to residual water table mounding from diversion of water to Spreading Area B in the mid-1980s. This mounding is thought to be limited to a small area in the vicinity of Well 88. The observed depression at Well 117 is almost certainly caused by borehole deviation problems.

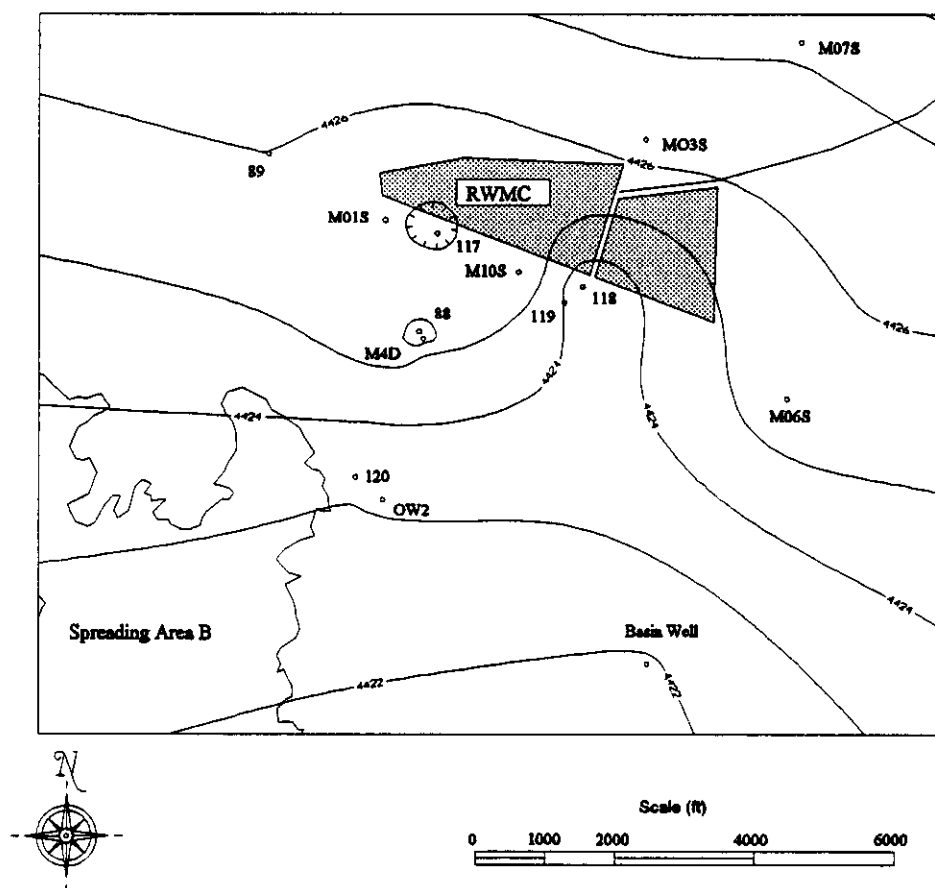


Figure 6. October 1994 water table in the vicinity of the RWMC(only wells used in contouring are posted).

Conceptual Model

Aquifer permeability is largely controlled by the distribution of basalt interflow zones (zone between the top of a basalt flow and the bottom of the overlying basalt flow) with some additional permeability contributed by fractures, vesicles, and intergranular pore spaces (Mundorff et al., 1964). Figure 7 shows a schematic cross section of a typical basalt flow. This figure illustrates collapse zones, cooling fractures, and a higher frequency of jointing in the outer rind of the flow. The individual basalt flows ideally consist of four elements: an upper vesicular element, a central nonvesicular element, a bottom vesicular element, and a substratum. The observed median thicknesses of the three upper elements are 6, 7.5, and 1.5 ft, respectively (Knutson et al., 1989). On the scale of the aquifer test (100's to 1,000's of ft) dense basalt flow interiors act as "grains" while the "intergranular porosity" is reflected in the interflow zones between the dense interiors (Whitehead, 1992). These "grains" are formed as basalt flow sequences are deposited in an overlapping and coalescing manner, where younger flows build on the complex undulating topography of previous flows. Flow through the aquifer follows a tortuous path, around, through, and between large particles in the general direction of the regional hydraulic gradient. This hydrological conceptual model agrees well with the plains-style volcanism described by Greeley (1982).

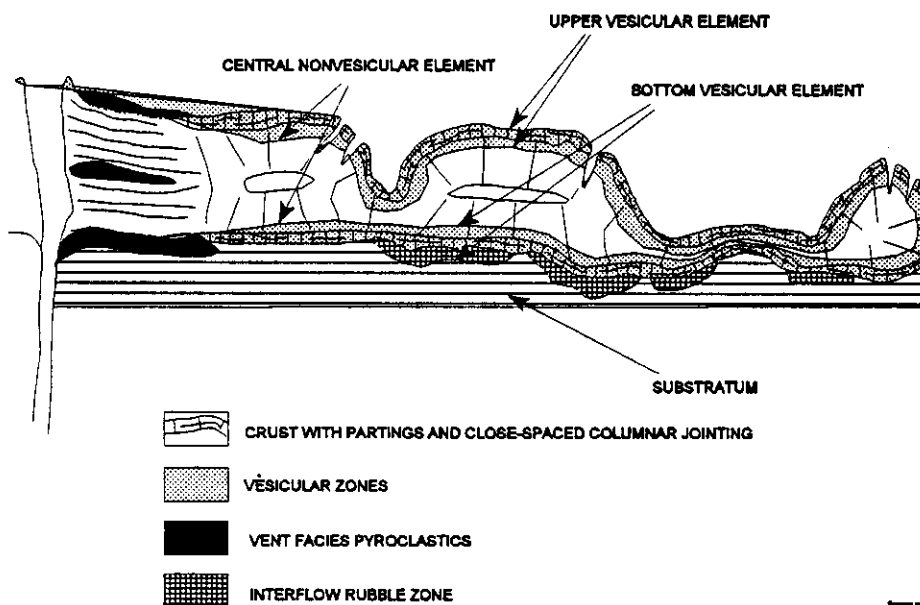


Figure 7. Schematic of a basalt flow cross section (from Knutson et al., 1989).

Numerous aquifer tests have been conducted in the Snake River Plain Aquifer to calculate aquifer transmissivity. A reliable aquifer storage coefficient has not been calculated because there are so few long-term multiple well tests. Mundorff et al (1964) discusses 15 multiple well tests, although none of the tests lasted 36 days. Figure 8 shows a normal probability plot and a frequency histogram of the natural log of transmissivity (ft²/day) using data compiled from Ackerman (1991), Wylie (1993), Wylie and Hubbell (1994), and Kaminsky et al, (1993). These data include results from slug tests, single well tests, and multiple well tests. The normal probability plot approximates a straight line, suggesting that transmissivity may be lognormally distributed. The mean and confidence interval may then be calculated in log space and a back transform conducted. Using this technique the calculated average transmissivity is 6×10^3 ft²/day, with a 95% confidence interval for the mean between 3×10^3 and 1.2×10^4 ft²/day. Transmissivity in this sample ranges from 1.1 to 1.2×10^7 ft²/day, nearly seven orders of magnitude. Hydraulic conductivity, calculated by dividing transmissivity by the portion of the well open to the aquifer, ranges from 1.0×10^{-2} to 7.4×10^3 ft/day.

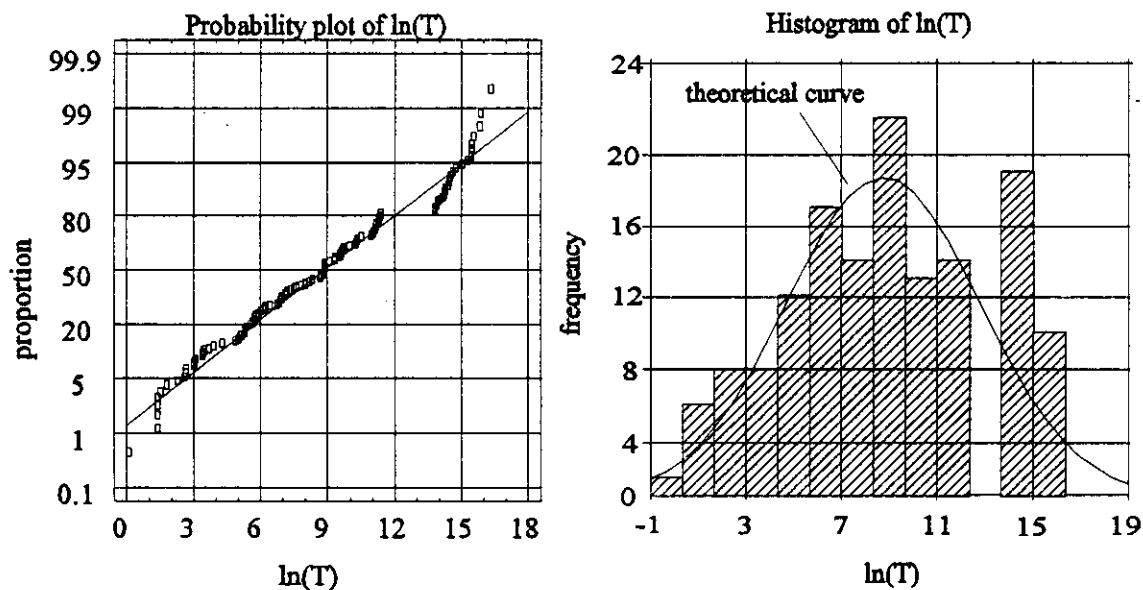


Figure 8. Normal probability plot and histogram of the natural log of transmissivity (ft²/day).

Aquifer Test Design

This section outlines test procedures used to conduct the pumping test including well location and well design, step test, data acquisition system, antecedent trend data, and pump and discharge system design. Analysis will follow in later sections. More detail concerning test design can be found in Wylie (1994a) and Wylie et al. (1994).

Well Location and Well Design

The Test Well is 200 ft east of Well 120; Observation Well One (OW1) and Observation Well Two (OW2) are located 110 ft N30E of the Test Well, and 378 ft S30E of the Test Well respectively (Figure 5). The two observation wells were drilled to 1,000 ft and cased to 600 ft with a forward rotary drill equipped with a downhole hammer. The Test Well was drilled to a total depth of about 857 ft with a cabletool rig and cased to 440 ft. Well construction data are in Table 1 and diagrams for the two observation wells and the Test Well are provided in Appendix A.

Step Test

On April 12, 1994, a single well step drawdown test was conducted in the Test Well to determine whether or not the Test Well would yield sufficient water for the infiltration portion of the experiment, refine the preliminary drawdown and radius of influence calculations, and use this information to refine the design of the data acquisition system. The Step Test was conducted with a 10-in. Layne & Bouler pump with a 10-in. column driven by a 450 hp engine. The test included:

- collecting antecedent trend data,
- pumping the well at 1,000 gpm for one hour,
- pumping the well at 1,500 gpm for one hour,
- pumping the well at 2,000 gpm for one hour, and
- pumping the well at 2,300 gpm for 15 minutes.

The fourth step at 2,300 gpm, was the pump's maximum pumping rate, and could not be maintained for a full hour because of the possibility of damaging the pump engine. Discharge was measured using a manometer. Drawdown was measured in the Test Well using an electric water level sounding tape and a HERMIT 100 psi transducer connected to a HERMIT 1000 datalogger. The test started at 10:00 and concluded at 13:15 after pumping about 304,500 gal with a maximum observed drawdown of 4.78 ft in the pumping well. Figure 9 shows a plot of drawdown versus time during the test.

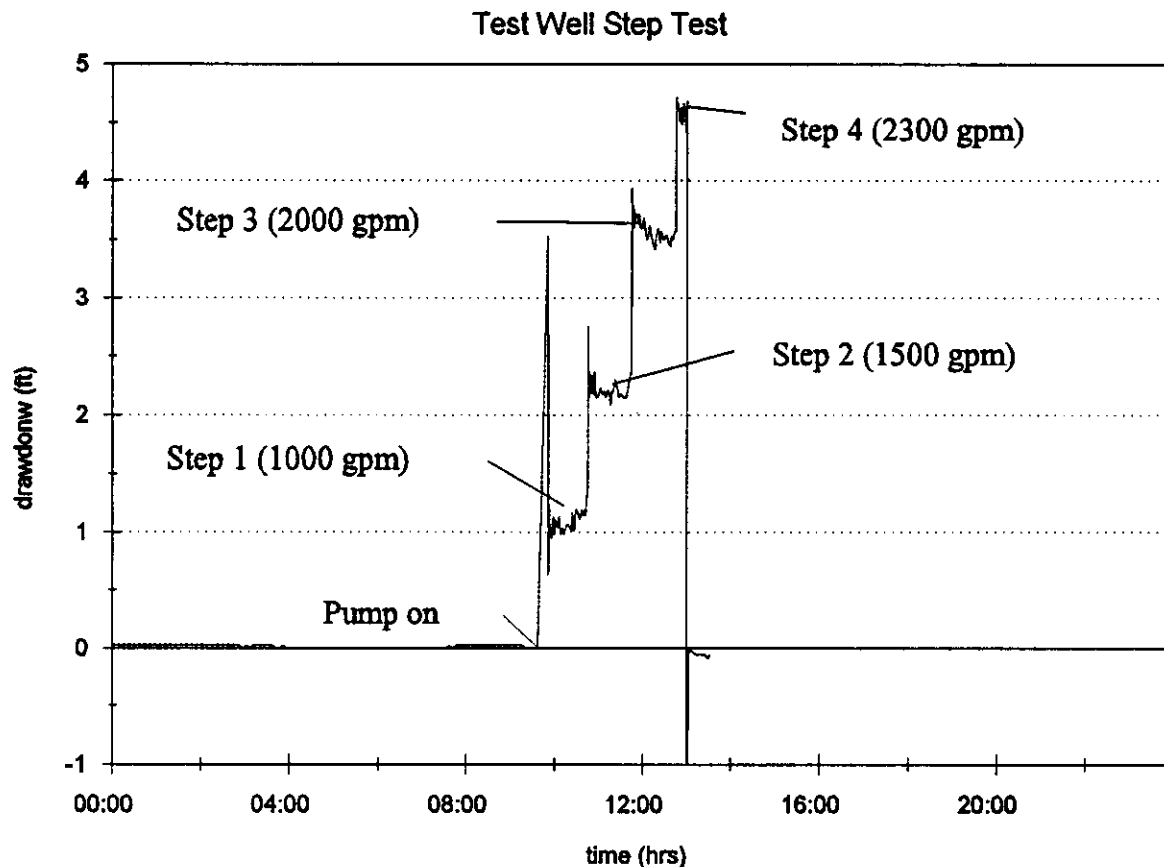


Figure 9. Time drawdown plot for the Step Test at the Test Well.

Data Acquisition System

An eight-channel HERMIT data logger manufactured by In-Situ Inc. was placed at OW1. The eight channels were connected to transducers (XD) as follows:

Channel number	Use
1	30 psi XD to monitor the Test Well
2	10 psi XD to monitor Well 120
3	10 psi XD to monitor upper zone in OW1
4	10 psi XD to monitor lower zone in OW1
5	10 psi XD to monitor the upper zone in OW2
6	10 psi XD to monitor the lower zone in OW2
7	barometer (In Situ, Inc.)
8	barometer (INW)

Wells 88, M4D, 118, 9 and the aquifer well in the Infiltration Basin (BW) were also monitored as follows:

<u>Well</u>	<u>Monitor</u>
88	10 psi XD and HERMIT data logger
M4D	10 psi XD and HERMIT data logger
118	10 psi XD and HERMIT data logger
9	10 psi XD and HERMIT data logger
BW	10 psi XD and HERMIT data logger

Well locations are shown in Figure 5.

Antecedent Trend for the Main Test

On June 28, packers were installed in OW1 and OW2, and trend data were collected from zones both above and below the packers. The packer in OW1 was set at 735-740 ft below land surface (bls); the packer in OW2 was set at 777-782 ft bls (Figure 4).

The packer locations were picked after analyzing geophysical logs. Gamma logs were analyzed to correlate sedimentary interbeds and basalt flow groups as discussed by Anderson and Lewis (1989), and caliper and flow meter logs were analyzed to identify the more transmissive zones in the wells. Zones in which the well was out of gauge and experiencing high flow were presumed to be the more transmissive zones. The packer in Well OW2 was placed just below the lowest transmissive zone. The lowest transmissive zone in Well OW1 was below an unstable zone, so the packer was located above the unstable zone to make packer retrieval following the test more likely.

Antecedent water level trend data were collected for about 1 month prior to start of the test. These data were used to establish prepumping water levels and identify natural and manmade water level fluctuations that could interfere with the test. Any interferences were subtracted from the data during analysis. The water level trends in the Test Well and OW1 Upper (614 -735 ft bls), OW1 Lower (740-1000 ft bls), Well 120 (638-705 ft bls), OW2 Upper (621-777 ft bls) and OW2 Lower (782-1000 ft bls) are similar. Hydrographs from the wells are presented in Appendix B. Figure 10 contains a hydrograph for Well 120 with pretest trend data. A well with an unusual trend could have indicated the presence of unidentified discontinuities in the aquifer, or that the well may not be in hydrologic communication with the aquifer.

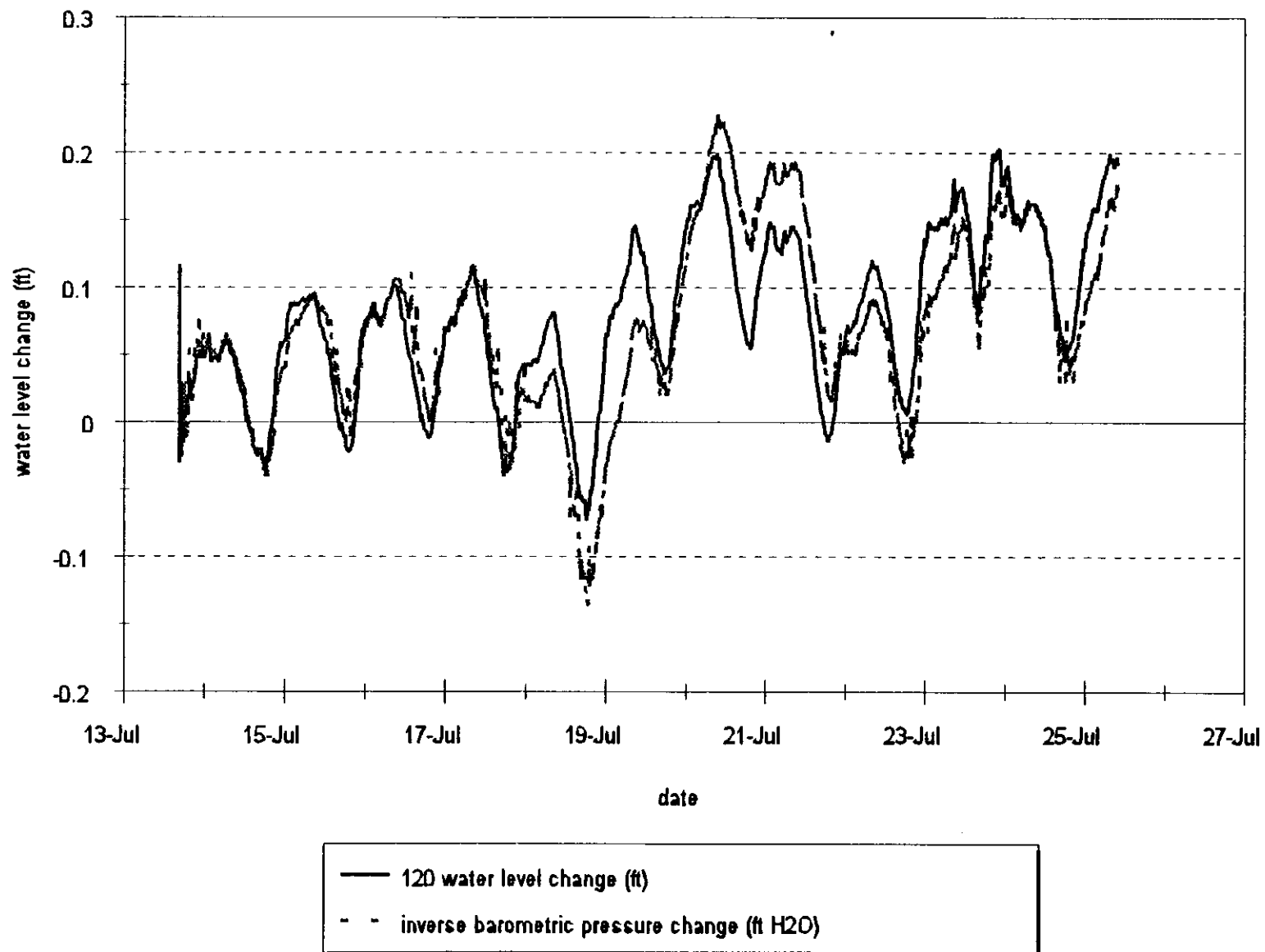


Figure 10. Water level and barometric pressure fluctuations prior to start of the pumping test.

Pump and Water Discharge System

The pump used during the main part of the test was a Layne & Bouler 15-stage, line-shaft, turbine pump with 12-in. bowls and a 12-in. pump column driven by an 800-hp General Electric motor. A 125-hp booster pump was used to move the water along the 5,000 ft of pipe required to reach the infiltration basin. Flow of an anticipated 3,000 gallons per minute (gpm) required a pipe with a minimum diameter of 16-in. in order to keep the flow velocity below a recommended 5 ft/s. Once the basin was full, excess water was routed to Spreading Area A (Figure 5).

Pumping History

On July 13, a trial test was conducted to test the pump, discharge system, and team coordination. Drawdown was observed in the Test Well, Well 120, OW1 Upper, OW1 Lower, and OW1 Upper; however, the flow meters were not correctly installed and did not function properly. This problem was identified and corrected before the start of the main portion of the test. The data loggers were reset to collect antecedent trend data.

On July 25 at 11:22, the pump was turned on to start the test.

On August 6 at about 06:02, the controller for the pump failed and the pump stopped. At 15:02 repairs were completed and the pump was restarted.

On August 8 at 09:47, the generator was shut down for routine servicing. After servicing was complete, the pump could not be restarted. Repairs were completed on the controller at 18:47 and the pump restarted.

On August 30 at 18:15, the pump was stopped and the recovery test was initiated. 148 million gal of water were pumped from the Test Well in 36.18 days for a time weighted average pumping rate of 2.8×10^3 gpm (Starr, 1994).

Data Analysis

This section outlines the analytical techniques used to interpret the data. The raw data will be presented then corrections to the raw data will be discussed. After making necessary corrections, the data are analyzed using standard analytical techniques and numerical methods. Well 120 was arbitrarily selected to illustrate the analysis in this document. Analysis for the other wells are presented in Appendix C.

All the wells monitored with transducers and data loggers have similar water level trends, and are therefore presumed to be in hydrologic communication and suitable as observation wells.

Water level data show two responses associated with changes in atmospheric (barometric) pressure. Diurnal fluctuations of about 0.1 ft are due to barometric pressure changes associated with diurnal temperature/barometric pressure changes. These are lowest in the winter months and greatest in the summer. Atmospheric barometric pressure changes cause larger water level fluctuations (0.3 ft) than the diurnal fluctuations.

Influence of changing barometric pressure was observed in the field by field personnel who noted that the wells frequently were 'blowing or sucking' air when downloading dataloggers. Changes in atmospheric pressure cause a difference in pressure between the well and the basalt surrounding the well. The pressure change is transmitted instantaneously in the well but is delayed by confining layers in the basalt thus causing a pressure difference in the aquifer. The time (lag in time) it takes for the pressure in the atmosphere to be transmitted to the aquifer at 615 ft is in the order of 1 to 3 days, during which the well will blow or suck air. This pressure difference between the well and the basalt causes the water in the well to either rise or fall in response to the pressure difference. The water level change is the inverse of the barometric pressure change. If barometric pressure decreases the water level will increase. Figure 10 presents the water level and inverse barometric pressure change observed at Well 120 from July 13 to July 25.

The barometric "efficiency" of a well relates to the effectiveness of the pressure transmittal and is dependant upon the rigidity of the geologic media and the overall permeability of the rock. A maximum barometric efficiency of 1.0 means that the water level will change in a 1 to 1 ratio with the pressure change, where as a 0.5 barometric efficiency will change the water level 50% of the barometric pressure change. Barometric efficiency generally varies between 0.2 to 0.75 (Todd, 1959). Unfortunately due to the lag time, variations in lag time by location, and that barometric pressure is continuously changing, it is impossible to correct all water levels for changes in barometric pressure fluctuations.

The calculated barometric efficiency for the well monitored as part of this test is about 90% for diurnal barometric fluctuations and 60% for longer term barometric fluctuations (Figure 10). Perhaps this difference is because diurnal fluctuations occur before a pressure change can equilibrate throughout the vadose zone, but long-term barometric changes associated with a weather front have more time to equilibrate.

Figure 11 contains a hydrograph of the raw data from the pretest trend through recovery for Well 120, 200 ft from the Test Well. The signal-to-noise ratio is unfavorable, the measurable response due to pumping is overwhelmed by barometric affects, and some filtering must be done to remove the background noise from the data. Several techniques were tried including:

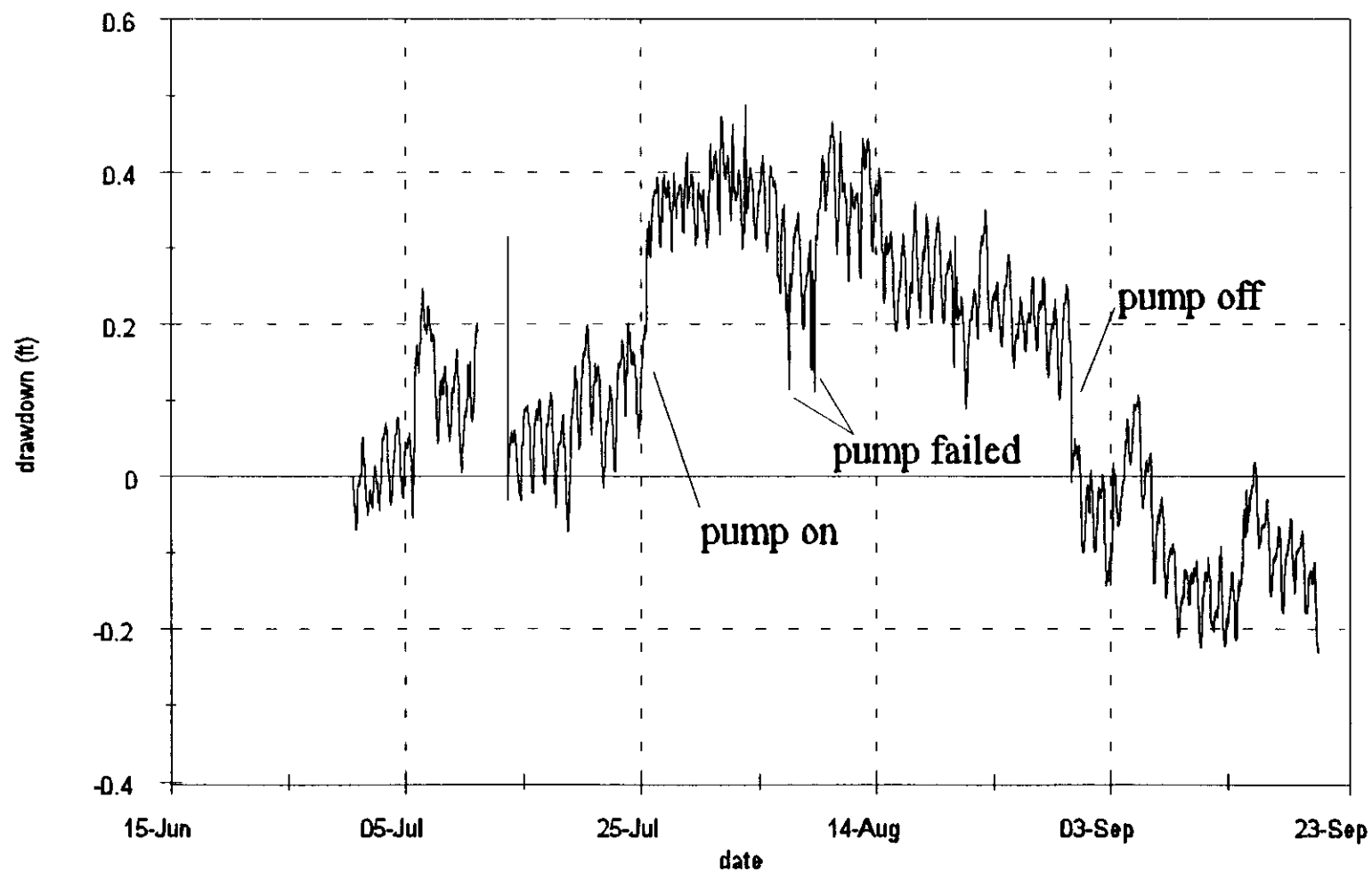


Figure 11. Raw water level data for well 120 June to September 1994.

- Correcting for water table trend and barometric effects (Figure 12-a),
- Subtracting the data collected at Well 88 (Figure 12-b),
- Transforming the Well 88 and 120 data using Fourier transforms and subtracting the spectrum from Well 88 from the spectrum from Well 120 (Figure 12-c), and
- Subtracting water level data collected in OW2 Lower, which has no detectable drawdown, from water level data from Well 120 (Figure 12-d).

Figure 12a through d contains hydrographs of the data collected from Well 120 after filtering with each of these techniques. Drawdown must be steadily increasing before it can be analyzed with any analytical technique. The only filter that yields data in which drawdown does not significantly decrease through time is the OW2 Lower filter. This filter also yields the smoothest data set.

Subtracting out barometric effects and water level changes observed in an outlier well are standard filtering techniques in groundwater hydrology which are described in Kruseman and de Ridder (1991). The Fourier transform technique is used to filter out noise in the geophysical industry (Dobrin 1976). Subtracting out water level changes observed in OW2 Lower requires justification because some effects from pumping could be subtracted out. Figure 13 contains hydrographs from OW2 Lower, Well 120, and Well 88 for noon August 5 through noon August 7. The Test Well pump failed on August 6 at 06:02, and was not restarted until 15:02. Note that a pressure transient is visible in the hydrograph for OW2 Lower and Well 120, however, the hydrograph for OW2 Lower shows that the potentiometric head returned to its original level quickly and that head in Well 120 did not. The raw data plots in Appendix B show significant differences in the character of the hydrograph for OW2 Lower and the other wells in the Test Well cluster. The head in OW2 Lower tended to rise during the test as did the head in the outlier wells (Well 9, Well 88, and Well 118) and the head in the other wells in the Test Well cluster tended to drop. Although some aspect of the signal may be subtracted out by using OW2 Lower to remove background noise, this effect is probably negligible.

Well 88 was selected for use as a filtering mechanism because it was the closest well to the Teat Well cluster completed in the G(1) or H(1) flow groups. Although Burgess et al. (1993) implied that it may not be in good hydraulic communication with the aquifer, it had the same barometric response and trend as wells in the Test Well cluster.

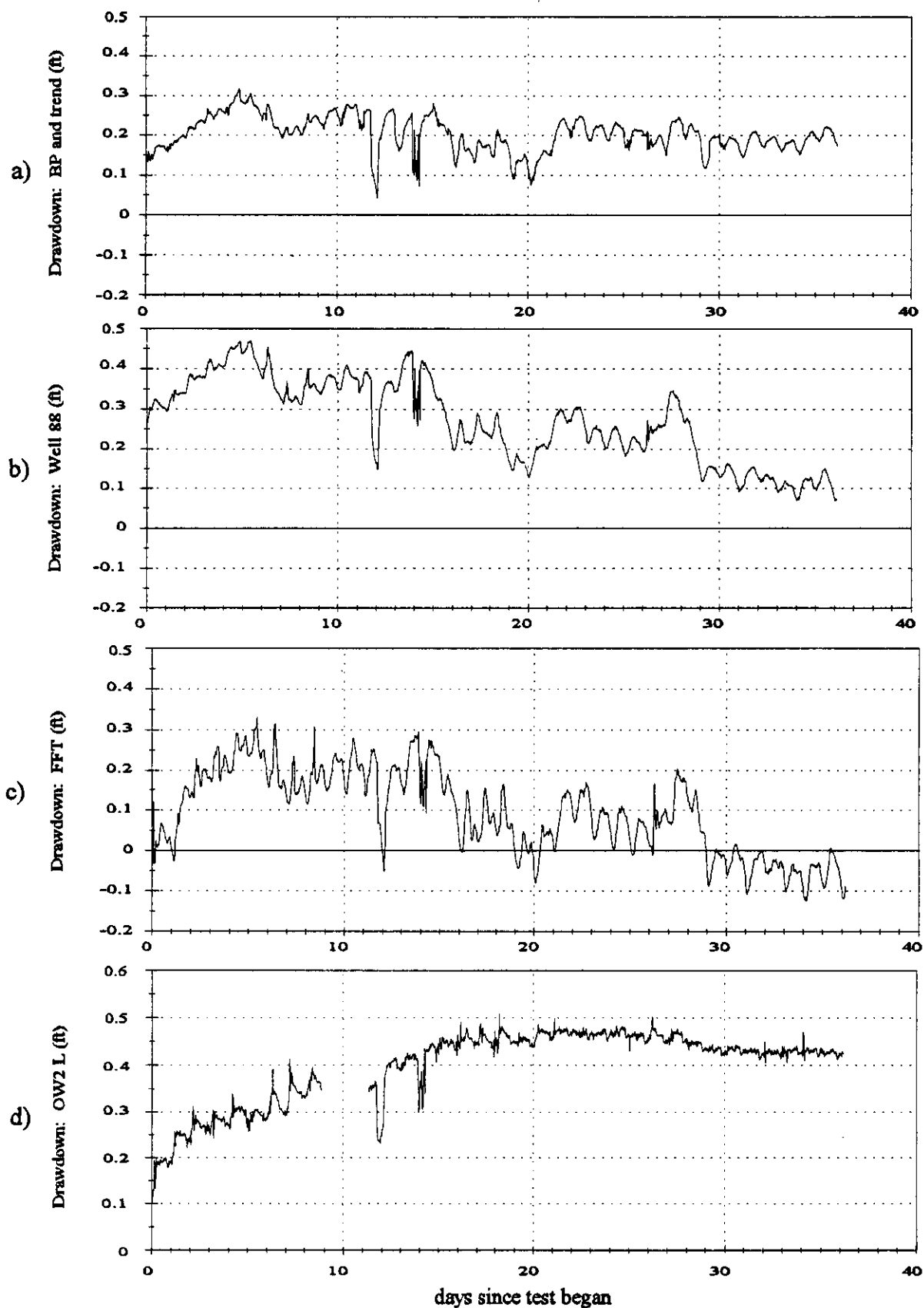


Figure 12. Comparison of different filtering techniques for Well 120.

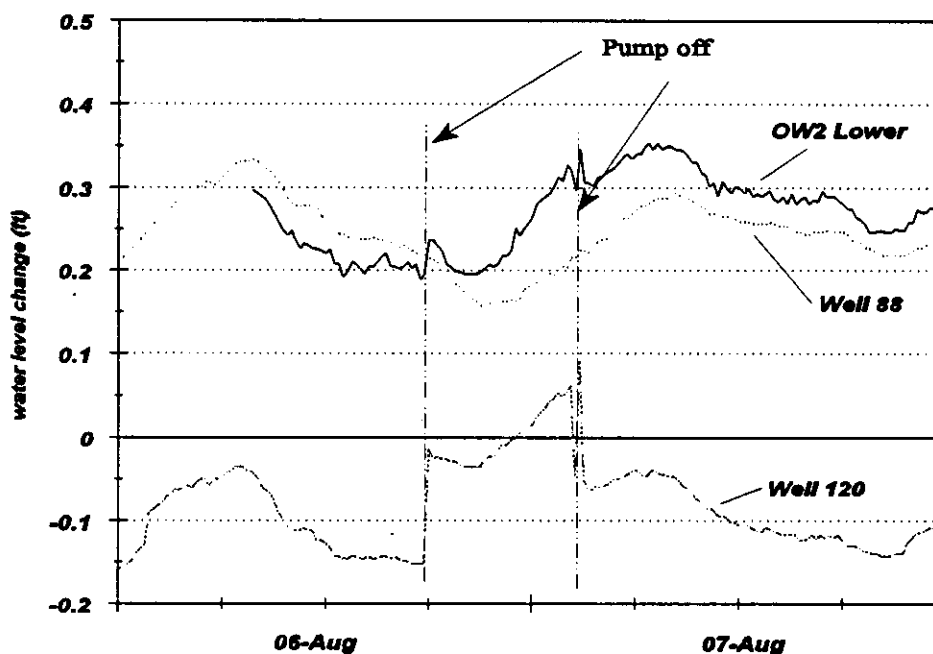


Figure 13. Comparison of OW2 Lower, Well 120, and Well 88 hydrographs for 12:00 August 5 through 12:00 on August 7.

Analysis of the Step Test

Aquifer test analysis of the water level response in the Test Well during the Step Test was conducted by hand and using the computer program AQTESOLV (Duffield and Rumbaugh, 1991). Analytical results from step one are summarized in Table 2. These calculations were made using the Cooper and Jacob (1946) and Theis (1935) techniques. The data from the first step are generally considered most reliable because analysis for later steps require corrections for the effect of all previous steps, as well as the antecedent trend.

The Step Test was also analyzed using the Hantush-Bierschenk method (Hantush, 1964). These calculations predicted the Test Well would be about 29% efficient at 3,000 gpm and have a drawdown of about 7.07 ft. Assuming a transmissivity of 4×10^5 ft²/day and a specific yield of 0.1, the predicted drawdowns at the end of the test at OW1, 120, and OW2 were 1.12 ft, 1.02 ft, and 0.82 ft respectively (Wylie, 1994b).

Analysis of the Main Test

Several possible solution techniques for analyzing the test results were attempted. The results are summarized in the following sections.

Table 2: Calculated transmissivities.

Pumping rate (gpm)	Maximum Observed Drawdown (ft)	Specific Capacity (gpm/ft)	Analytical Method	Transmissivity (ft ² /day)
1,000	1.14	877.19	Cooper/ Jacob (hand)	5×10^5
1,000	1.14	877.19	Cooper/ Jacob (AQTESOLV)	3×10^5
1,000	1.14	877.19	Theis (AQTESOLV)	3×10^5
Mean				4×10^5

Cooper-Jacob and Theis evaluations.

Because no drawdown was observed in OW2 Lower, the base of the aquifer is assumed to be at 777 ft below land surface and the Test Well is considered fully penetrating. The G(1) and H(1) flow groups are assumed to consist of the effective aquifer at the pumping test site (Figure 4). All production is assumed to come from the 155 ft thick zone comprising these two flow groups.

Figures 13 and 14 contain plots of drawdown data for Well 120 using the Cooper-Jacob and Theis evaluations which assume the aquifer is fully confined. The poor fit early in the drawdown curve is probably caused by a decrease in pumping rate as the riser pipe filled with water, increasing the lifting head on the pump. Once the lifting head stabilized, the pumping rate stabilized at 2.8×10^3 gpm. After about 3 days, the data showed more drawdown than the theoretical curves predict. This could be a result of either boundary effects or gravity drainage from an unconfined aquifer. Appendix C contains Cooper-Jacob and Theis evaluations for Well 120 and the other wells in the Test Well cluster.

Semiconfined evaluation

In a semiconfined (leaky) aquifer the hydraulic head in the pumped aquifer lowers, creating a hydraulic gradient in the aquifer and between the aquifer and aquitard. The water that the pumped aquifer contributes to well discharge comes from storage within the aquifer. Water contributed by the aquitard comes from

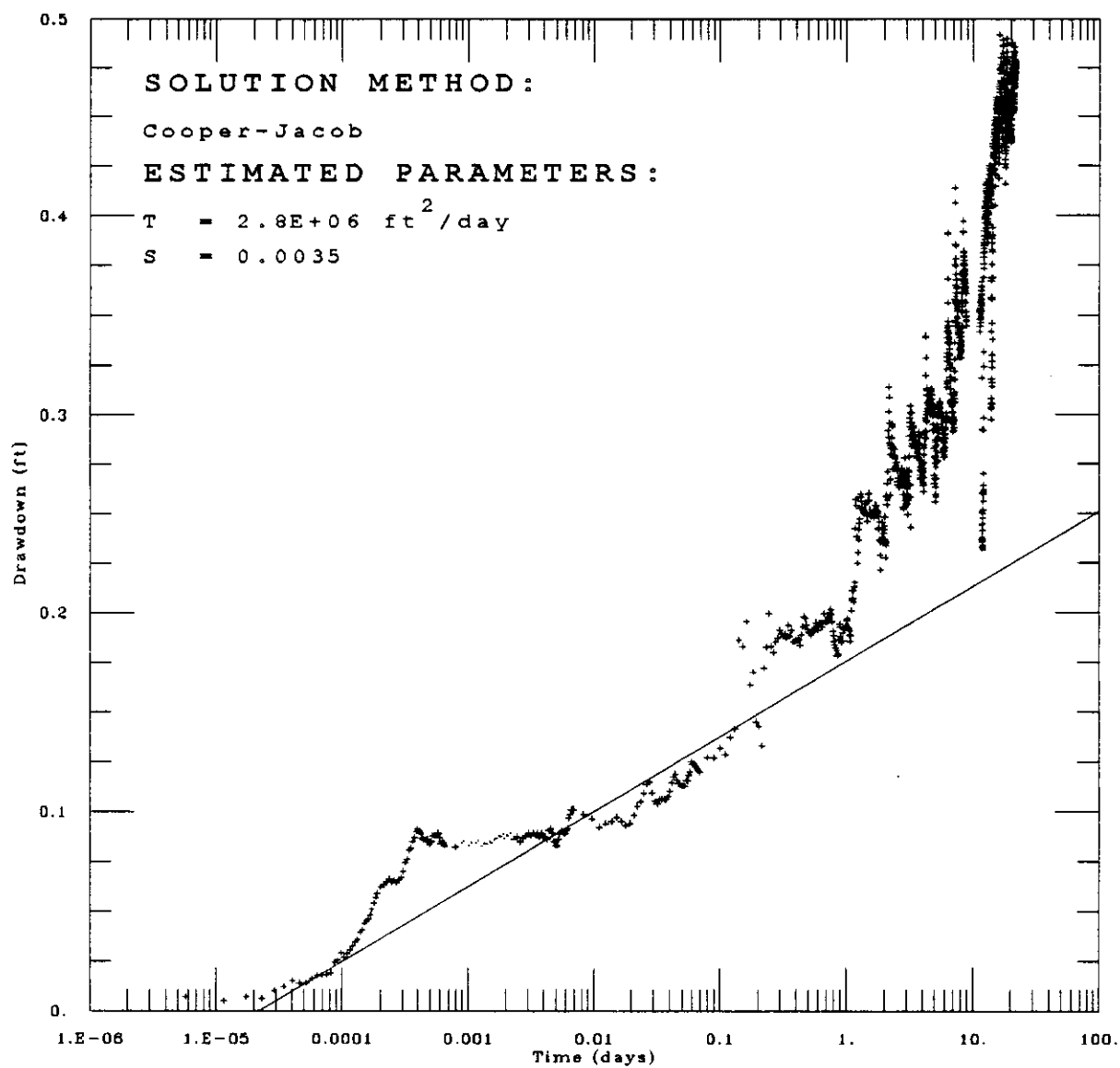


Figure 14. Cooper-Jacob plot from Well 120.

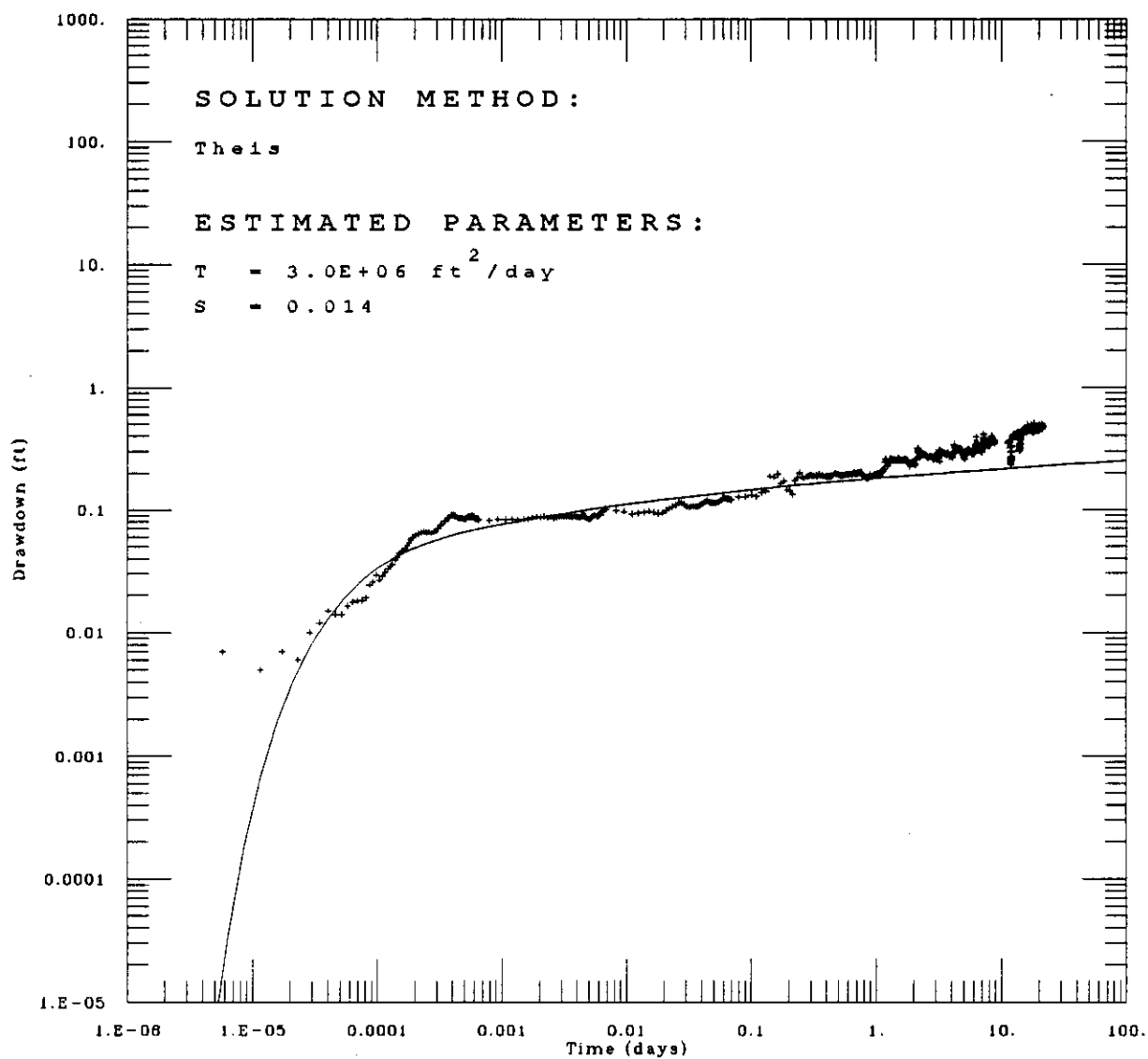


Figure 15. Theis drawdown plot for Well 120.

storage within the aquitard and leakage through it from an adjacent unpumped aquifer. As pumping continues, more of the water comes from leakage from the unpumped aquifer and less from aquitard storage. In time, well discharge comes into equilibrium with leakage through the aquitard and steady-state flow is attained. Under such conditions, the aquitard serves as a water-transmitting medium, and the water contributed from its storage can be neglected. When pumping starts, the drawdown data follow the Theis curve while water is delivered primarily from storage within the aquifer. As pumping continues and more water is contributed from aquitard storage and/or leakage there is a decrease in the slope of the time-drawdown curve relative to the Theis curve because water is delivered to the well from outside the aquifer and yield is greater than that which would be delivered by an equal decline in the potentiometric surface of a fully confined aquifer. When steady-state flow is attained, the drawdown curve is flat (Kruseman and de Ridder, 1991). The data do not show the above mentioned response, so an attempted match will not be illustrated.

Boundary calculations

Appendix C contains calculations for the distance to an impermeable boundary. These calculations were conducted as described by the Bureau of Reclamation (1977). Based on these calculations, the distance to an image well approximating an impermeable boundary from OW1 Upper is 19,000 ft, from Well 120 it is 4,100 ft, and from OW2 Upper it is 490 ft. To locate the boundary, a circle is drawn on a map of the test site using a radius equal to the distance computed for each observation well. If there were a linear boundary it would be located one half the distance from the pumped well to the point where the circles intersect. There is about an order of magnitude decrease in the distance to the image well as the radial distance from the observation well to the Test Well increases, however, all the observation wells are within 100 to 400 ft from the Test Well, so none of these circles intersect. It is therefore unlikely that the observed increased in drawdown is due to an impermeable boundary.

Neuman evaluation

In an unconfined aquifer, after the pump is turned on, water is released instantaneously from storage by compaction of the aquifer and by the expansion of water and time-drawdown data conform to the Theis curve. During the second phase, the effects of gravity drainage are felt. There is a decrease in the slope of the time-drawdown curve relative to the Theis curve because water is delivered to the well by dewatering that portion of the aquifer above the now lowered potentiometric surface and the yield is greater than that which would be delivered by an equal decline in the potentiometric surface of a confined aquifer. In the third phase, time-drawdown data once again conform to the Theis curve as water flows from the aquifer into the well from aquifer storage

Figure 15 shows a plot of a Neuman (1975) analysis of Well 120 data. Once again, the data do not fit the early part of the curve, but the later data fit

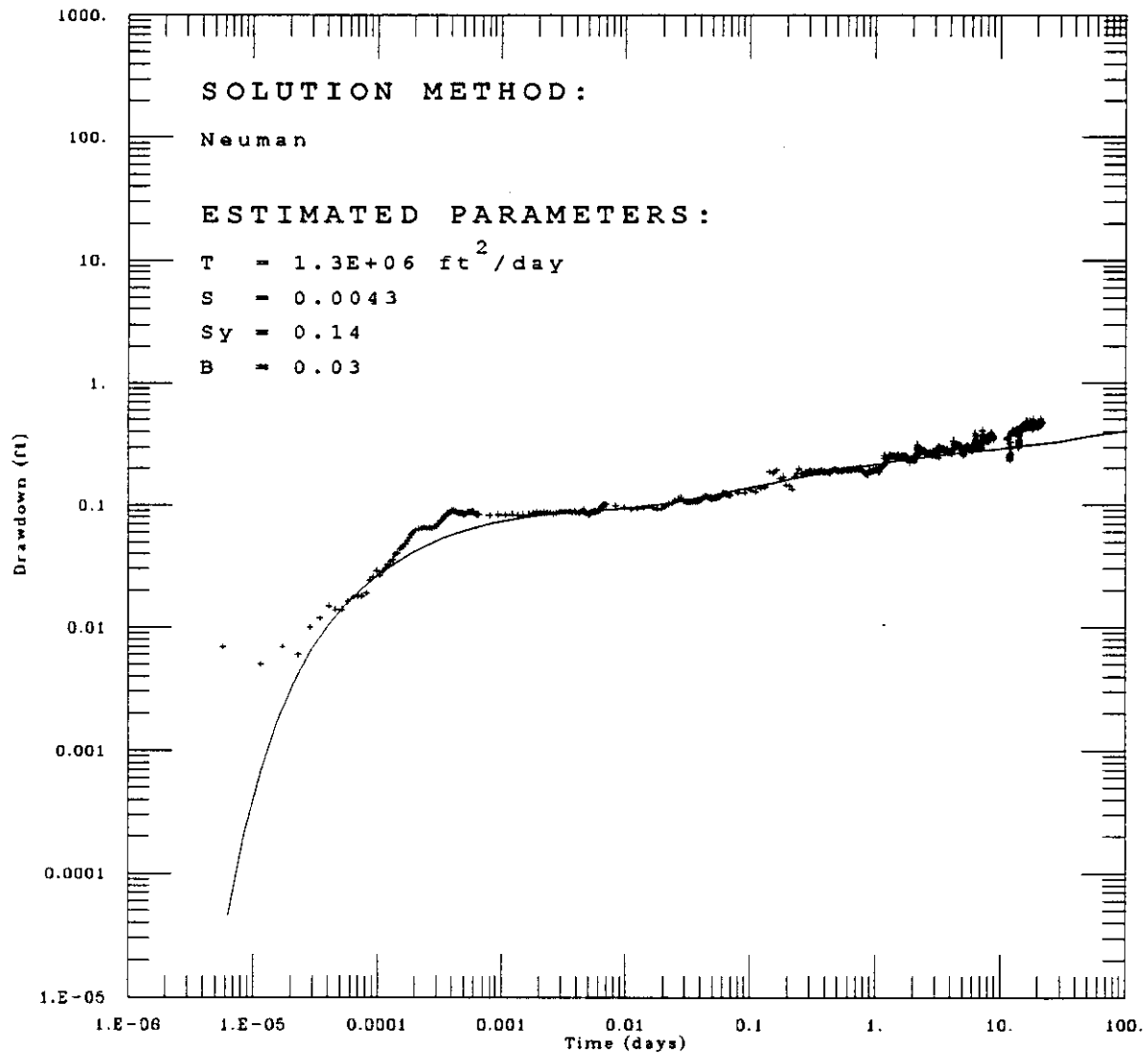


Figure 16. Neuman analysis of time-drawdown plot of Well 120 data.

much better, indicating the unconfined aquifer conceptual model describes the data from this test better than the confined conceptual model. The calculated Kh/Kv ratio is 60 using the parameters shown in Figure 15. Neuman analysis and Kh/Kv ratio calculations for Well 120 and the other observation wells in the Test Well cluster are presented in Appendix C. The match with OW2 is not as good as the match for the other wells, however, this match is also much better than the Theis or Cooper-Jacob match.

Evaluation of recovery data.

Figure 16 shows a plot of the corrected recovery data from Well 120 analyzed using the Theis recovery method as modified by Neuman (1975). The Test Well did not have a check valve to prevent water in the pump column from draining back into the aquifer; however, there was a valve at land surface to prevent water in the above-ground piping system from being siphoned back into the well. A calculated 3,600 gal of water drained back into the aquifer when the pump was turned off. This creates a significant deviation from the type curve early during the recovery test and makes analysis of the data questionable. Note that, for Well 120, the storage coefficients for the recovery analysis differ more significantly from the drawdown analysis than transmissivity, 1.2×10^6 vs. 1.3×10^6 ft²/day for transmissivity and 1.4×10^{-1} vs. 5.0×10^{-2} for specific yield. This may be due to the injection of water that occurred as the pump was turned off. For this reason, recovery analysis is used as a check on the transmissivity values from the drawdown analysis only. Recovery analysis for Well 120 and the other observation wells in the Test Well cluster are presented in Appendix C.

Distance drawdown analysis.

A semilog distance-drawdown graph can be constructed using drawdowns observed in at least 3 observation wells at different distances from the Test Well. This graph is a plot of the cone of depression and can be used to calculate aquifer coefficients, well efficiency and the theoretical zone of influence for the pumped well. These calculations were conducted as described by Driscoll (1986). Drawdowns observed three days into the test, when deviations from the Theis curve were not pronounced were used for this analysis. The results are presented in Figure 17 and calculations are in Appendix C.

The observed and predicted drawdown in the Test Well were 9.53 ft and 0.56 ft respectively and the calculated well efficiency is 6%, the calculated point of zero drawdown is 10,000 ft from the Test Well. Note that the well efficiency is 6%, yet the Test Well is completed as an open hole. An open hole is the most efficient well design possible. Well efficiency is low because permeability is not evenly distributed throughout the thickness of the G(1) and H(1) flow groups. The more permeable sections of the flow groups are isolated in only a few feet of the well resulting in converging and turbulent flow into the well, reducing well efficiency.

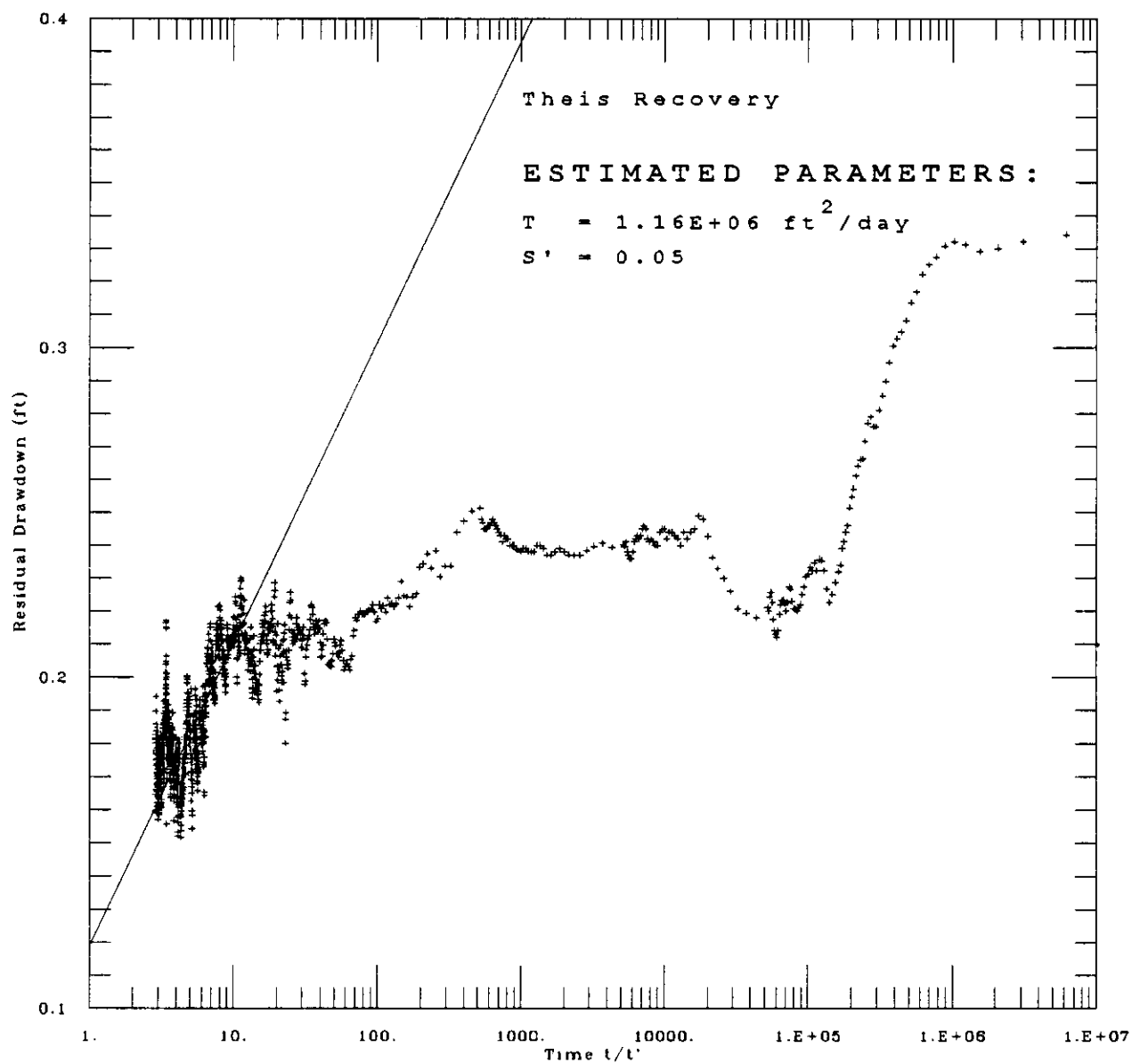


Figure 17. Recovery analysis for Well 120.

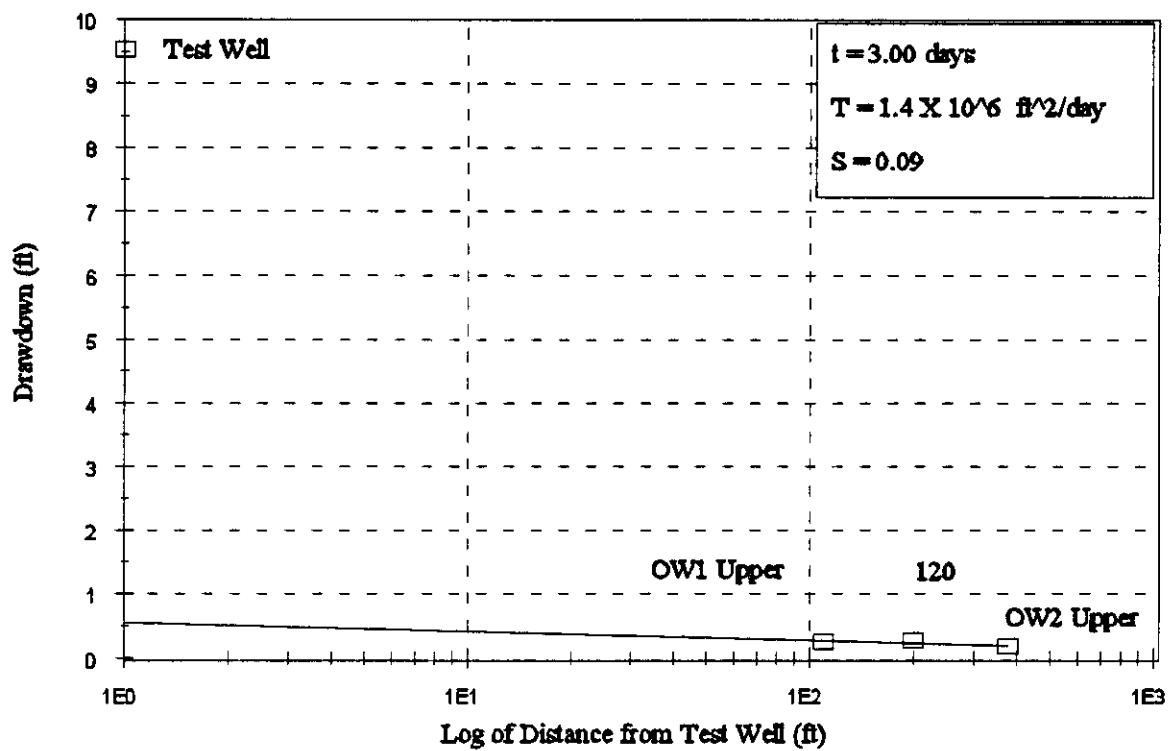


Figure 18. Distance drawdown plot.

Analysis of aquifer anisotropy.

Knowing whether a formation is anisotropic, and to what extent, is important for developing mathematical models, contaminant migration studies, and hydrologic studies. Aquifer anisotropy was analyzed using PAPADOP, a program by In-Situ Inc., which uses a technique by Way and McKee (1982). Program output is presented in Appendix C. The PAPADOP program uses data from multi-well pumping tests (one pumping well and a minimum of three observation wells) to obtain mean directional transmissivity based on all possible three-well combinations. This analysis indicates that the major transmissivity axis of 1.6×10^6 ft²/day is north 6.9° east and the minor axis is 1.4×10^6 ft²/day (Figure 19).

There are only three observation wells and only one combination that can be analyzed to evaluate aquifer anisotropy; thus, the analysis cannot be cross-checked.

Summary of Analytical Analysis

The Test Well is completed in the G(1), H(1) flow groups. OW1 and OW2 are deeper; however, packers were placed in the wells in an attempt to isolate the G(1) and H(1) units from the remainder of the hole. The packer in OW1 could not

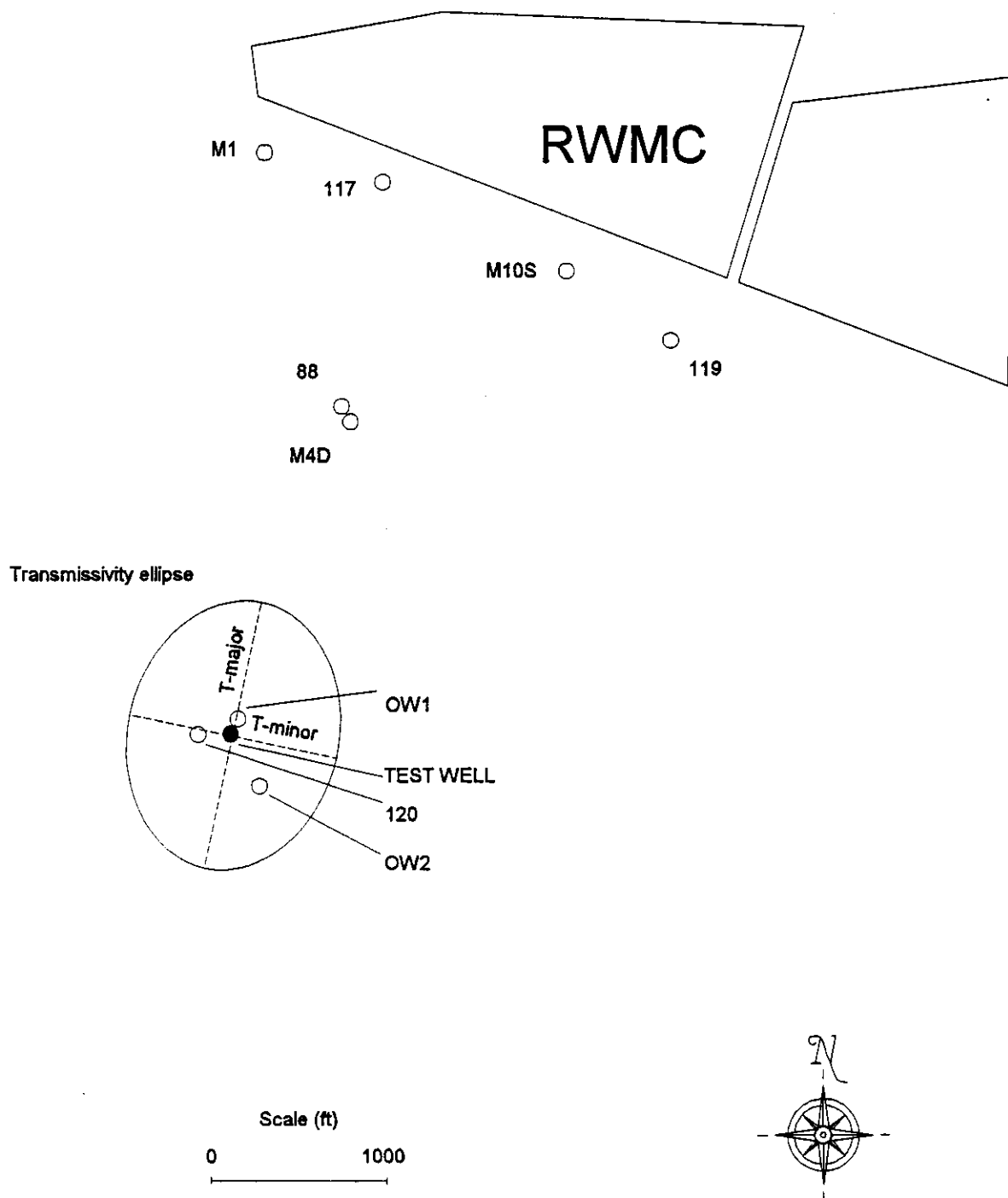


Figure 19. Transmissivity ellipse showing the major and minor transmissivity axis.

be placed in the optimal location because of hole stability problems. Aquifer response suggests that most of the flow into the Test Well was from the G(1) and H(1) flow groups.

The raw data had to be corrected before analysis because of the small observed drawdowns and large water level fluctuations due to barometric pressure changes. Diurnal fluctuations appear to be about 90% efficient, while barometric pressure changes associated with weather frontal systems appear to be about 60% efficient. A difficult part of the analysis was selecting a filter to remove the noise and not affect any aquifer response due to pumping the Test Well. The filter that appeared to work best was subtracting data collected at a nearby well which apparently did not respond to any pumping. The high observed barometric efficiency suggests that the aquifer is confined.

Analysis of the step test indicated that the transmissivity in the vicinity of the Test Well was $4 \times 10^2 \text{ ft}^2/\text{day}$ and that the aquifer would yield sufficient water to conduct the infiltration portion of the test.

The drawdown data from the main portion of the test fit unconfined type curves best, suggesting that, at this location and scale, the Snake River Plain aquifer responds as an unconfined aquifer. This seems to be inconsistent with the analysis of the pretest data, which indicated that the aquifer had a barometric efficiency between 60 and 90% suggesting that the aquifer is confined. Perhaps the units isolating the aquifer from barometric pressure fluctuations are not acting as aquitards, or are above the potentiometric surface of the aquifer. The recovery data is not felt to be as accurate as the drawdown data because there was no check valve in the pump to prevent water from draining out of the pump column into the aquifer. Table 3 contains a summary of the analytical results.

Even though the Test Well was completed as an open hole, the well efficiency is about 6%. This may indicate that preferential flow paths exist and that permeability is not evenly distributed throughout the G(1) and H(1) flow groups, and water is entering the well at only a few isolated horizons.

Analysis of vertical anisotropy indicates that the K_h/K_v ratio is between 30 and 100, suggesting that vertical communication within the aquifer is limited. Analysis of horizontal anisotropy indicates the T-major/T-minor ratio is about 1.2, indicating that the aquifer is only modestly anisotropic horizontally. This is consistent with the basalt flow geometry and the conceptual model of flow within the aquifer. Horizontal flow within the aquifer should be less impacted by long, slender, and flat basalt flows than vertical flow.

Table 3: Calculated aquifer coefficients.

Observation Well	Transmissivity (ft ² /day)	Storage	Kh/Kv ratio	Analytical Method
OW1 Upper	1.5 x 10 ⁶ ft ² /day	1.3 x 10 ⁻¹	1 x 10 ²	Neuman drawdown
	5.9 x 10 ⁶ ft ² /day	5.3 x 10 ⁻²		Theis recovery
OW1 Lower	5.5 x 10 ⁶ ft ² /day	1.8 x 10 ⁻¹		Neuman drawdown
	3.5 x 10 ⁶ ft ² /day	2.3 x 10 ⁻²		Theis recovery
120	1.3 x 10 ⁶ ft ² /day	1.4 x 10 ⁻¹	6 x 10 ¹	Neuman drawdown
	1.2 x 10 ⁶ ft ² /day	5.0 x 10 ⁻²		Theis recovery
OW2 Upper	1.5 x 10 ⁶ ft ² /day	1.4 x 10 ⁻¹	3 x 10 ¹	Neuman drawdown
	7.8 x 10 ⁶ ft ² /day	4.2 x 10 ⁻²		Theis recovery
	1.4 x 10 ⁶ ft ² /day	9.0 x 10 ⁻²		distance drawdown
	1.4 x 10 ⁶ ft ² /day	1.3 x 10 ⁻¹		anisotropy drawdown
	heterogeneous			anisotropy recovery

Numerical Modeling

Pumping test results were also analyzed using MODFLOWP (Hill, 1992). MODFLOWP is a finite difference model with automatic parameter estimation capabilities. MODFLOW (McDonald and Harbaugh, 1988) is the groundwater flow simulation model used in MODFLOWP. MODFLOW is capable of modeling one, two, or three dimensional groundwater flow.

Transmissivity and specific yield distribution in the vicinity of the pumping test is not well understood; however, different simulation models with different parameter distributions can be hypothesized and tested using a numerical model. A numerical model can simulate a heterogeneous and anisotropic aquifer. For each hypothesized pumping test simulation model, parameter values are chosen that allow the model to best reproduce the drawdowns observed during the pumping test. Using the numerical model, the aquifer can be divided into different transmissivity and specific yield zones and tested to explain the discrepancies between the observed drawdowns from the pumping test and the results expected based on the Theis and Neuman analysis presented in this report.

The following assumptions were made to simulate the pumping test:

- Two-dimensional horizontal flow in a single layer,
- Unconfined,
- Domain is a square, 24,560 ft on a side, with the pumping well situated in the middle,
- The initial hydraulic head is defined as zero so that the MODFLOW hydraulic

- head solution is equal to the negative of the drawdown,
- A prescribed head of zero is used for all boundaries,
 - The domain is oriented so that OW1 is situated along the +y axis, OW2 is situated along a line 30° below the +x axis, and Well 120 is situated along a line 30° below the -x axis (Figure 20),
 - OW1, Well 120, and OW2 are situated 110 , 200 , and 385 ft from the pumping well, respectively,
 - The aquifer is assumed to be 155 feet thick and
 - The pumping well pumped at a nearly constant rate of 3,000 gpm except for the periods from 11.78 to 12.15 and 13.93 to 14.31 days when it was turned off.

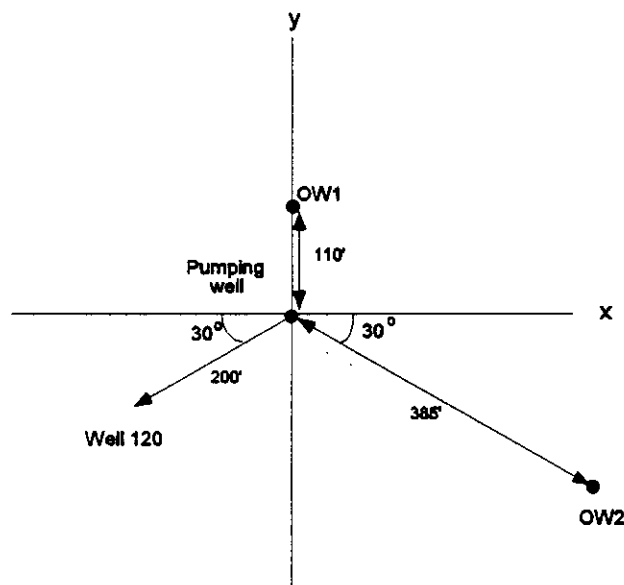


Figure 20. Layout of the pumping and observation wells.

The domain width and length were chosen based on the distance drawdown analysis presented earlier in this report and a series of numerical simulations performed with various size domains. The distance drawdown analysis indicated that the boundary needed to be 10,000 ft from the pumping well. The numerical simulations were performed to verify that distance. The measured drawdowns indicate that after about 21 days, the drawdown leveled off, indicating that the water pumped was being replaced by a boundary rather than removed from storage in the aquifer. Therefore, the simulation model domain must be sufficiently large so that a larger domain would not significantly increase the simulated drawdown at the observation wells after 21 days of pumping. The results of the numerical simulations performed to determine the required domain size are shown in Table 4. The difference between the simulated drawdown after

21 days of pumping for the 10,410 and 24,560 ft domains is about 10%. The difference in the drawdown after 21 days for the 24,560-and 34,560-ft domains is only 0.2%. Therefore, the 24,560-ft domain was chosen for the simulations. The domain sizes identified with the distance drawdown analysis (10,000 ft) and the numerical simulations are about the same.

Table 4. Comparison of the simulated drawdown for numerical model domains of different length and width.

Well	Domain Geometry	Domain Length and Width (feet)				Actual
		5,730	10,410	24,560	34,560	
	Time Step (days)	Drawdown (feet)	Drawdown (feet)	Drawdown (feet)	Drawdown (feet)	Drawdown (feet)
OW1	1	0.300	0.303	0.303	0.303	0.22
	8	0.394	0.446	0.456	0.456	0.35
	21	0.393	0.459	0.506	0.507	0.53
	36	0.395	0.466	0.540	0.545	0.57
120	1	0.231	0.233	0.233	0.233	0.19
	8	0.323	0.375	0.385	0.385	0.33
	21	0.322	0.388	0.435	0.436	0.45
	36	0.324	0.395	0.469	0.474	0.43
OW2	1	0.157	0.160	0.160	0.160	0.10
	8	0.245	0.297	0.307	0.307	0.31
	21	0.244	0.310	0.357	0.358	0.53
	36	0.246	0.317	0.391	0.396	0.54

The simulated drawdown is very sensitive to the aquifer domain dimensions,

particularly at the later stages of the test; therefore, the aquifer domain dimensions must be treated as a calibration parameter. The sensitivity of the estimated storativity and transmissivity to the domain size is evaluated and presented later.

The numerical domain was discretized into 201 rows and 201 columns. The pumping well was positioned in the center of the domain. A variable grid was used that ranges in size from 10' by 10' in the area of the pumping well to 400' by 400' on the boundary. The domain is symmetric about the center (location of the pumping well). Table 5 is a list of the row and column numbers and the cell width for each. As shown in Table 5, rows 1-10 discretize the northern most 4000' of the domain into 10 rows of 400' each, and columns 1-10 discretize the western most 4000' of the domain into 10 rows of 400' each.

Table 5. Cell widths along the rows and columns.

Row / Column numbers	Cell Width Along the Rows or Columns	Total Length of the Domain Defined by these Rows and Columns
	(feet)	(feet)
1 - 10	400	4,000
11 - 20	300	3,000
21 - 40	200	4,000
41 - 55	50	750
56 - 60	25	125
61 - 141	10	810
142 - 146	25	125
147 - 161	50	750
162 - 181	200	4,000
182 - 191	300	3,000
192 - 201	400	4,000
Total		Total 24,560

As explained in earlier sections of this report, the signal-to-noise ratio for

the pumping test was very low. However, a reasonable set of drawdowns at the observation wells was extracted from the measured hydraulic heads at the observation wells. The estimated drawdown every 24 hours after the pumping test started were used as the model calibration observation set. There were no data for days 9, 10, and 11 because of equipment problems during the test. Three observations (8.88, 11.3, and 36.2 days) were added to the data set for a total of 36 observations for each of the three observation wells. Recovery data were also taken after the pump was turned off, but the confidence in the recovery data is relatively low and, therefore, was not used for this analysis.

The simulated drawdown is very sensitive to the aquifer domain dimensions, particularly at the later stages of the test; therefore, the aquifer domain dimensions must be treated as a parameter in the calibration. The sensitivity of the estimated storativity and transmissivity to the domain size is evaluated and presented later in this paper. There is no unique solution to this parameter estimation problem, therefore, the results of 10 different scenarios are presented. The scenarios vary the number of transmissivity and specific yield zones as well as the extent of the modeled domain. For the first seven scenarios, the aquifer domain is assumed to be square with sides of 24,560 ft. The assumed aquifer parameter zones are shown in Figure 21. The test runs can be divided into four categories: (1) homogeneous transmissivity, (2) two transmissivity zones (combine zones 1, 2, and 3 in Figure 21 into one zone), (3) four transmissivity zones, and (4) sensitivity of the parameter estimates to the assumed dimensions of the aquifer. The homogeneous transmissivity test runs presented are:

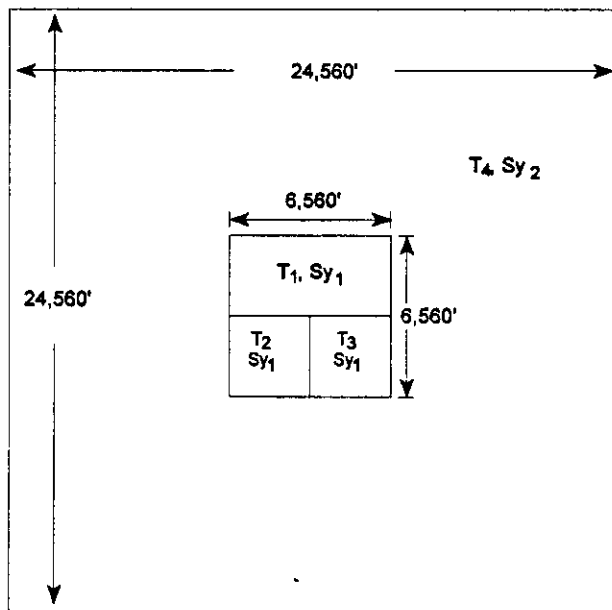


Figure 21. Assumed aquifer parameter zones.

1. Transmissivity is assumed to be homogeneous, and the specific yield is

assumed to be 0.13. MODFLOWP identifies an optimal value for the transmissivity.

2. Transmissivity and specific yield are both assumed to be homogeneous. MODFLOWP identifies optimal values for both the transmissivity and specific yield.
3. Transmissivity and specific yield are both assumed to be homogeneous, and the aquifer thickness is reduced from 155 ft to 5 ft. An aquifer thickness of 5 feet was chosen to simulate the assumed thickness of the interflow zones intersected by the pumping well. MODFLOWP identifies optimal values for both the transmissivity and specific yield.

The test runs that assume two transmissivity zones are:

4. The aquifer is divided into two transmissivity zones (combine zones 1,2, and 3 in Figure 21 into one zone), and the specific yield is assumed to be 0.13. MODFLOWP identifies the two optimal parameter transmissivity values.
5. The aquifer is divided into two transmissivity zones (combine zones 1,2, and 3 in Figure 21 into one zone), and the specific yield is assumed to be homogeneous. MODFLOWP identifies the three optimal parameter values.
6. The aquifer is divided into two transmissivity and two specific yield zones (combine zones 1,2, and 3 in Figure 21 into one zone). MODFLOWP identifies the four optimal parameter values.

The test run that assumes four transmissivity zones is:

7. The aquifer is divided into four transmissivity zones (shown in Figure 21), and the specific yield is assumed to be homogeneous. MODFLOWP identifies the five optimal parameter values.

The results of the test runs are shown in Table 6. The simulation results are judged based on a least squares fit to the actual drawdown. Comparison of the drawdown values used for the calibration and the simulated drawdowns for test run 5 are shown in Figure 22a, b, and c for OW1, well 120, and OW2, respectively. The comparisons for test runs 1, 2, 4 and 7 are included in Appendix D. The input files used for test run 5 is include in Appendix E.

For the most part, the drawdown data follow a pattern that can be reproduced by the simulation model with two transmissivity zones. The data that do not conform to the conceptual model simulated are the decrease in drawdown in well 120 after 25 days (see Figure 22b) and the significant decrease in drawdown observed when the pumps were twice temporarily turned off (see Figure 22). In each case the pumping well was off for about 0.37 days. The well was first turned off 11.8 days after the test began and then again 13.9 days after the test started.

Table 6. Comparison of the parameter values identified by MODFLOWP for different test runs simulating the pumping test.

Run #	Run	T ₁ (ft ² /day)	T ₂ (ft ² /day)	T ₃ (ft ² /day)	T ₄ (ft ² /day)	Sy ₁	Sy ₂	Sum of Squared Err
1	Homo_T_Sy=0.13	827,700	827,700	827,700	827,700	0.13	0.13	1.14
2	Homo_T_and_Sy	726,950	726,950	726,950	726,950	0.50	0.50	0.91
3	Homo_T_and_Sy_thickness=5	760,000	760,000	760,000	760,000	0.54	0.54	0.93
4	2T_Sy=0.13	2,356,000	2,356,000	2,356,000	229,400	0.13	0.13	0.33
5	2_T_homo_Sy	3,131,000	3,131,000	3,131,000	229,400	0.10	0.10	0.32
6	2_T_2_Sy	2,402,500	2,402,500	2,402,500	252,650	0.22	0.034	0.31
7	4_T_homo_Sy	132,525	3.92(10 ⁶)	3,286,000	277,450	0.13	0.13	0.29
8	2_T_homo_Sy_dom_5730	2,495,500	2,495,500	2,495,500	125,860	0.83	0.83	0.33
9	2_T_homo_Sy_dom_10410	2,588,500	2,588,500	2,588,500	150,660	0.32	0.32	0.32
10	2_T_homo_Sy_dom_34560	3,472,000	3,472,000	3,472,000	260,400	0.06	0.06	0.32

The optimal transmissivity for the homogeneous parameter estimation test runs is about 800,000 ft²/day (test cases 1 and 2). As shown in test cases 4, 5, and 6, when the aquifer is divided into one zone surrounding the pumping and observation wells (Zones 1, 2, and 3) and another for the rest of the aquifer (Zone 4), the observational data can be better simulated by increasing the transmissivity around the wells by factor of 3 to 4 and decreasing the transmissivity in the rest of the aquifer by a factor of 3 to 4. The improvement in the fit is significant, decreasing the sum of the squared errors from 0.9 to 0.3. When the aquifer is divided into four zones (test case 7), the simulation models fit to the observational data is further improved but only marginally (0.32 to 0.29). The transmissivity in zones 1, 2, and 3 differ over four orders of magnitude without significantly changing the fit because the sum of the squared errors is not very sensitive to the parameter values and there is significant correlation between the parameters. Because of the correlation, one parameter value can be increased and the other

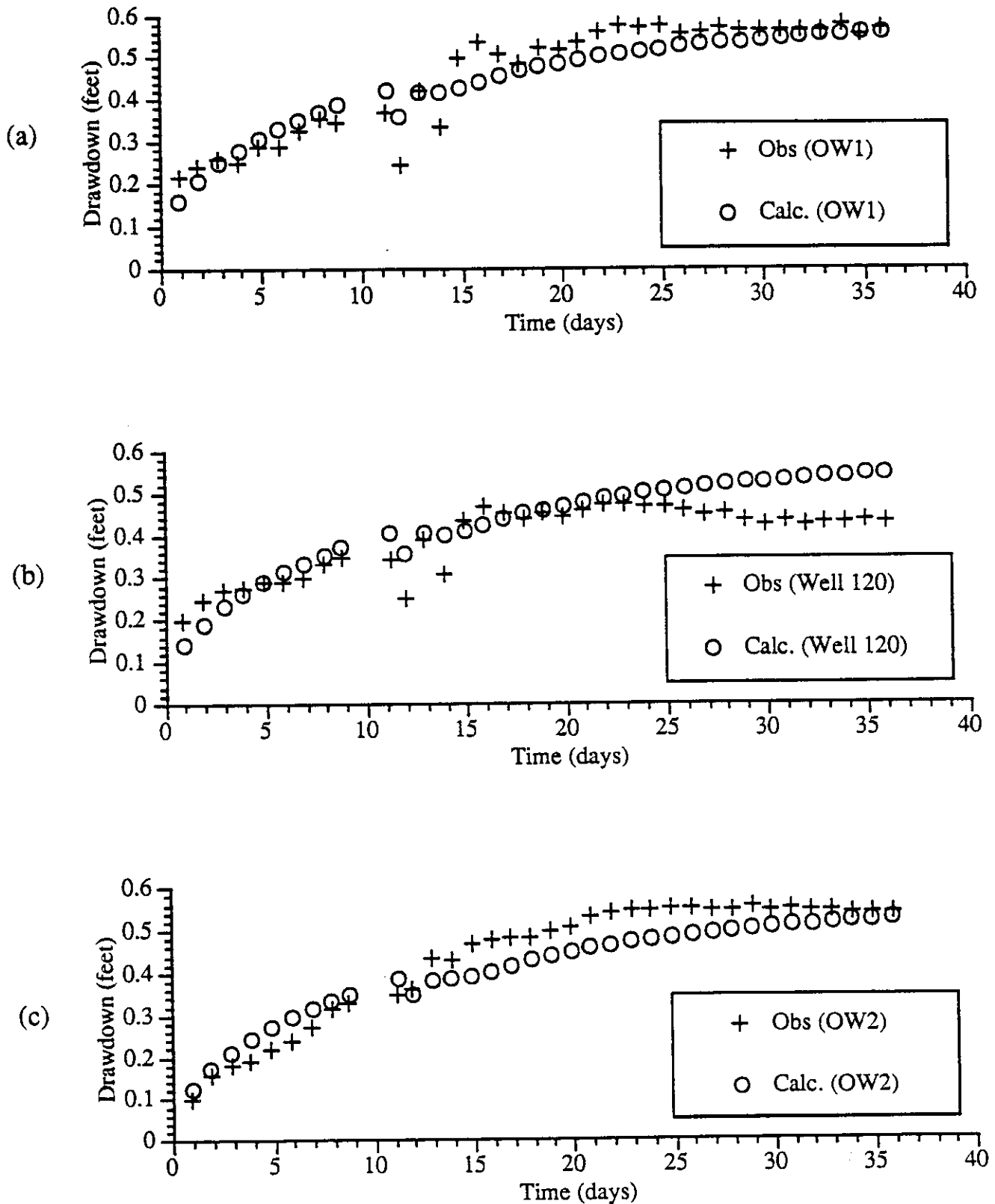


Figure 23. Comparison of OW1 Upper (a), Well 120 (b), and OW2 Upper (c) observed drawdown values with the simulated drawdowns from test run 5.

decreased without significantly changing the sum of the squared errors. For systems with perfectly correlated parameters, there is an infinite number of solutions. For problems such as this with significant parameter correlation, the solutions are not unique but can be used to imply parameter values that approximate the optimal solution.

MODFLOWP identified an optimal specific yield of 0.5 (test run 2) when the aquifer was assumed to be homogeneous. However, the transmissivity and specific yield are strongly correlated for this problem (correlation coefficient of -0.96) which implies that there is little confidence in this value. The parameter correlation coefficient is calculated in MODFLOWP and explained in detail in the MODFLOWP documentation (Hill, 1992). If the correlation coefficient for two parameters approaches one (greater than 0.9) then the parameter values are correlated and it will be difficult to identify a unique solution.

If the drawdown for the pumping test is small, then it is difficult to separate the drawdown effects of the transmissivity from the effects of the storativity. To illustrate this problem, consider Jacob's equation that describes the drawdown that results from pumping in a confined aquifer;

$$s = \frac{Q}{4\pi T} [-0.5772 - \ln(\frac{r^2 S}{4 T t})] \quad (1)$$

Where;

- s drawdown (f)
- Q pumping rate (f³/day)
- T transmissivity (f²/day)
- S storativity (unitless)
- r distance from the pumping well to the observation well (f)
- t time (day)

In order to compare the sensitivity of the drawdown to storativity and transmissivity, consider the calculated drawdown for $Q = 5.77\text{e}5 \text{ ft}^3/\text{day}$, $t = 10 \text{ day}$, $r = 110 \text{ ft}$, $S = 0.13$ and $T = 1(10^6) \text{ ft}^2/\text{day}$. Defining the drawdown sensitivity to the storativity and transmissivity as a drawdown percent change for a 10% change in the parameter value, the sensitivity to the storativity is approximately 1% and the sensitivity to the transmissivity is approximately 10% (see Table 7). For this high transmissivity example, the sensitivity of the storativity is an order of magnitude smaller than the sensitivity to the transmissivity and the change in the drawdown for a 10% change in the parameter values is similar in magnitude to the error in the data. Therefore, it is very difficult to separate the drawdown effects of the transmissivity from the effects of the storativity. For a low transmissivity example (see Table 7) the sensitivity to the transmissivity is less than twice the sensitivity to the storativity. In addition, the change in the drawdown for a 10% change in the parameter

values is large in comparison to expected measurement errors. Therefore, as the transmissivity decreases, it is easier to separate the drawdown effects of the transmissivity and storativity and identify unique parameter values that best represent the transmissivity and storativity in the aquifer.

Table 7. Sensitivity of the drawdown to 10% changes in the transmissivity and storativity.

Transmissivity	Storativity	Drawdown	Fractional Change in Drawdown
(ft ² /d)		(ft)	
High Transmissivity			
1,100,000	0.13	0.403	-0.08
1,000,000	0.13	0.439	-
900,000	0.13	0.482	0.10
1,000,000	0.143	0.434	-0.01
1,000,000	0.13	0.439	-
1,000,000	0.117	0.444	0.01
Low Transmissivity			
1,100	0.13	114.91	-0.06
1,000	0.13	122.02	-
900	0.13	130.21	0.07
1,000	0.143	117.65	-0.04
1,000	0.13	122.02	-
1,000	0.117	126.86	0.04

When the aquifer is divided into two transmissivity zones and one specific yield zone (test run 5) the optimal specific yield identified was 0.1, which is closer to the value that has been assumed in past modeling of the Snake River Plain aquifer. When the aquifer was divided into four transmissivity zones and one specific yield zone (Test Run 7) the optimal specific yield identified was 0.13, which is again close to the value that has been assumed in the Snake River Plain aquifer modeling in the past (based on the assumed effective porosity). When the aquifer was also divided into two specific yield zones (Test Run 5), specific yields of 0.22 and 0.34 were identified.

If the specific yield value of 0.5 is accurate, it could imply that the aquifer would be better modeled as a layered system with a large transmissivity and specific yield of 0.5 in small interflow zones, and small transmissivity and specific yield surrounding the interflow zones. This would be a significant change from the way that both flow and transport have been modeled in the past for the Snake River Plain aquifer.

The sensitivity of the transmissivity values to the simulated aquifer domain (test runs 8, 9, 5, and 10) is relatively small, and the sensitivity of the specific yield is relatively high. As the domain size increases (5,730; 10,410; 24,560, and 34,560 ft on a side), the identified specific yield values significantly decrease (0.83, 0.32, 0.10, and 0.06). The sum of the squared errors fit to the drawdowns is essentially the same in all cases. Therefore, the domain size assumed for the numerical simulations is very important to identifying a reasonable specific yield value.

Conclusion

The objectives of the test were to calculate a transmissivity representative of the aquifer, calculate a storage coefficient representative of the aquifer, determine if the aquifer is confined or unconfined, and supply sufficient water to conduct the infiltration test about 1 mile from the Test Well (Wylie, 1994a).

The analytical results indicate that:

- Transmissivity values ranged from 7.8×10^6 to 1.2×10^6 ft²/day with an arithmetic mean of 1.4×10^6 ft²/day,
- Storage coefficient ranged from 9.0×10^{-2} to 1.8×10^{-1} with an arithmetic mean of about 1.3×10^{-1} , and
- The aquifer test data best fit type curves based on an unconfined aquifer analytical model.

Numerical modeling results imply that:

- The pumping test stressed a sufficient portion of the aquifer that flow can be approximated with an equivalent porous media model.
- Although there was not a unique transmissivity value identified, in our judgement, the value is probably within a factor of three of 1×10^6 ft²/day based on the test run results. With such a high transmissivity, it is very difficult to run a large-scale pumping test that would cause significant drawdown at wells outside the immediate vicinity of the pumping well.
- The aquifer in the immediate vicinity of the pumping and observation wells appears to have a higher transmissivity than the aquifer some distance from the wells. Recall that transmissivity value calculated using data from this test is well above the 95% confidence interval for the aquifer mean, therefore, this result should be expected.
- The specific yield estimate is uncertain. A more accurate conceptual model may allow the specific yield to be more accurately identified.
- The dimensions of the numerical domain strongly influence the estimated specific yield values; therefore, these dimensions are an important parameter in the pumping test analysis.

Historical data indicate that the 95% confidence interval for the mean of log transmissivity is between 3×10^3 and 1.2×10^4 ft²/day. The mean transmissivity calculated from this test is 1.4×10^6 ft²/day, two orders of magnitude above the 95% confidence interval. This test yielded a transmissivity much higher than expected because:

- The test site was selected in an area expected to yield 3000 gpm, and
- A long-term high pumping rate test yields a better estimate of aquifer properties because more aquifer material is stressed during the test and there are more data to better define the match with the type curve.

Ackerman (1991) reported a transmissivity of 2.2×10^5 ft²/day for Well 120 from a 60 min, 21.1 gpm test, the step test yielded a transmissivity of 3.7×10^5 ft²/day from a 60 min 1000 gpm test, and the value was refined to 1.4×10^6 ft²/day with a 36 day, 3000 gpm test. This test refined the transmissivity estimate upward by a factor of 6.4. It should be noted that the original estimate was well above the 95% confidence interval for the mean. This suggest that the high transmissivity values presented in Figure 8 may be underestimated. A close look a Figure 8 shows that the values below e^{12} (1.6×10^5 ft²/day) appear to closely approximate the theoretical curve, while the values above e^{12} do not follow along the theoretical curve as nicely. Perhaps higher estimates are not as

precise as the lower estimates. The stress applied to the aquifer in the original 21.1 gpm test may not have been sufficient to observe a response which allowed an accurate and precise estimate of aquifer properties.

The conceptual model suggesting that aquifer permeability is largely controlled by the distribution of basalt interflow zones has been verified by 1) interflow zones were identified as being the zones in which aquifer flow was taking place; 2) packer selections based on the conceptual model seemed to correctly identify preferential flowpaths in the aquifer; 3) the Test Well was highly inefficient, even though it was completed as an open hole; and 4) analysis of vertical anisotropy indicates that the K_h/K_v ratio is between 30 and 100, suggesting that vertical communication within the aquifer is limited. Nonetheless some data do not seem to support the conceptual model. If the conceptual model were correct either a fracture flow model as described by Kazemi et al. (1969) or the Moench (1984) double-porosity model should have been required to analyze the data. However, the data are adequately described by the Neuman model. Perhaps the permeability of the matrix material is sufficiently low and the interflow zones are distributed evenly enough that fluid flow can be approximated with an unconsolidated homogeneous analytical model. The aquifer was successfully simulated as an unconsolidated aquifer during numerical modeling, supporting this hypothesis.

Darcy's law can be used to calculate the diameter of the capture zone for a pumping well. Assuming the aquifer is homogeneous and isotropic, there are no boundary effects in the radius of influence of the pumping well, and there are no other pumping or injecting wells within the radius of influence of the pumping well, Darcy's law is:

$$Q = KIA \quad (2)$$

Where: Q is discharge, K is hydraulic conductivity, I is hydraulic gradient, and A is the cross-sectional area.

Aquifer transmissivity, T , is hydraulic conductivity, K , times aquifer thickness, b . So Darcy's law can be written as:

$$Q = TIL \quad (3)$$

Where: L is the length of the cross-sectional area of the aquifer yielding the discharge. Solving for L yields:

$$L = \frac{Q}{TI} \quad (4)$$

Using Equation (4), assuming an average gradient of 4 ft/mi (Barracough, and Jensen, 1976), and the 95% confidence interval for the transmissivity mean (3×10^3 to 1.2×10^4 ft²/day), an extraction well pumping at 100 gpm could be expected to have a capture zone between 4.2×10^3 to 1.1×10^3 ft wide. In a well field with several active extraction and injection wells, the results of this scoping calculation would not be valid because the capture zone would be affected by the presence of other active wells.

Areas where more study would be beneficial include:

- Experimenting with different filtering techniques to remove the fluctuations in the data introduced by barometric pressure changes.
- The response to the pump being turned off may be improved if the simulation model reinjects an estimated 3,600 gal of water that drained back into the aquifer from the well when the pump was turned off.
- Conducting multiple well packer tests to better define the vertical anisotropy of the aquifer.
- Conducting the test again with at least one additional monitoring well and a check valve in the pump collum. This could significantly refine the horizontal anisotropy estimate by allowing checks on the calculation with 3 more 3 well combinations and the recovery data.
- Image a partitioning tracer test using borehole to borehole tomography to better define the hydrogeological conceptual model and attempt to test the conceptual model in the presence of discontinuities and terminations in the interflow zones.
- Develop a flow and solute transport model that can be used for hypothesis testing to evaluate the range of possible transport responses based on different conceptual models. The current conceptual model assumes flow and transport through a porous media. How different would a plume move through a system where the flow is primarily in interflow zones that pinch off and force flow to move slowly through dense basalt, or move quickly through vertical fractures to other interflow zones?
- Conduct a sensitivity analysis using different conceptual models with a three dimensional contaminant transport groundwater model with dual porosity capabilities.
- Retest the wells in the geostatistical data set above 1.6×10^5 ft²/day.
- Conduct a complete geostatistical analysis using the refined data set including variography, kriging, and multiple aquifer simulations.

All the objectives of the test have been met. Results indicate that the transmissivity of the aquifer is between 7.8×10^6 to 3.3×10^5 ft²/day, the storage coefficient ranges from 6.0×10^{-2} to 1.8×10^{-1} with an average of about 1.3×10^{-1} based on the analytical results, while the results from numerical

modeling suggest it may be as high as 5.0×10^{-1} in preferential flow paths. Although the barometric efficiency was as high as 90%, the test results best fit an unconfined aquifer analytical model, and adequate water was supplied to conduct the infiltration experiment.

References

- Ackerman, D. J., 1991. Transmissivity of the Snake River Plain Aquifer at the Idaho National Engineering Laboratory, Idaho. Water-Resources Investigations Report 91-4058, U.S. Geological Survey.
- Anderson, S. R. and B. D. Lewis, 1989. Stratigraphy of the Unsaturated Zone at the Radioactive Waste Management Complex, Idaho National Engineering Laboratory, Idaho. Water-Resources Investigations Report 89-4065, U.S. Geological Survey.
- Anderson, S.R., 1994, Hydrologist, U.S. Geological Survey, Written Communication dated December 21, 1994 to Richard Smith, Geologist, LITCO.
- Barracough, J.T., and R.G. Jensen, 1976. Hydrologic Data for the Idaho National Engineering Laboratory Site, Idaho 1971 to 1973. USGS Open File Report 75-318.
- Bureau of Reclamation, 1977, Ground Water Manual, A Water Resources Technical publication. United States Government Printing Office Washington. Stock No 024-003-00106-6
- Burgess, J. D., B.D. Higgs, and T.R. Wood, 1993. WAG 7 Groundwater Pathway Draft Track 2 Summary Report. EGG-ER-10731.
- Cooper, H. H. Jr., and C. E. Jacob, 1946, A Generalized Graphical Method for Evaluating Formation Constants and Summarizing Well-Field History, American Geophysical Union Transactions, Vol. 27.
- Dobrin M.B., 1976, Introduction to Geophysical Prospecting. McGraw-Hill, Inc. New York
- Driscoll, F.G., 1986, Groundwater and Wells. Johnson Division, St. Paul, MN.
- Duffield, G. M., and J. O. Rumbaugh, III, 1991, AQTESOLV Aquifer Test Solver Version 1.00 Documentation, Geraghty & Miller Modeling Group, Reston, VA.
- Greeley, R., 1982, The Style of Basaltic Volcanism in the Eastern Snake River Plain, Idaho, in Cenozoic Geology of Idaho, (Bonnichsen and R. M. Breckenridge, eds.). Idaho Bureau of Mines and Geology Bulletin 26.
- Hantush, M.S., 1964, Hydraulics of wells, In: V.T. Chow (editor), Advances in hydroscience, Vol. 1, pp. 281-432, Academic Press, New York and London.

- Hill, M. C., 1992, A Computer Program (MODFLOWP) for Estimating Parameters of a Transient, Three-Dimensional, Ground-Water Flow Model Using Nonlinear Regression, USGS Open-File Report 91-484.
- Kazemi, H., M.S. Seth, and G.W. Thomas, 1969. The Interpretation of Interference Test in Naturally Fractured Reservoirs with Uniform Fracture Distribution. Society of Petroleum Engineers Journal, pp. 463-472.
- Kaminsky, J.F., K.N. Keck, A.L. Schafer-Perini, C.F. Hersley, R.P. Smith, G.J. Stormberg, and A.H. Wylie, 1993. Remedial Investigation Final Report with Addenda for the Test Area North Groundwater Operable Unit 1-07B at the Idaho National Engineering Laboratory. EGG-ER-10643.
- Knutson, C.F., K.A. McCormic, R.P. Smith, W.R. Hackett, J.P. O'Brien, J.C. Crocker, 1989, RWMC Vadose Zone Basalt Characterization. EGG-WM-8949
- Kruseman, G.P., and N.A. de Ridder, 1991. Analysis and Evaluation of Pumping Test Data. Wageningen, The Netherlands.
- McDonald, M. G. and A. W. Harbaugh, 1988, A Modular Three-Dimensional Finite-Difference Ground-Water Flow Model, In: Techniques of Water-Resources Investigations of the United States Geologic Survey, Book 6, Chapter A1, Scientific Software Group, Washington, D. C.
- Moench, A.F., 1984. Double-porosity Model for a Fissured Groundwater Reservoir With Fracture Skin, Water Resources Research, v 20, n0. 7, pp 831-846.
- Mundorff, M. J., E. G. Crosthwaite, C. Kilburn, 1964. Groundwater for Irrigation in the Snake River Basin in Idaho. Water Supply Paper 1654, U.S. Geological Survey, Reston, Virginia, p. 224.
- Neuman, S.P., 1975. Analysis of Pumping Test Data From Anisotropic Unconfined Aquifers Considering Delayed Gravity Response. Water Resources Res., Vol. 11, pp. 329-342.
- Porro, I., J.M. Hubbell, J.B. Sission, C.W. Bishop, J.D. Burgess, E. Neher, and T.K. Honeycutt. 1994. Integrated Large-Scale Aquifer Pumping and Infiltration Test Vadose Zone Monitoring Test Plan. EGG-ER-11369.
- SAIC, 1990. Final Report on the preliminary assessment of the hydrogeology at the Subsurface Disposal Area, Radioactive Waste Management Complex, Idaho National Engineering Laboratory. SAIC-89/1421

Starr, R.C., and M.J. Rohe, 1994. Large Scale Aquifer Stress Test and Infiltration Test Water Management System Operation and Results. INEL-95/059

Theis, C. V., 1935, The Relation Between the Lowering of the Piezometric Surface and the Rate and Duration of Discharge of a Well using Ground-Water Storage, American Geophysical Union Transactions, Vol. 5.

Todd, D.K., 1959. Ground Water Hydrology, John Wiley and sons, Inc., New York.

Way, Shao-Chih and C.R. McKee, 1982. In-situ Determination of Three-Dimensional Aquifer Permeabilities. Ground Water, v. 20, no. 5, pp. 594-603.

Whitehead, R.L., 1992, Geohydrologic Framework of the Snake River Plain Regional Aquifer system, Idaho and Eastern Oregon, U.S. Geological survey Professional Paper 1408-B.

Wood, T. R., and A. H. Wylie, 1991. Ground Water Characterization Plan for the Subsurface Disposal Area, Idaho National Engineering Laboratory. EGG-WM-9668.

Wylie, A.H., 1994a. Field Scale Aquifer Stress Test Data Collection Plan for Operable Uint 7-6. EGG-ER-11251

Wylie, A.H., 1994b. Interoffice Correspondence to K.J. Dooley, Step Test at RWMC Test Well. AHW-09-94.

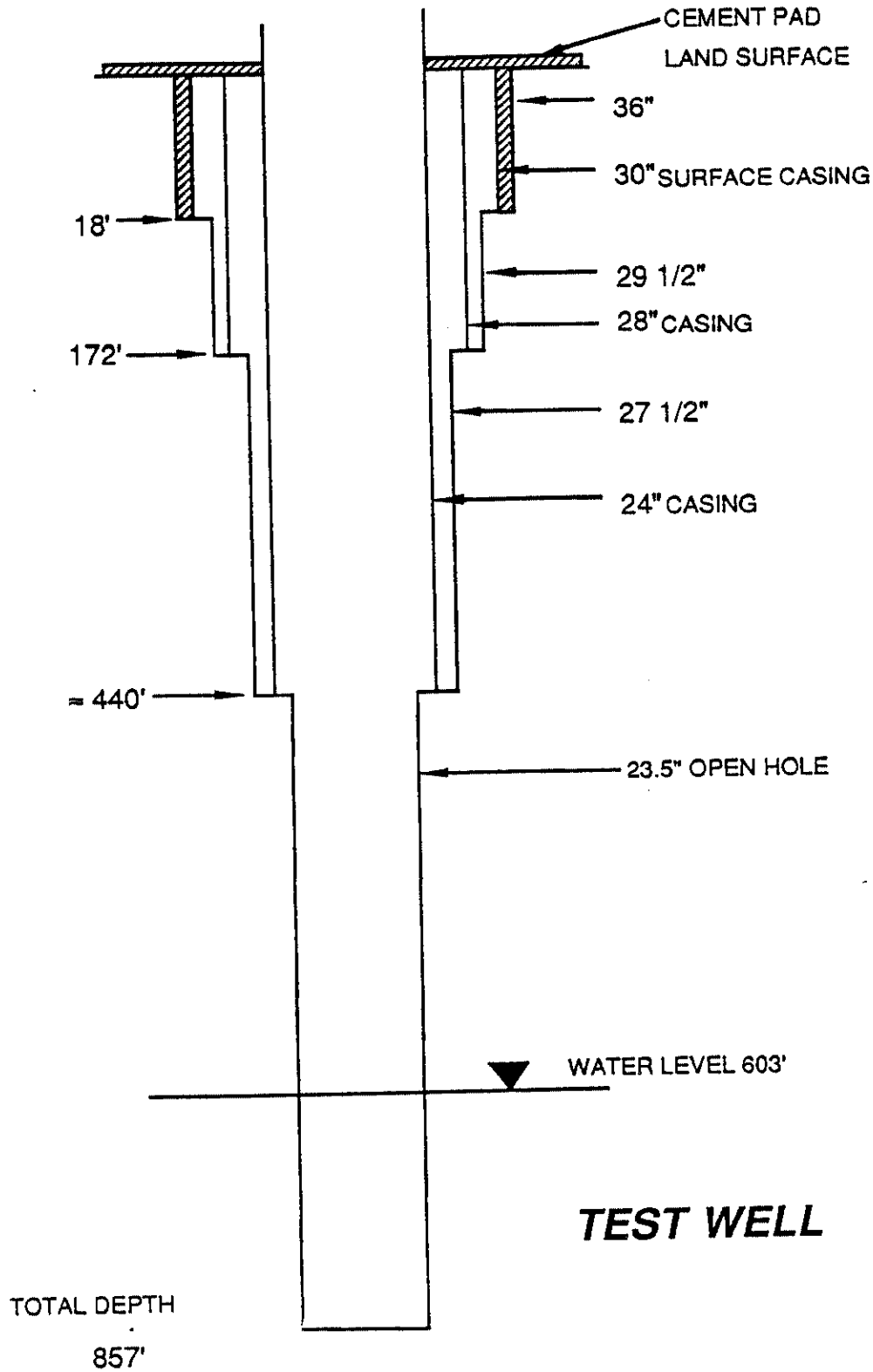
Wylie, A.H., 1993, TAN RI Aquifer Testing Results. ER-WAG1-25.

Wylie, A.H., and J.M. Hubbell, 1994. Aquifer Testing of Wells M1S, M3S, M4D, M6S, M7S, and M10S at the Radioactive Waste Management Complex. ER-WAG7-26.

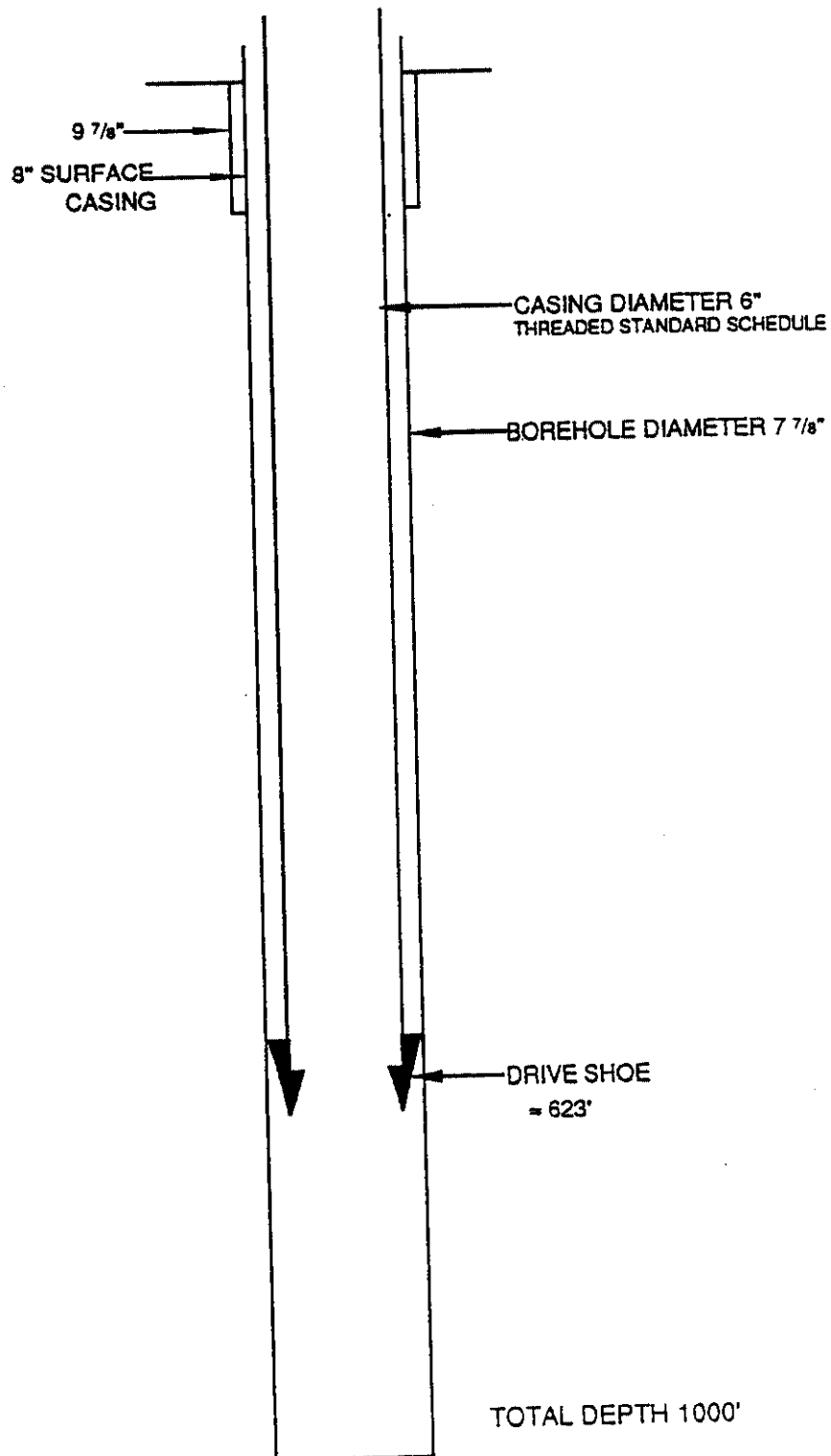
Wylie, A.H., T.R. Wood, and G.T. Norrell, 1994. Conceptual Design of the field Scale Aquifer Stress Test. ER-WAG7-48.

Appendix A

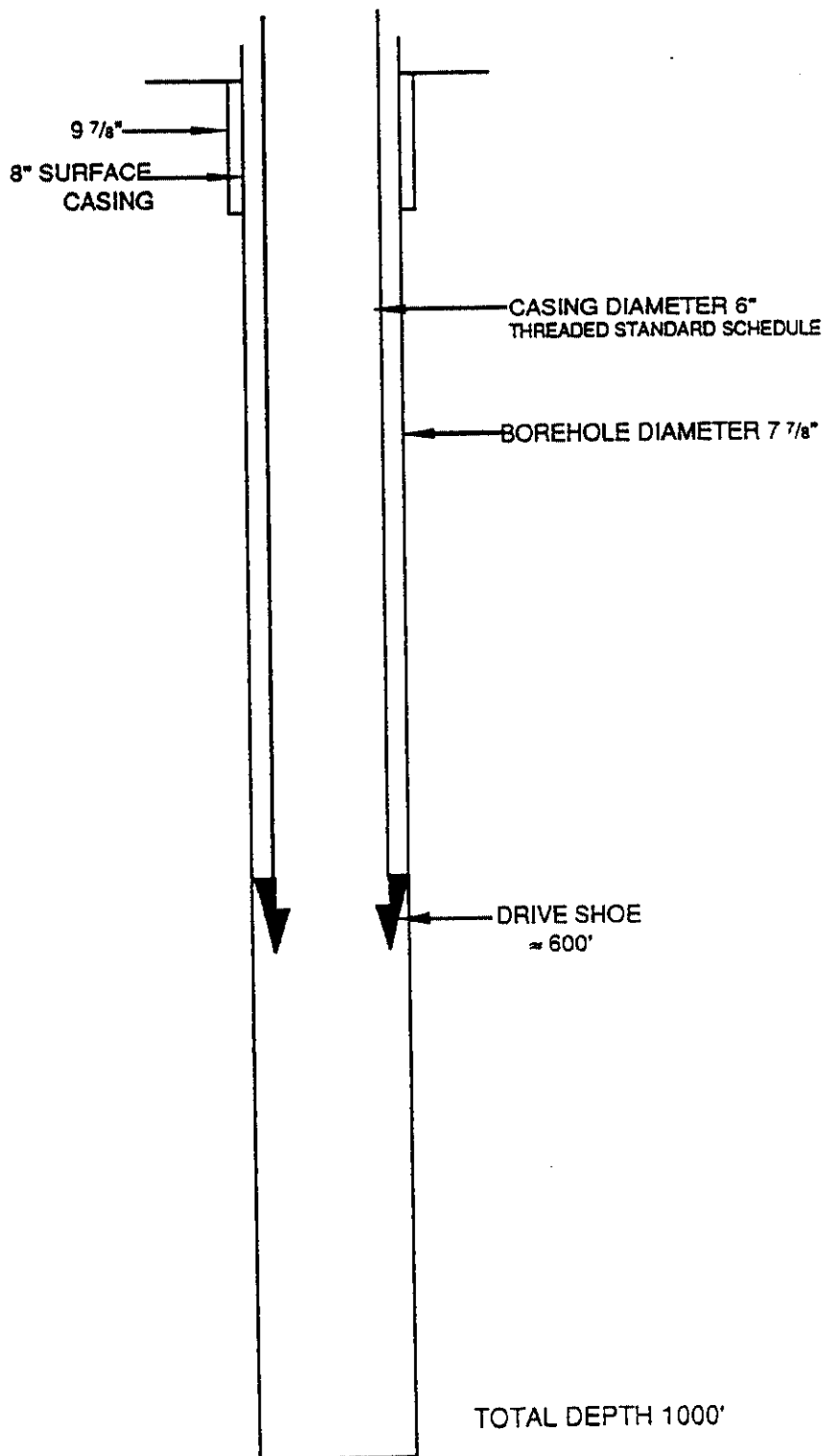
Well Construction Diagrams for OW1, OW2, and Test Well



OW-1



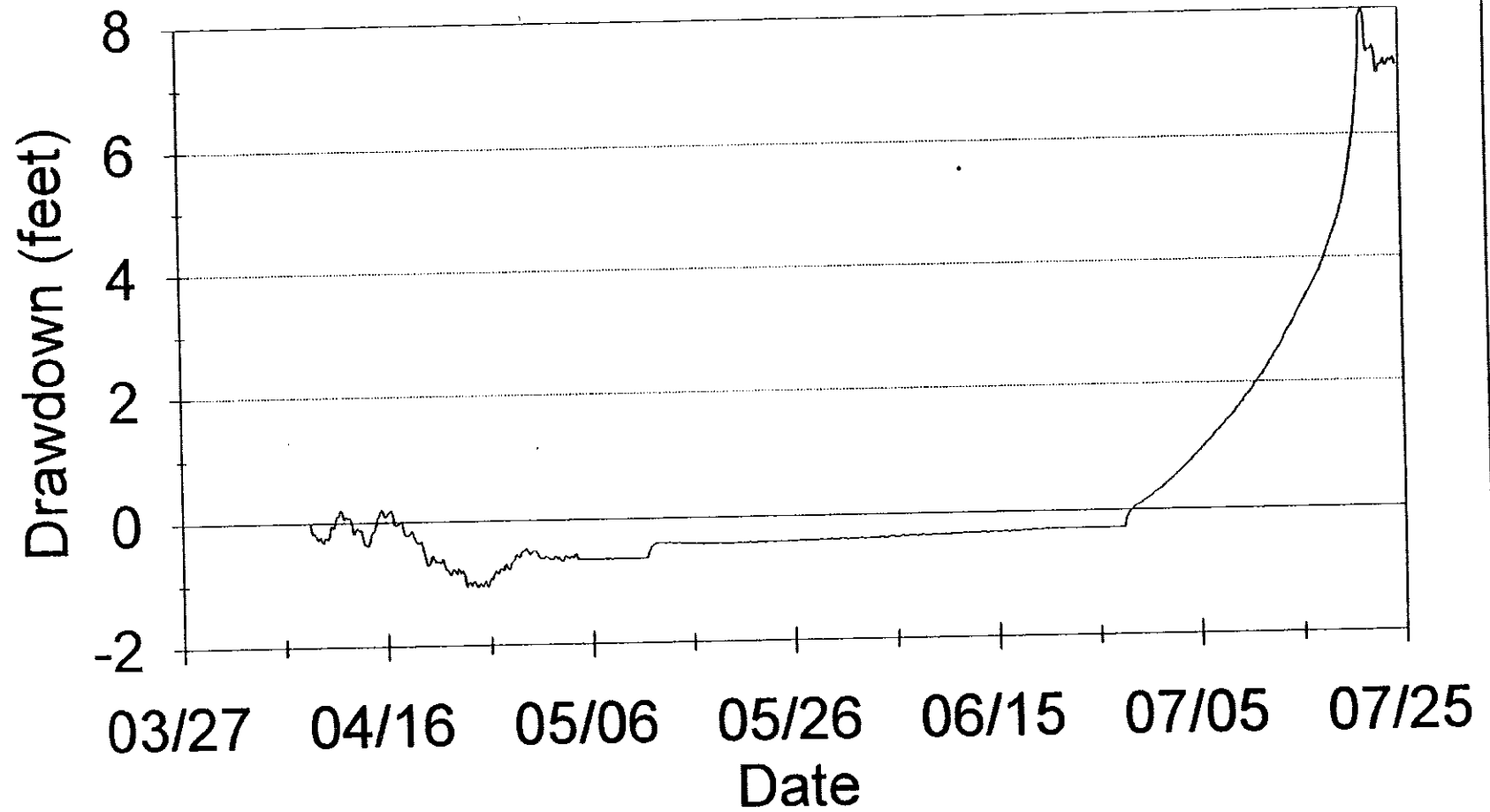
OW-2



Appendix B

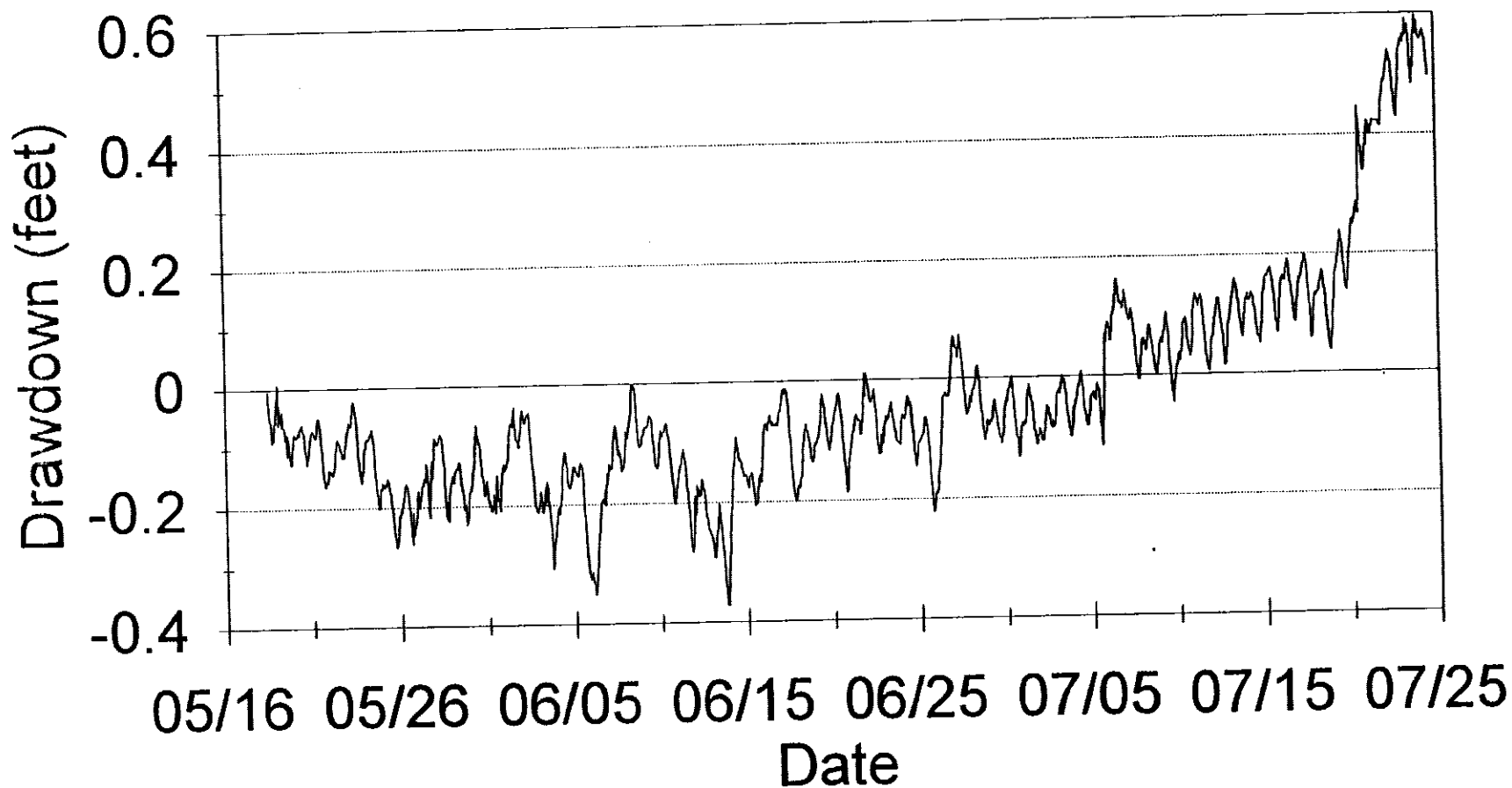
Hydrographs

M4D Pre-Test Trend Data



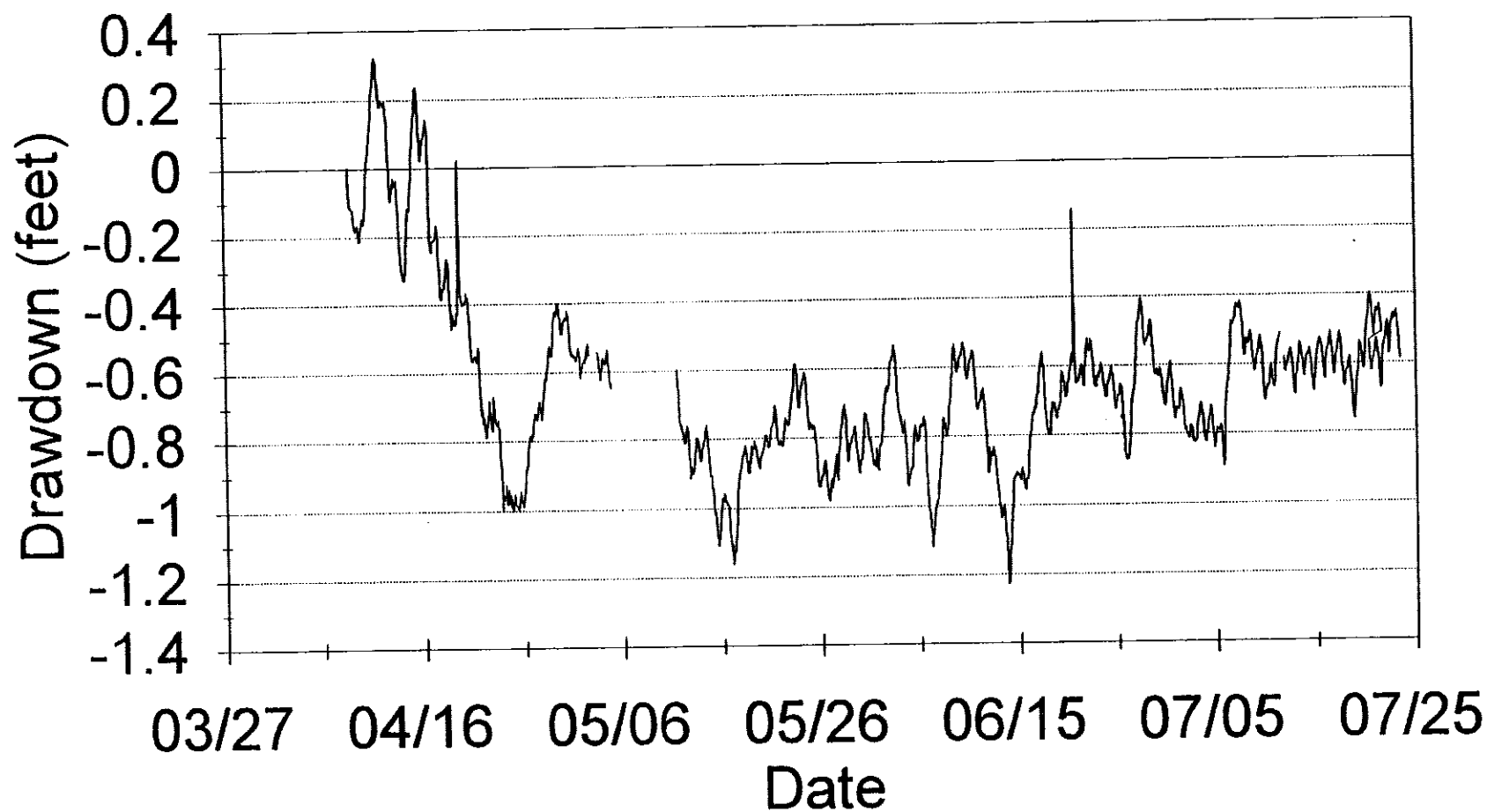
USGS 9

Pre-Test Trend Data



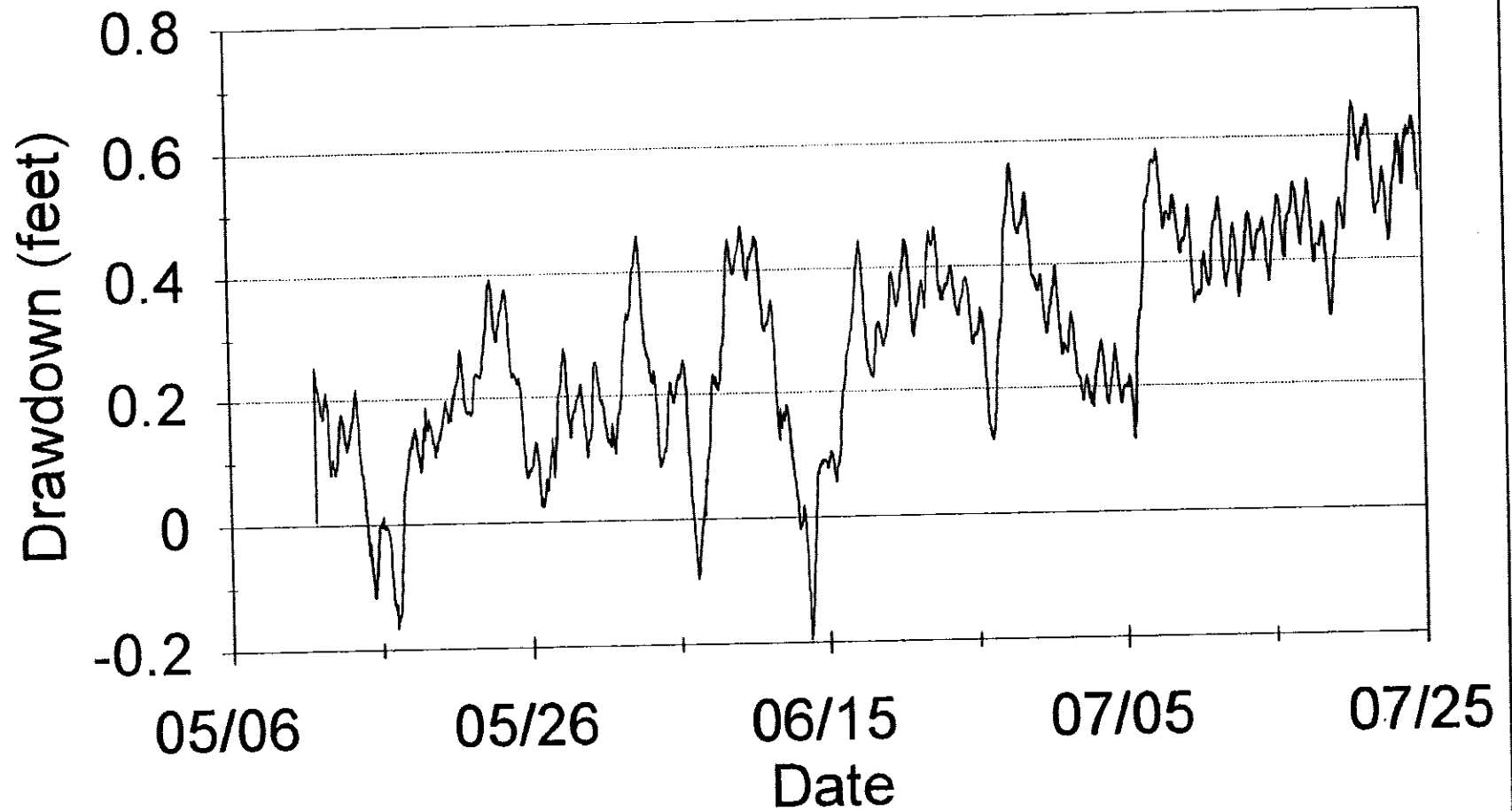
USGS 88

Pre-Test Trend Data



USGS 118

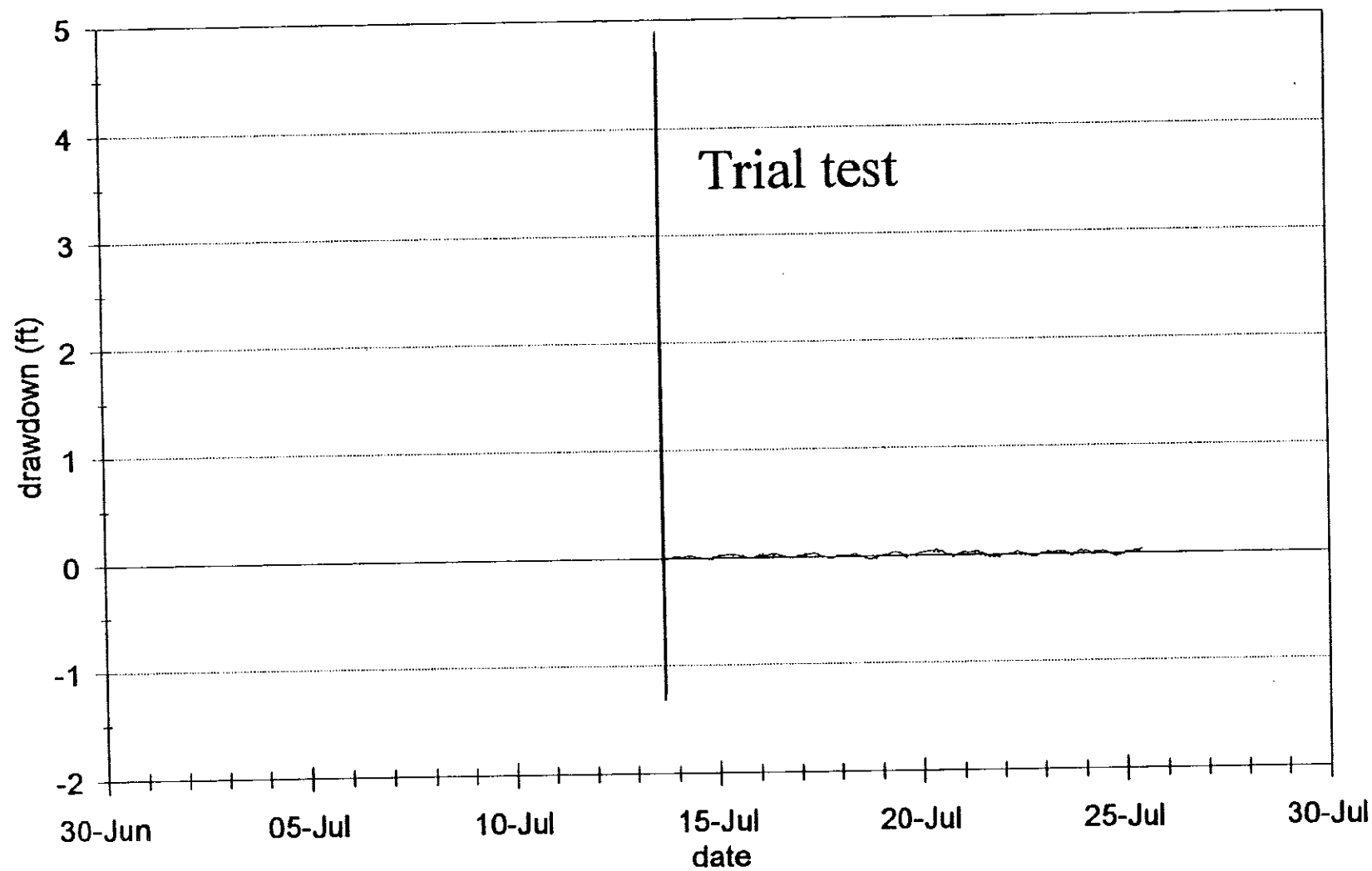
Pre-Test Trend Data



Test Well

pretest

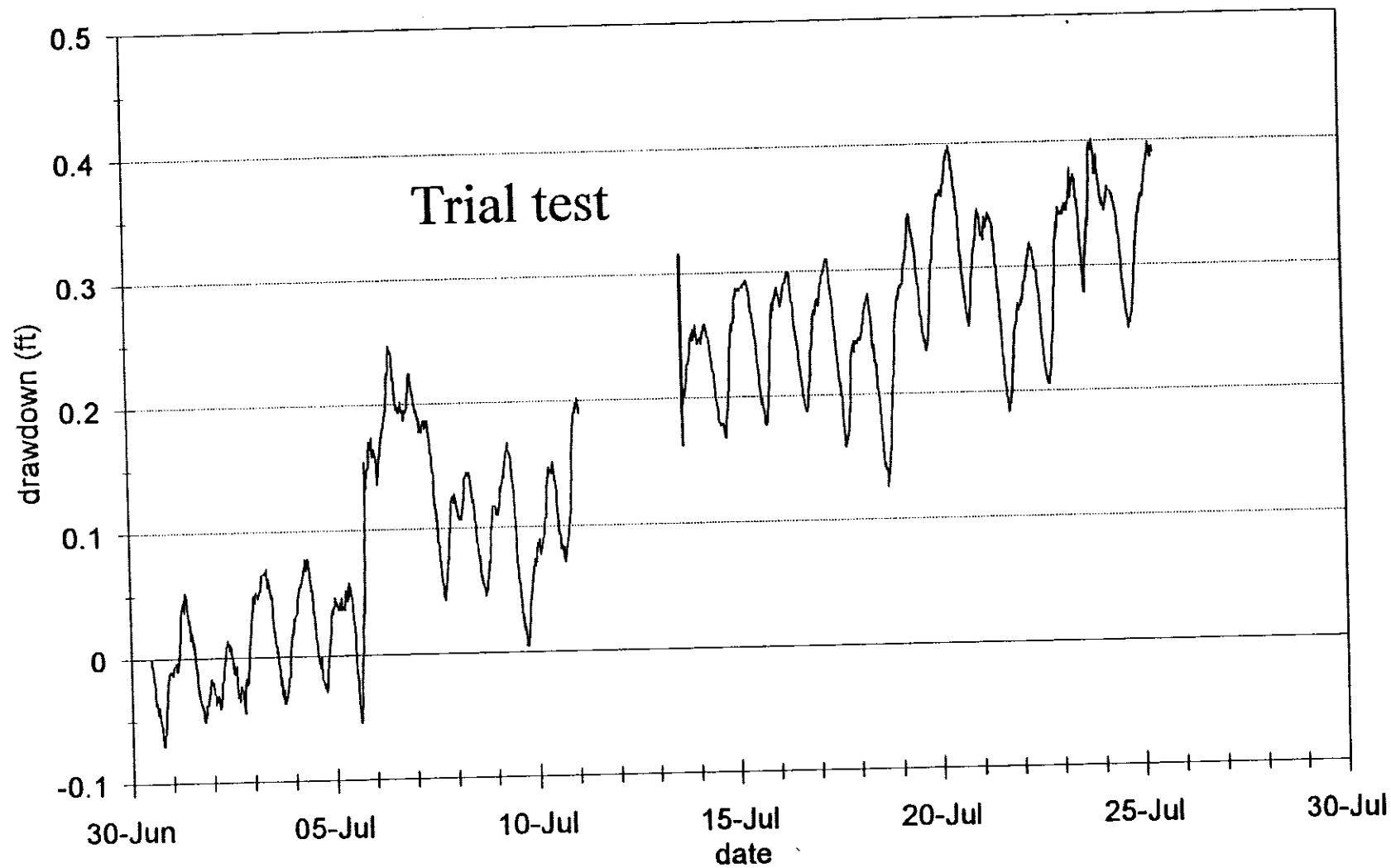
EG&G Idaho, Inc.
FORM EGG-2631#
(Rev. 01-92)



120

pretest

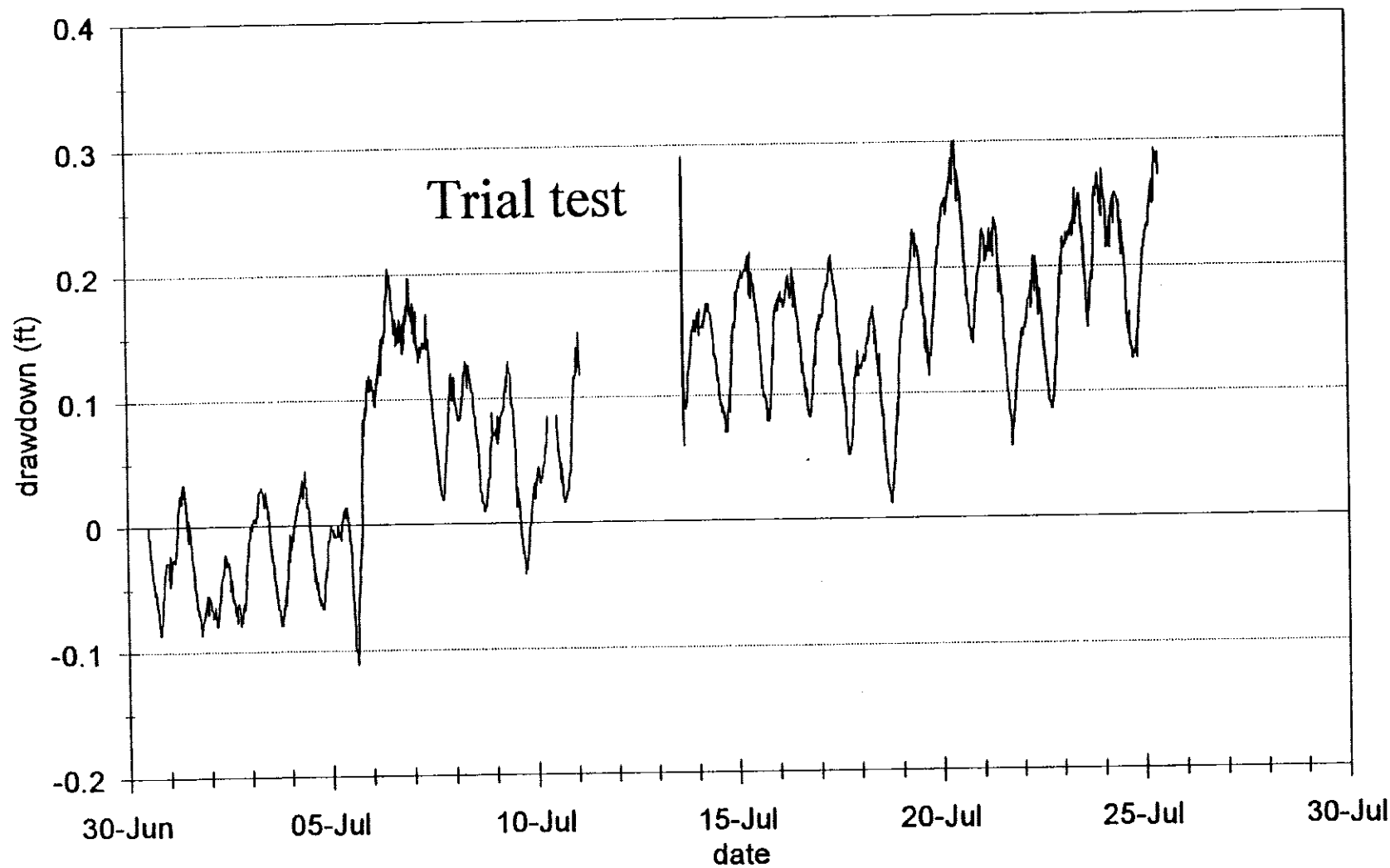
EG&G Idaho, Inc.
FORM EGG-2631#
(Rev. 01-92)



OW1 upper

pretest

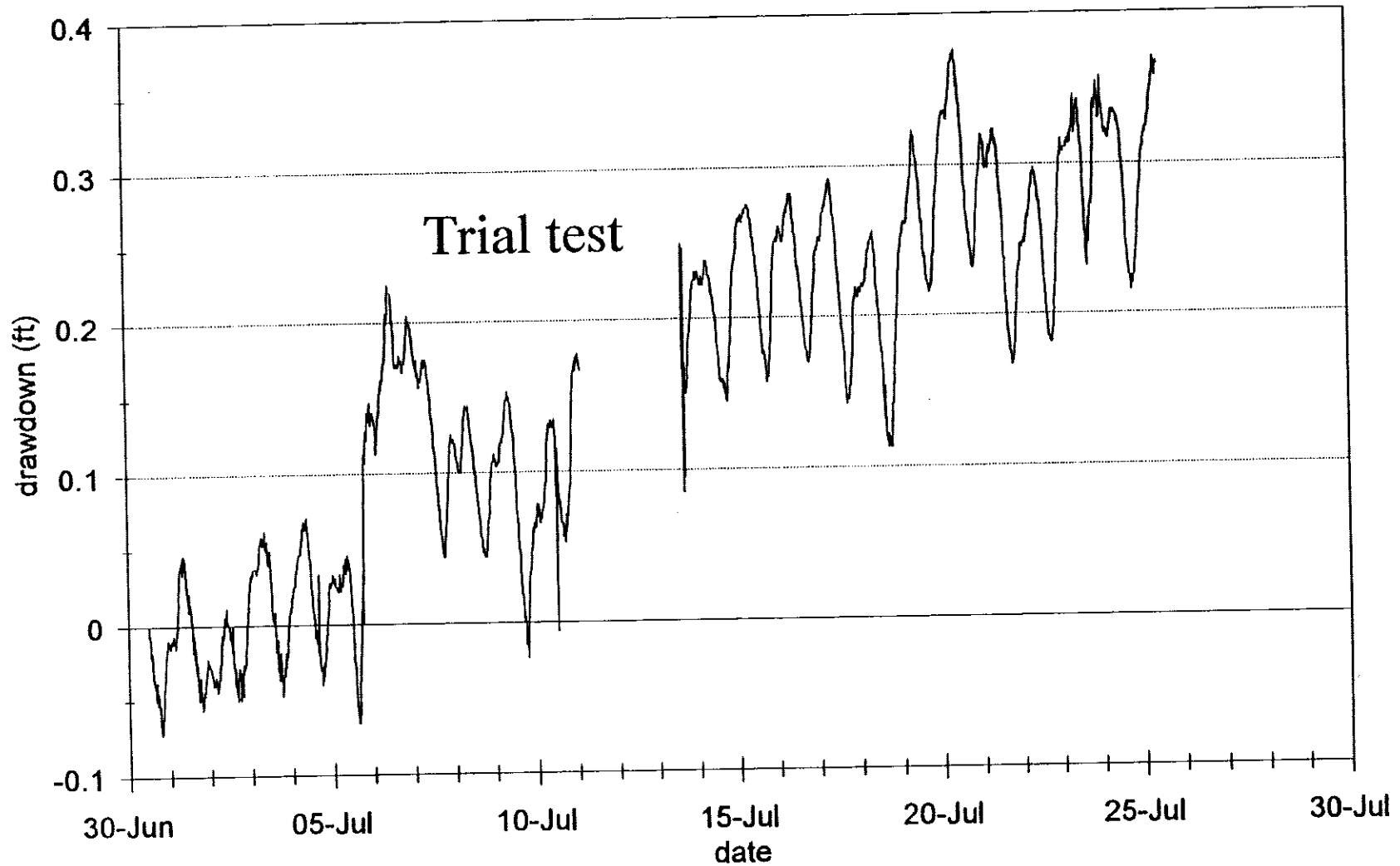
EG&G Idaho, Inc.
FORM EGG-2631#
(Rev. 01-92)



OW1 lower

pretest

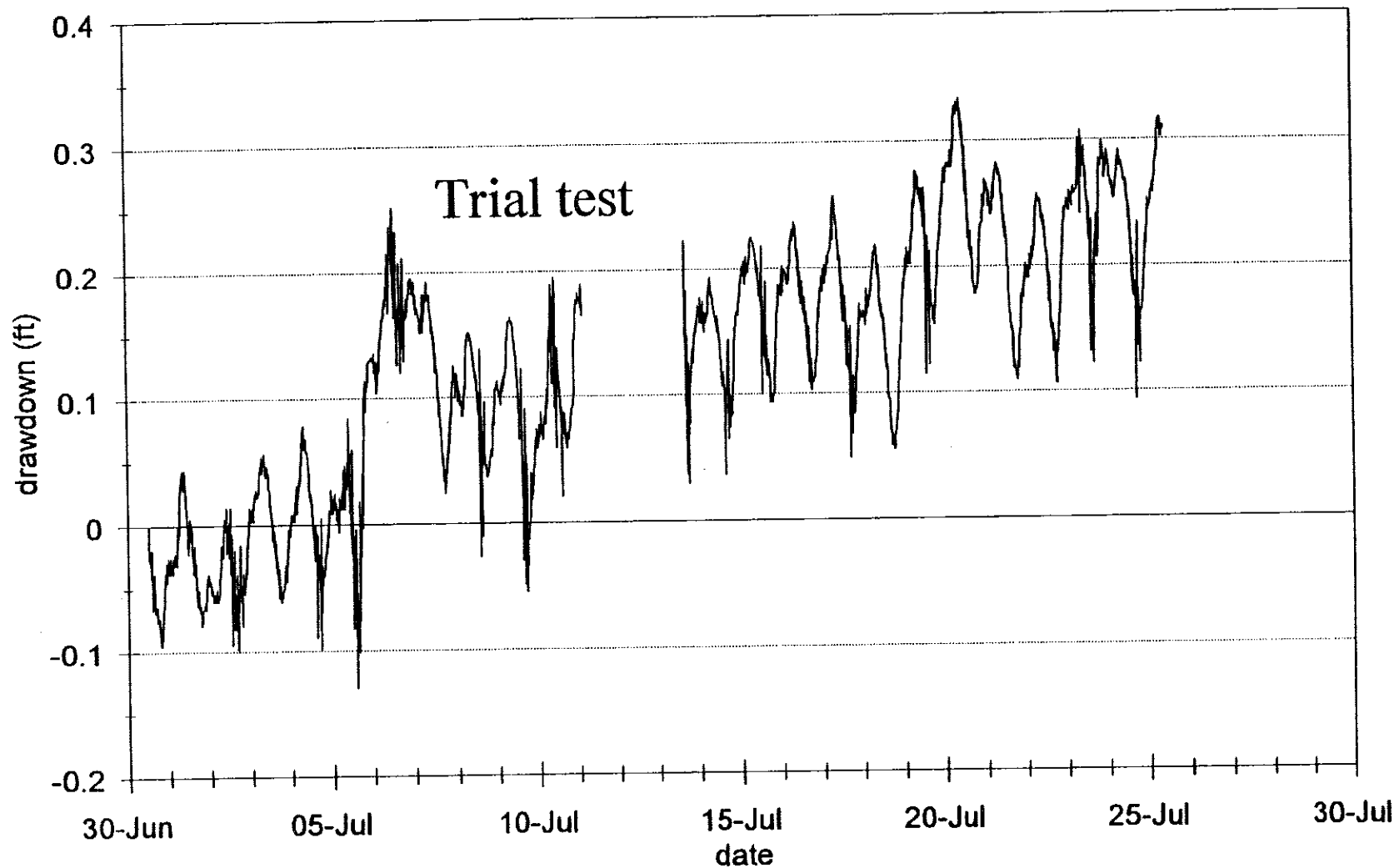
EG&G Idaho, Inc.
FORM EGG-2631#
(Rev. 01-92)



OW2 upper

pretest

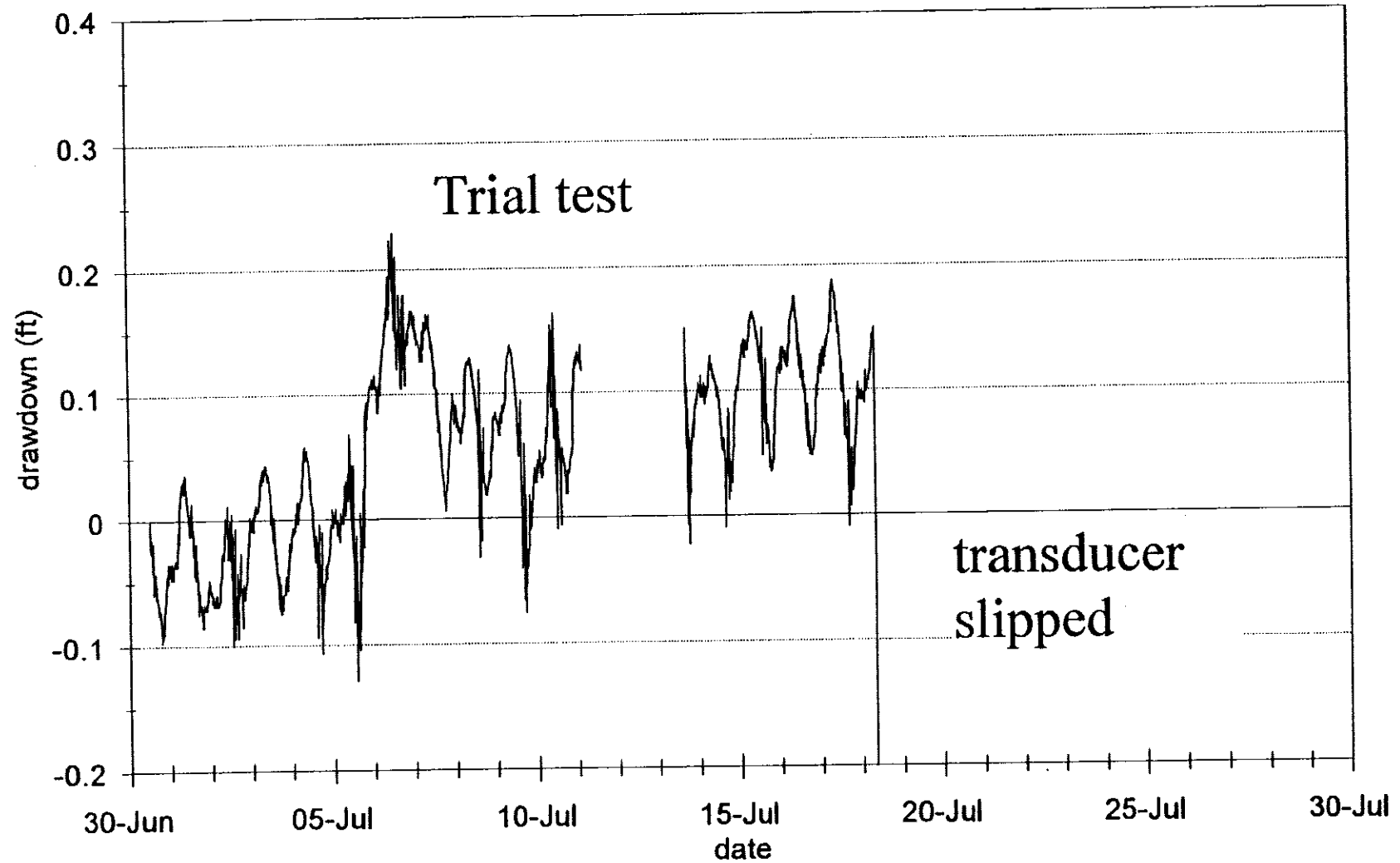
EG&G Idaho, Inc.
FORM EGG-2631 #
(Rev. 01-92)



OW2 lower

pretest

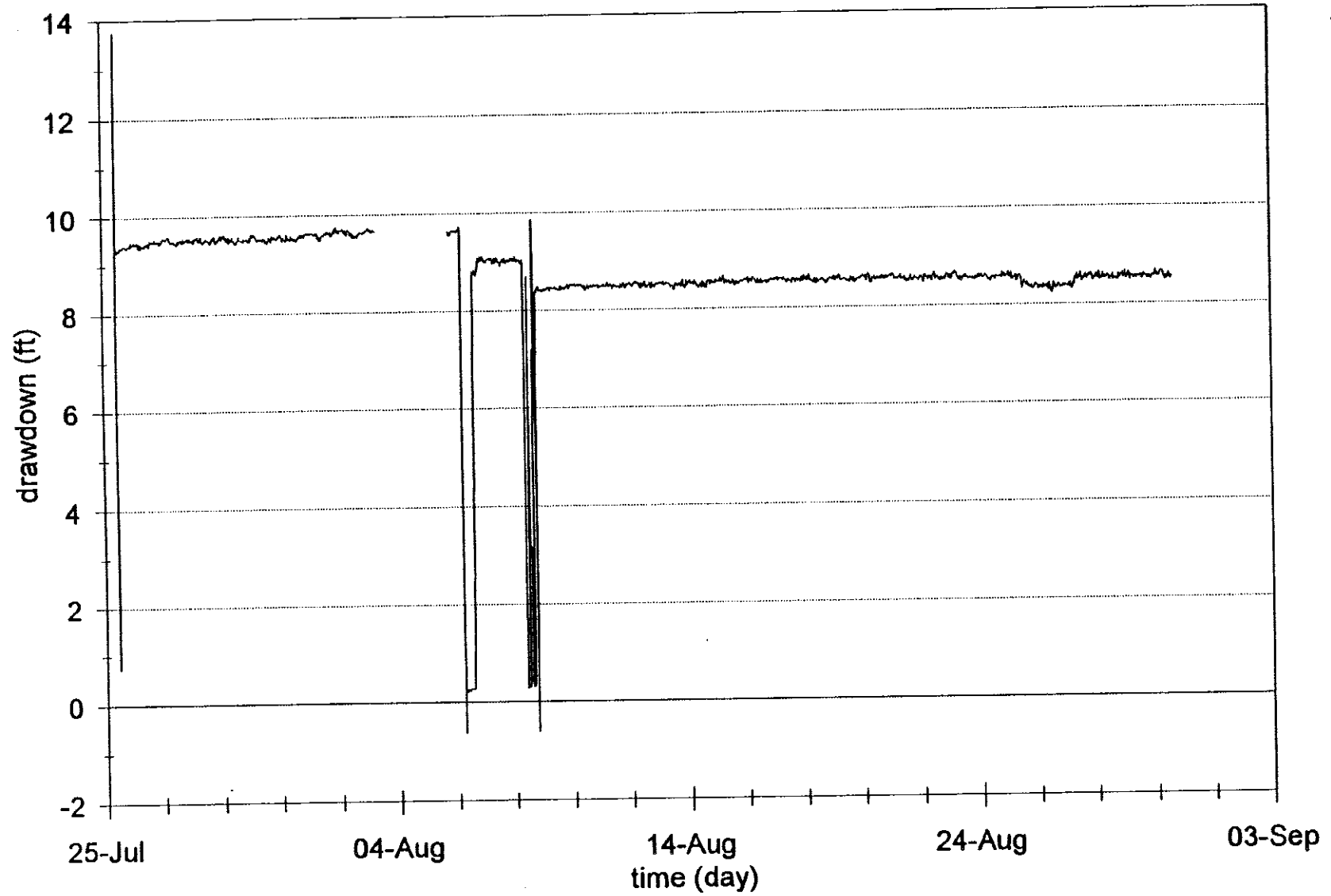
EG&G Idaho, Inc.
FORM EGG-2651#
(Rev. 01-92)



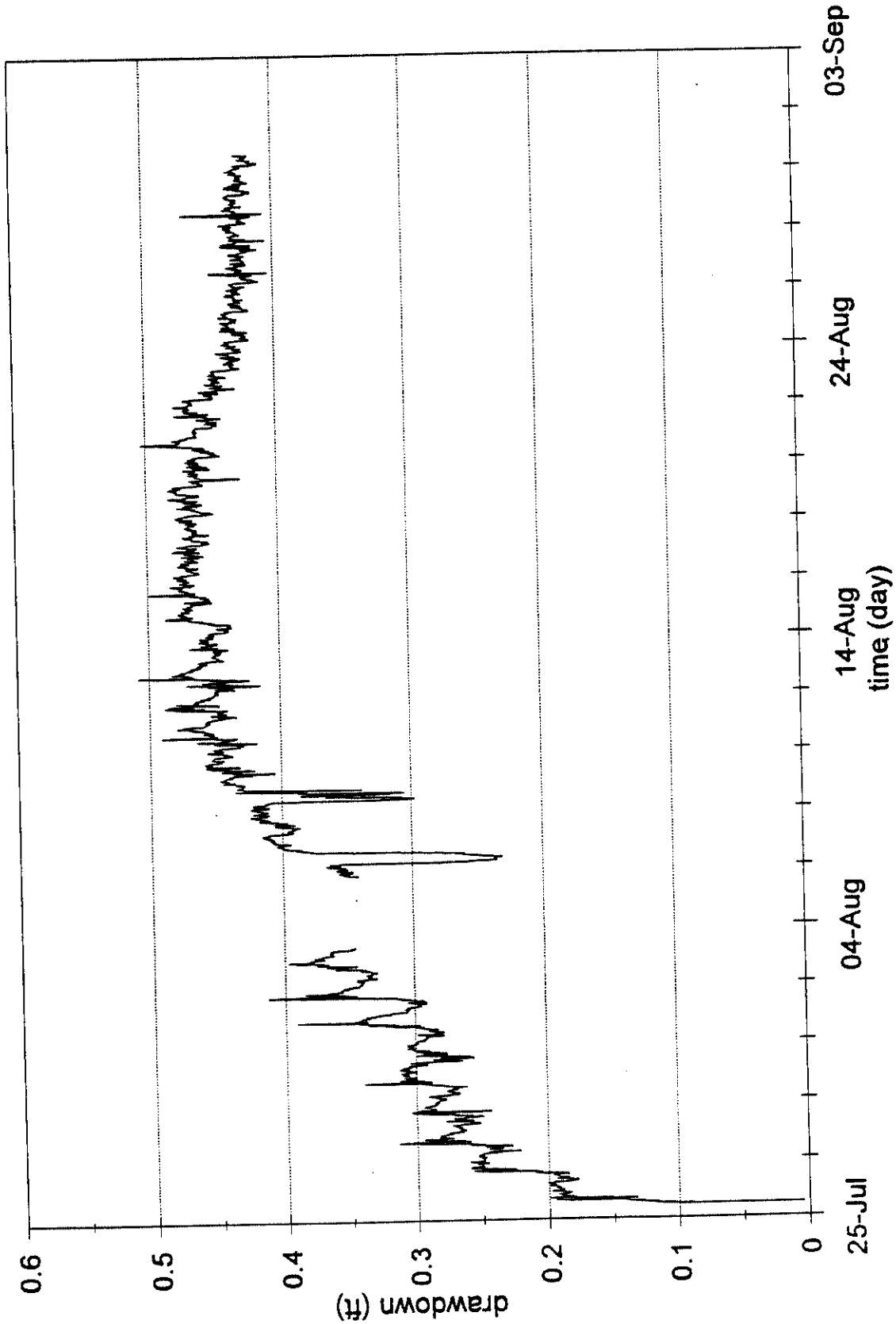
Test Well

filtered

EG&G Idaho, Inc.
FORM EG-2631#
(Rev. 01-92)

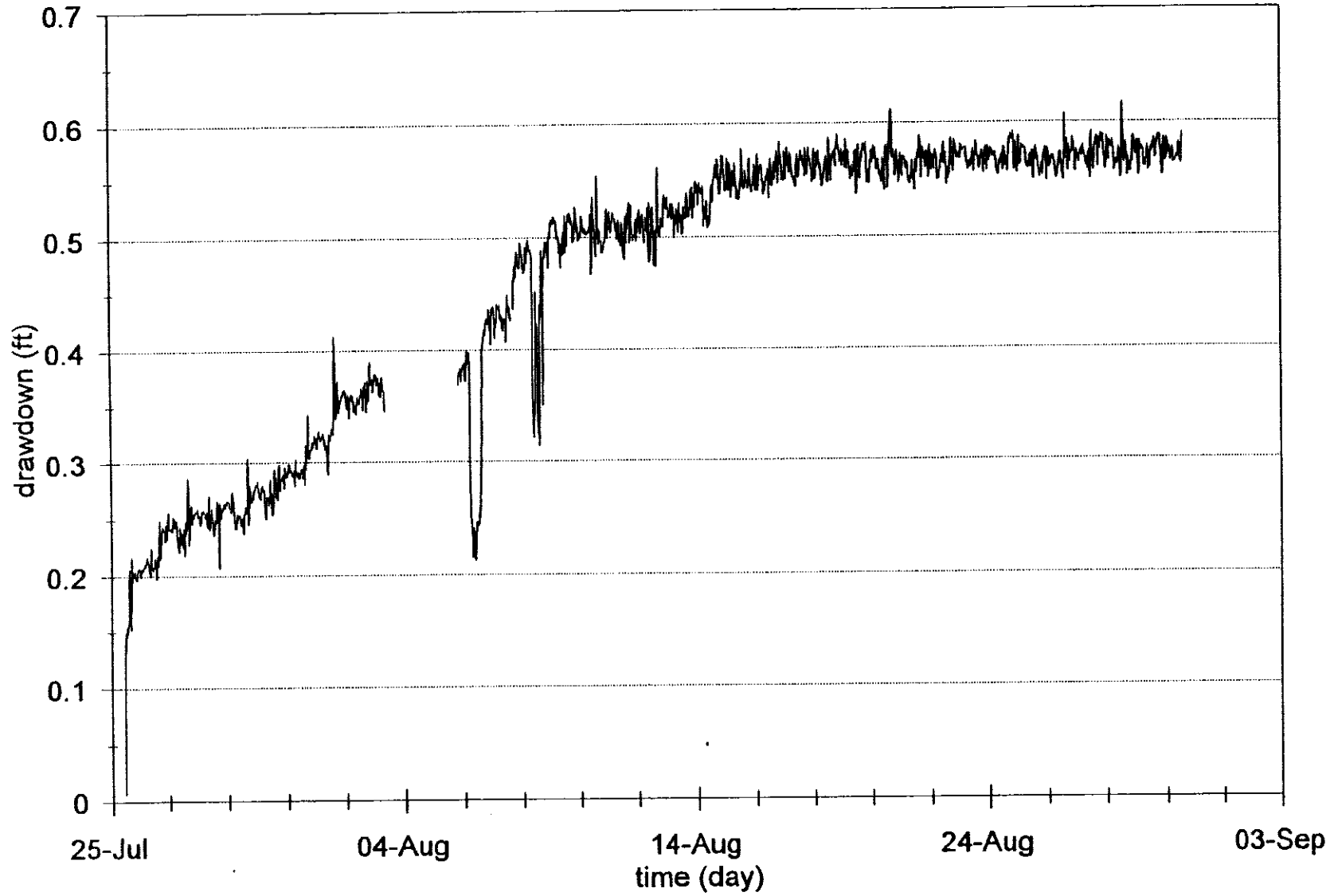


120
filtered



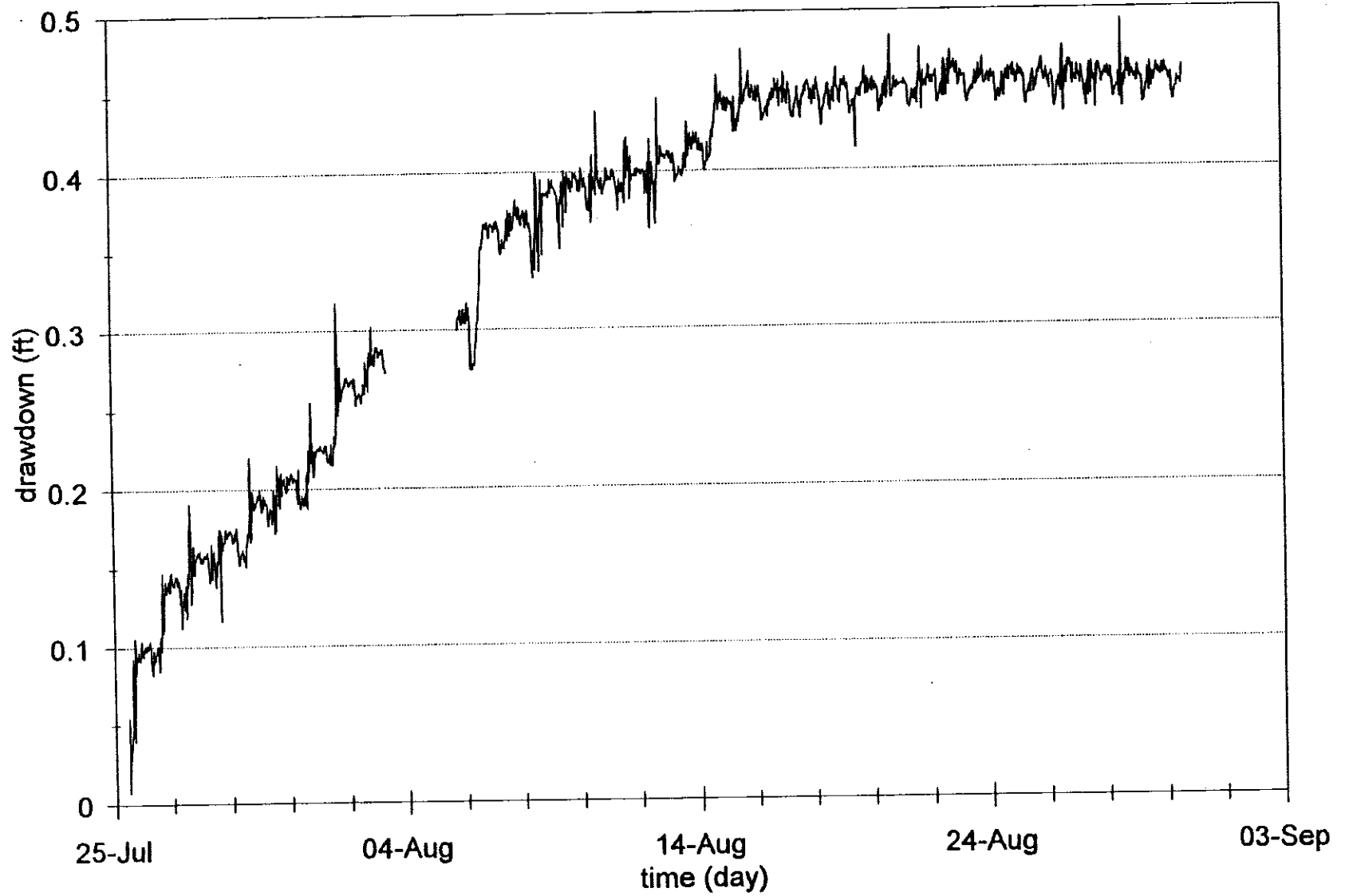
OW1 upper filtered

EG&G Idaho, Inc.
FORM EGG-2631#
(Rev. 01-92)



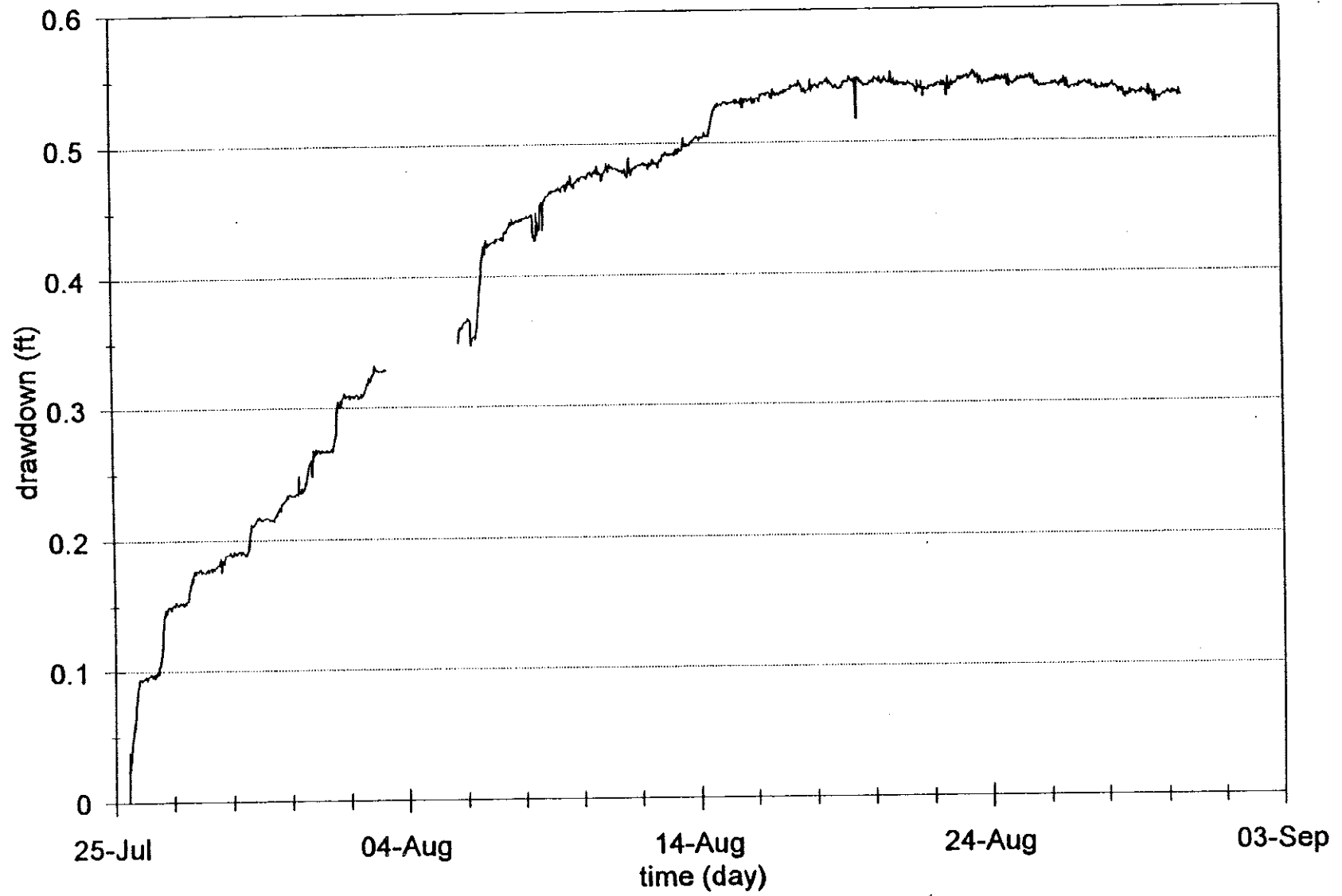
OW1 lower

filtered



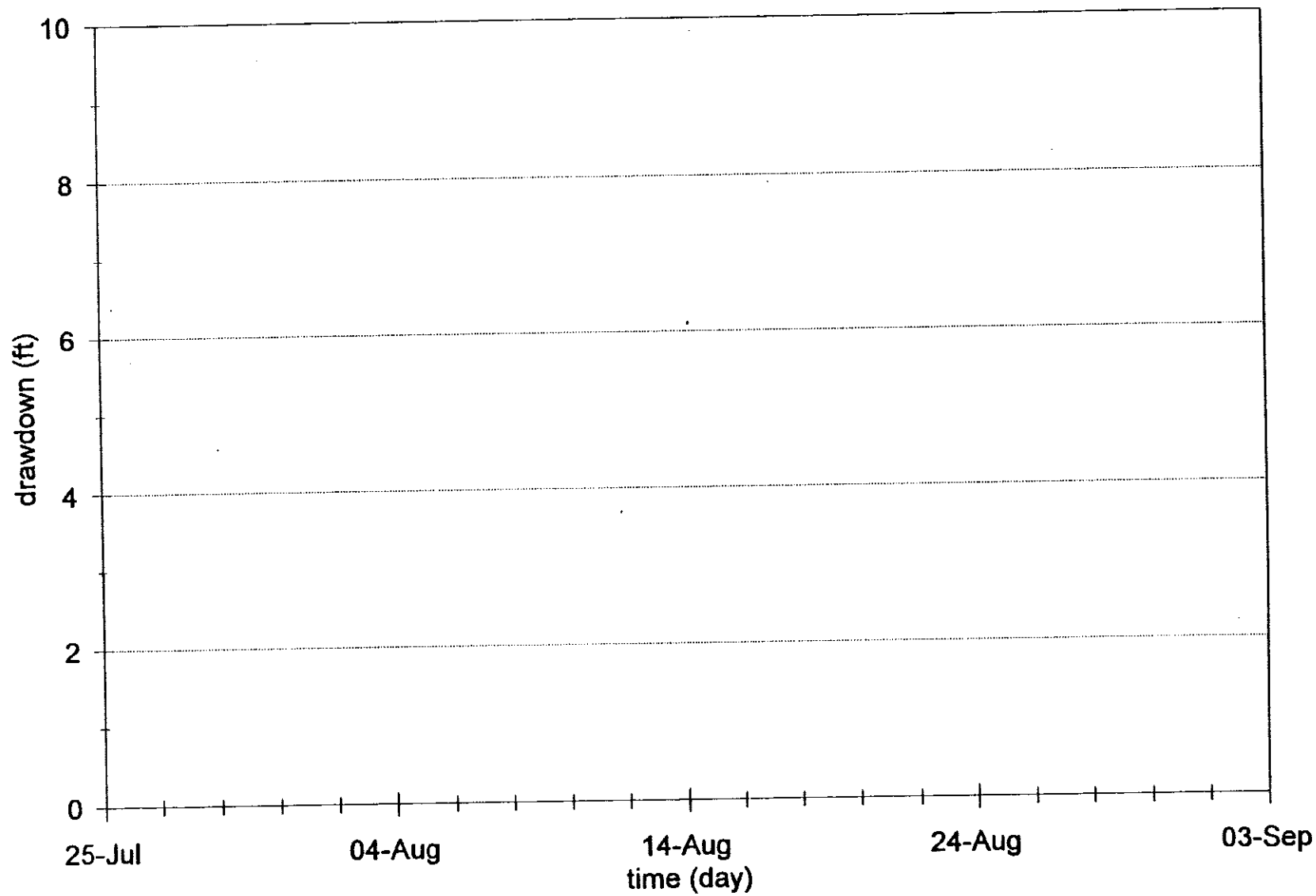
OW2 upper filtered

EG&G Idaho, Inc.
FORM EG&G-2631#
(Rev. 01-92)



OW2 lower

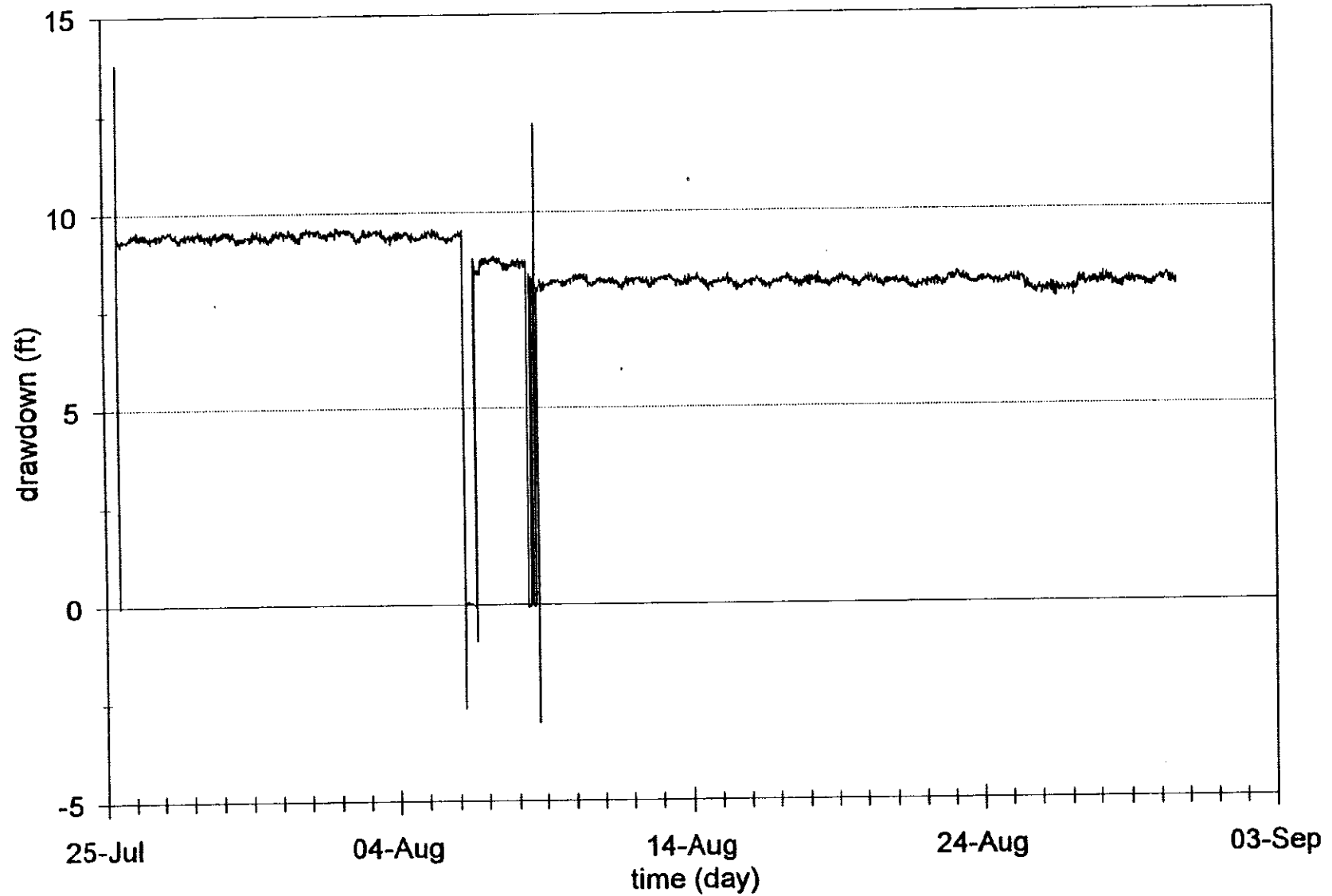
filtered



Test Well

raw data

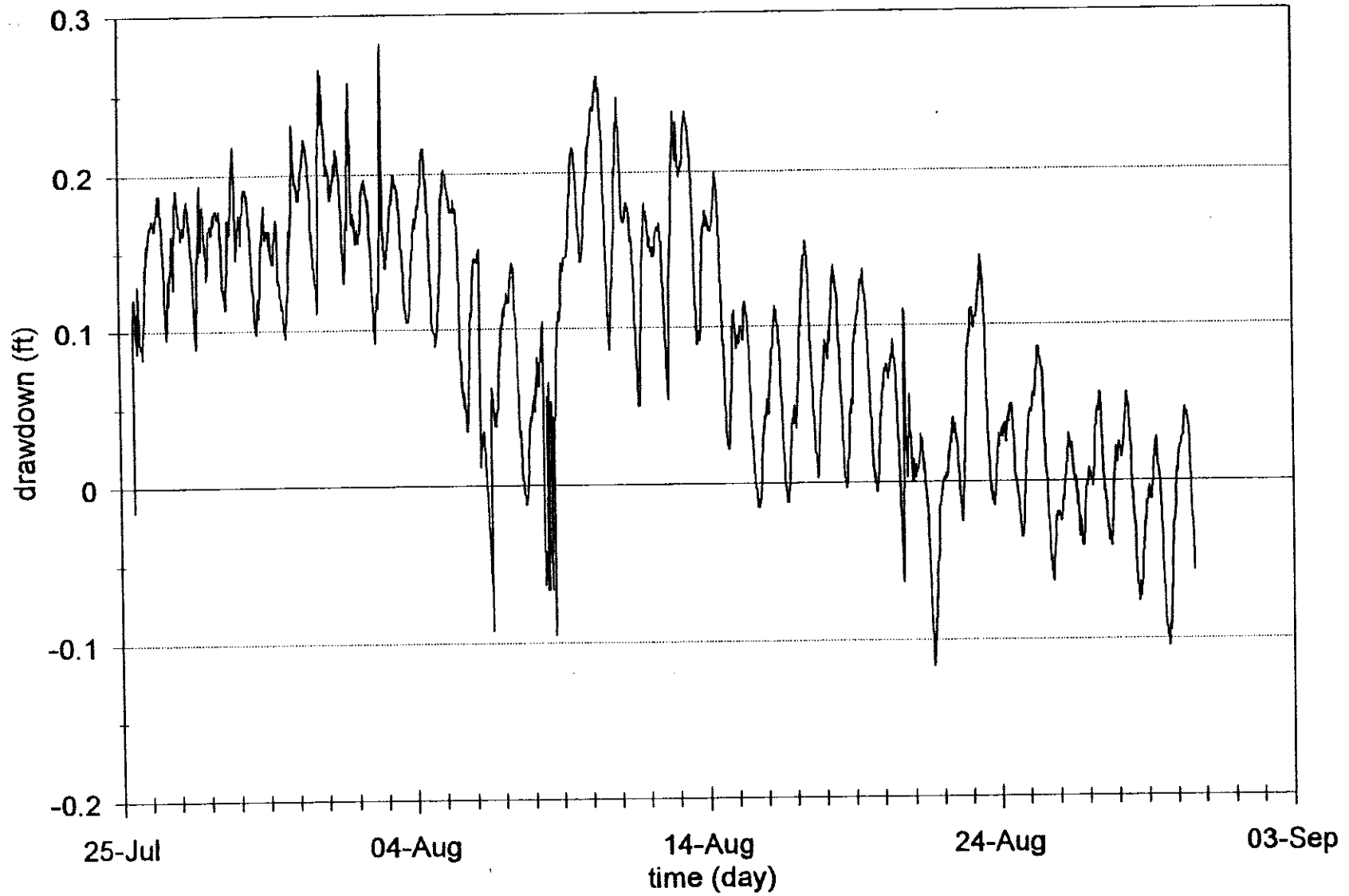
EG&G Idaho, Inc.
FORM EG&G-2631#
(Rev. 01-92)



120

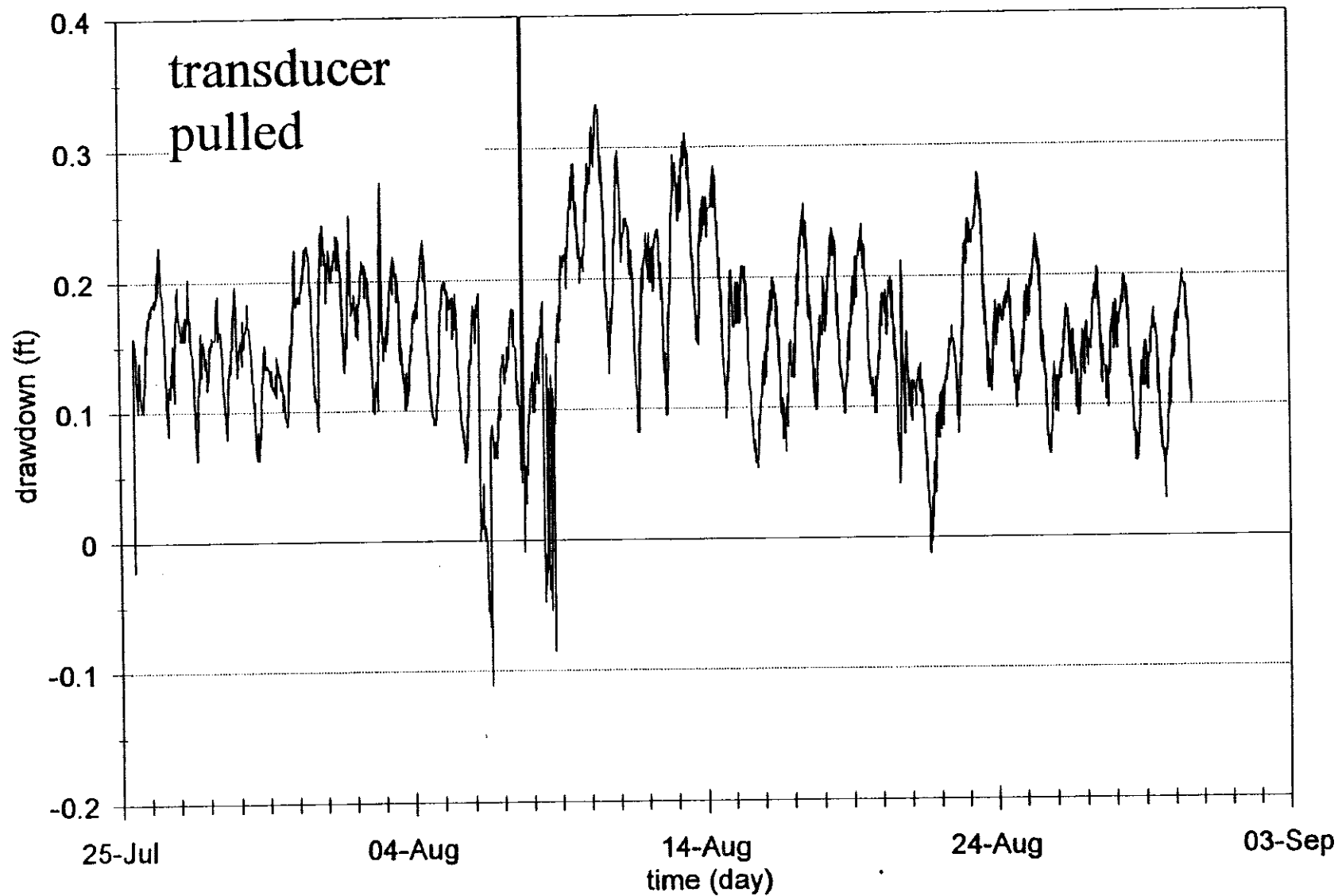
raw data

EG&G Idaho, Inc.
FORM EGG-2631#
(Rev. 01-92)



OW1 upper

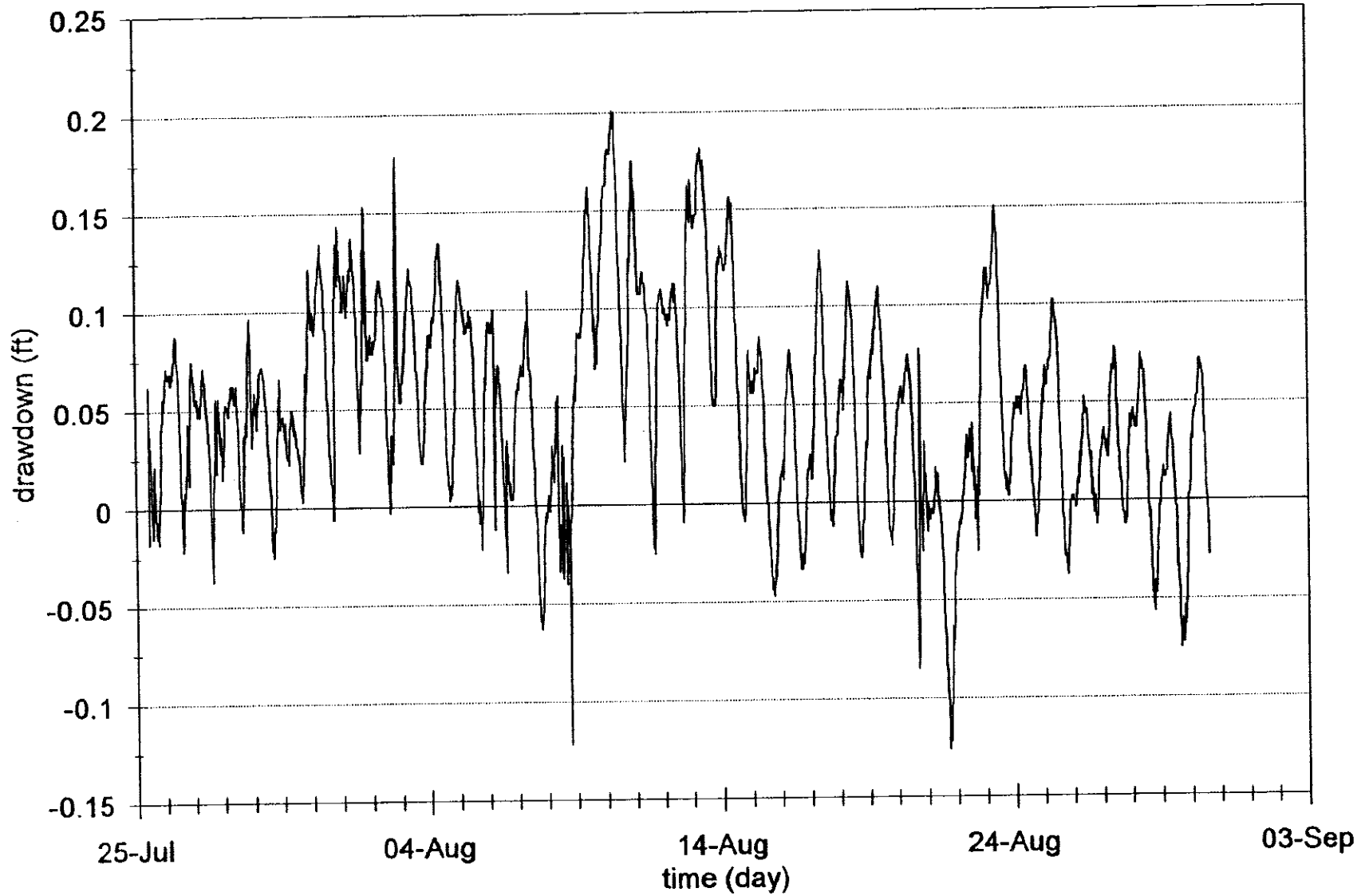
raw data



OW1 lower

raw data

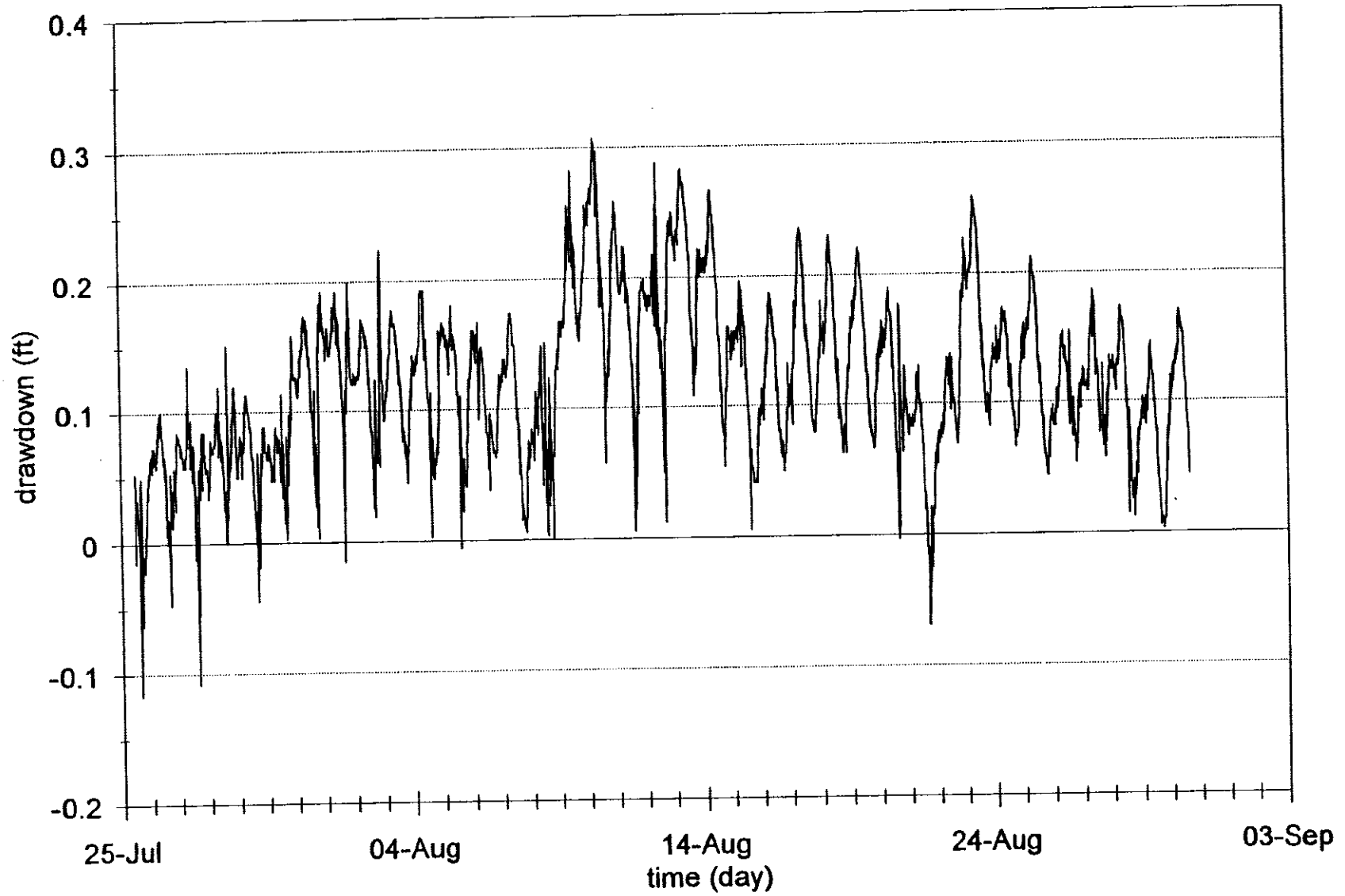
EG&G Idaho, Inc.
FORM EGG-2631#
(Rev. 01-92)



OW2 upper

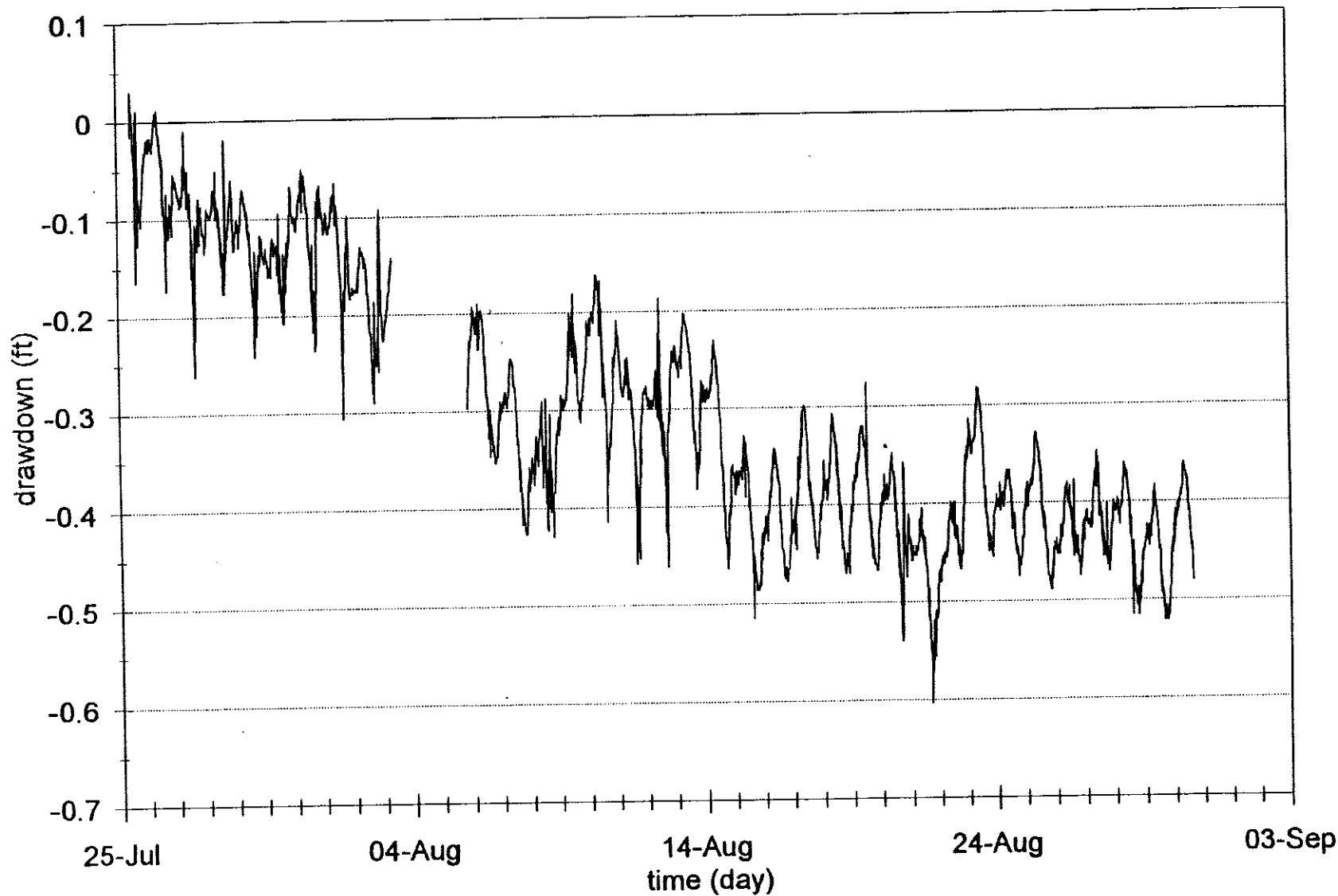
raw data

EG&G Idaho, Inc.
FORM EGG-2631#
(Rev. 01-92)



OW2 lower

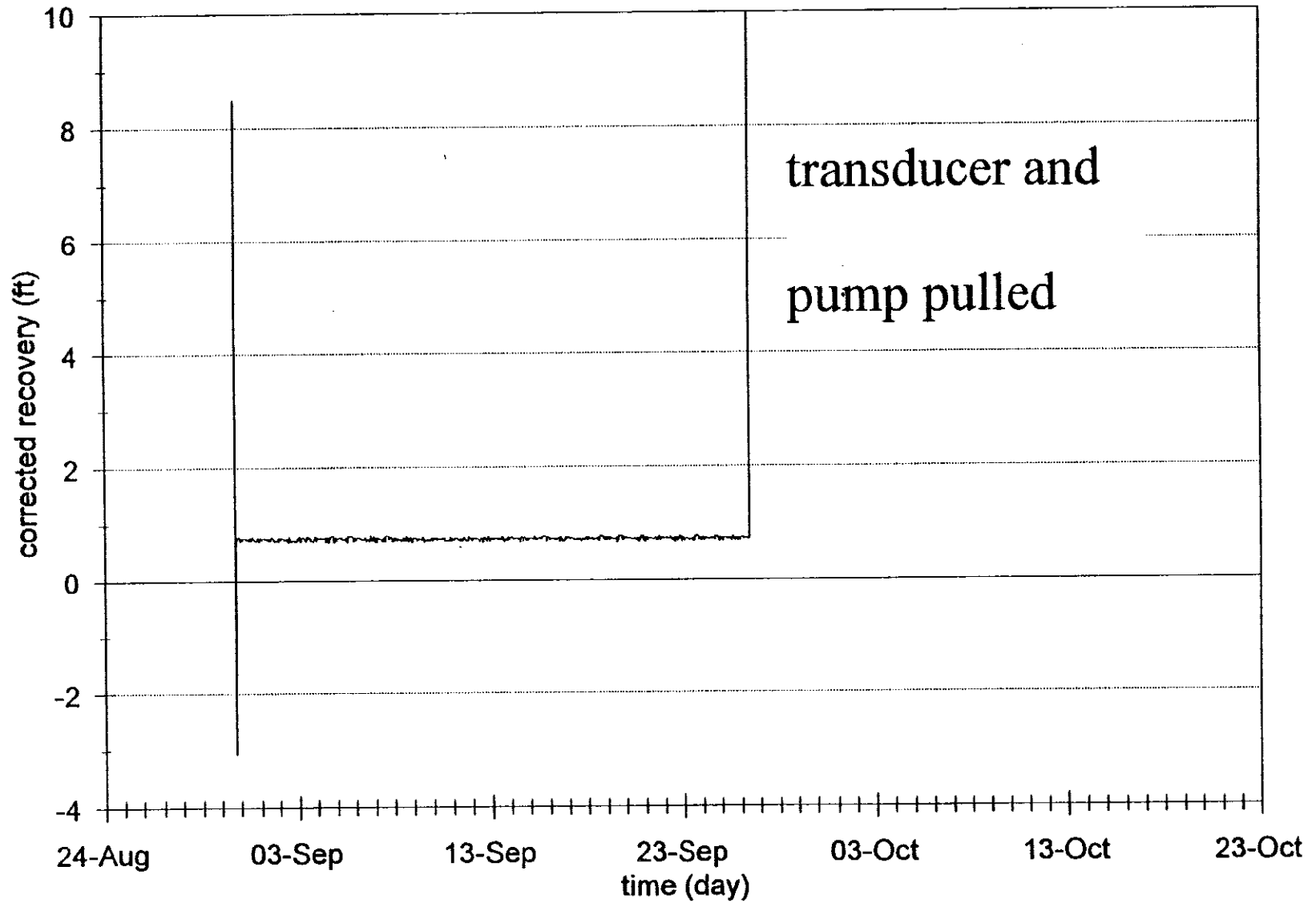
raw data



Test Well

filtered data

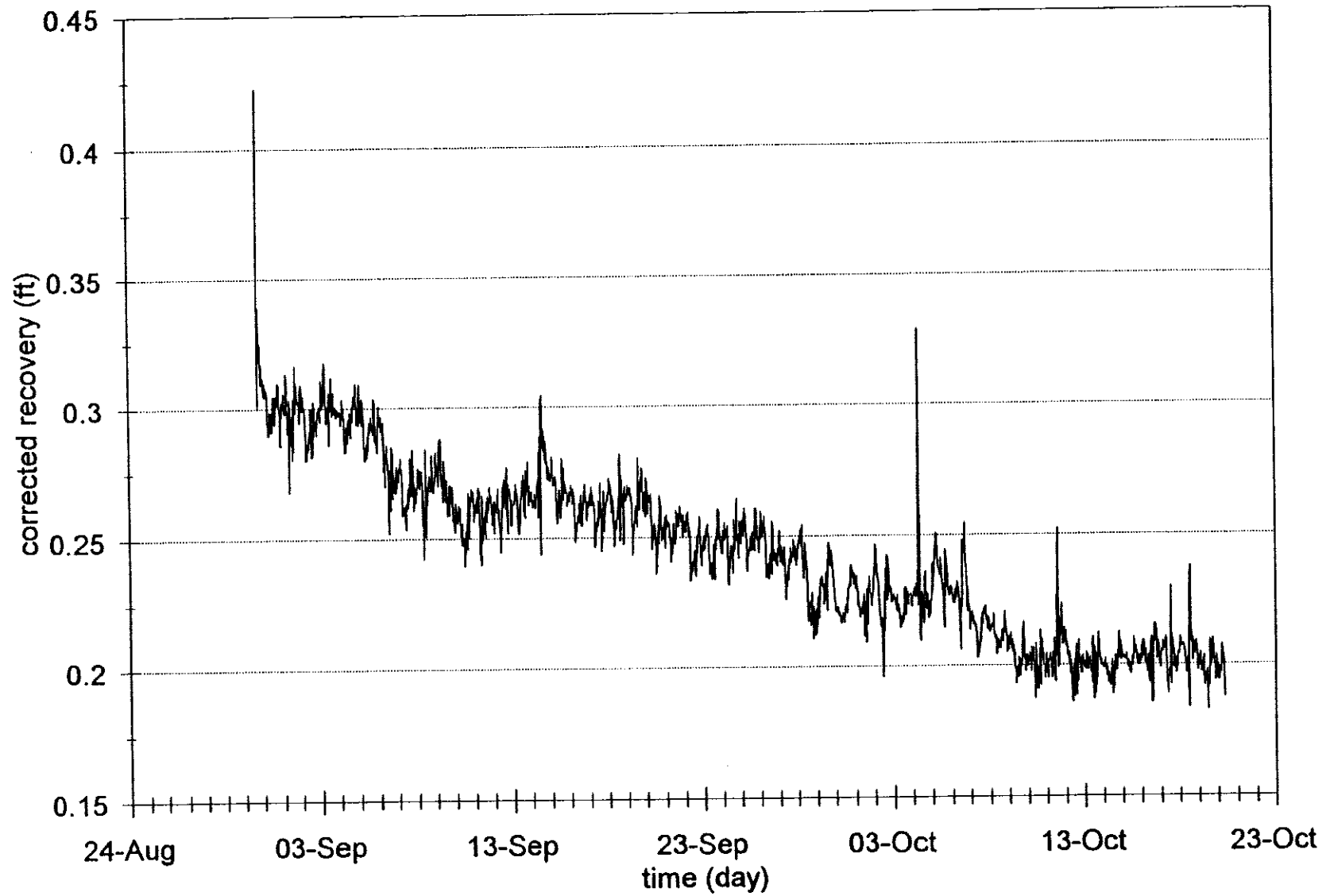
EG&G Idaho, Inc.
FORM EGG-2631#
(Rev. 01-92)



120

filtered data

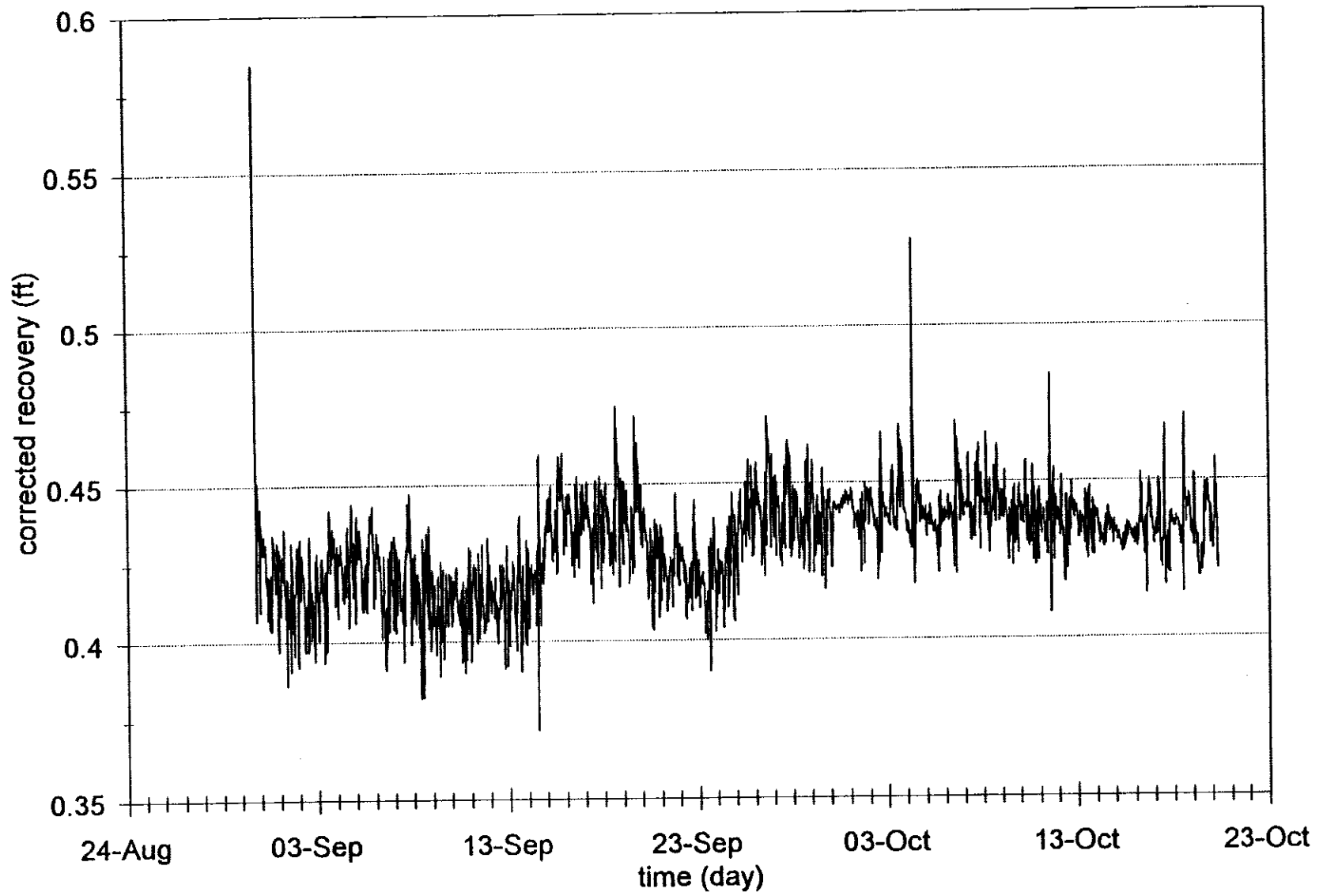
EG&G Idaho, Inc.
FORM EG&G-2631#
(Rev. 01-92)



OW1 upper

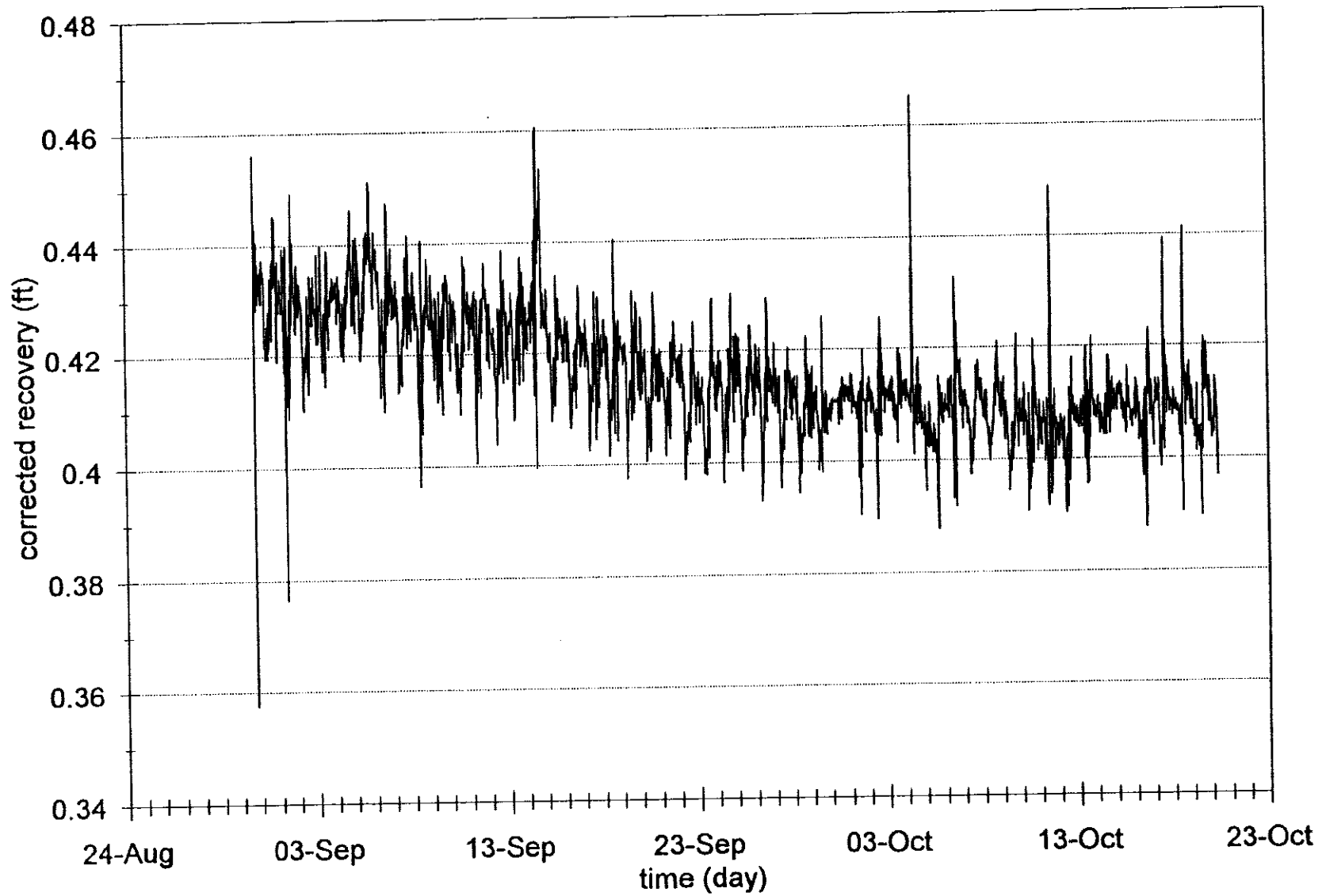
filtered data

EG&G Idaho, Inc.
FORM EGG-2631#
(Rev. 01-92)



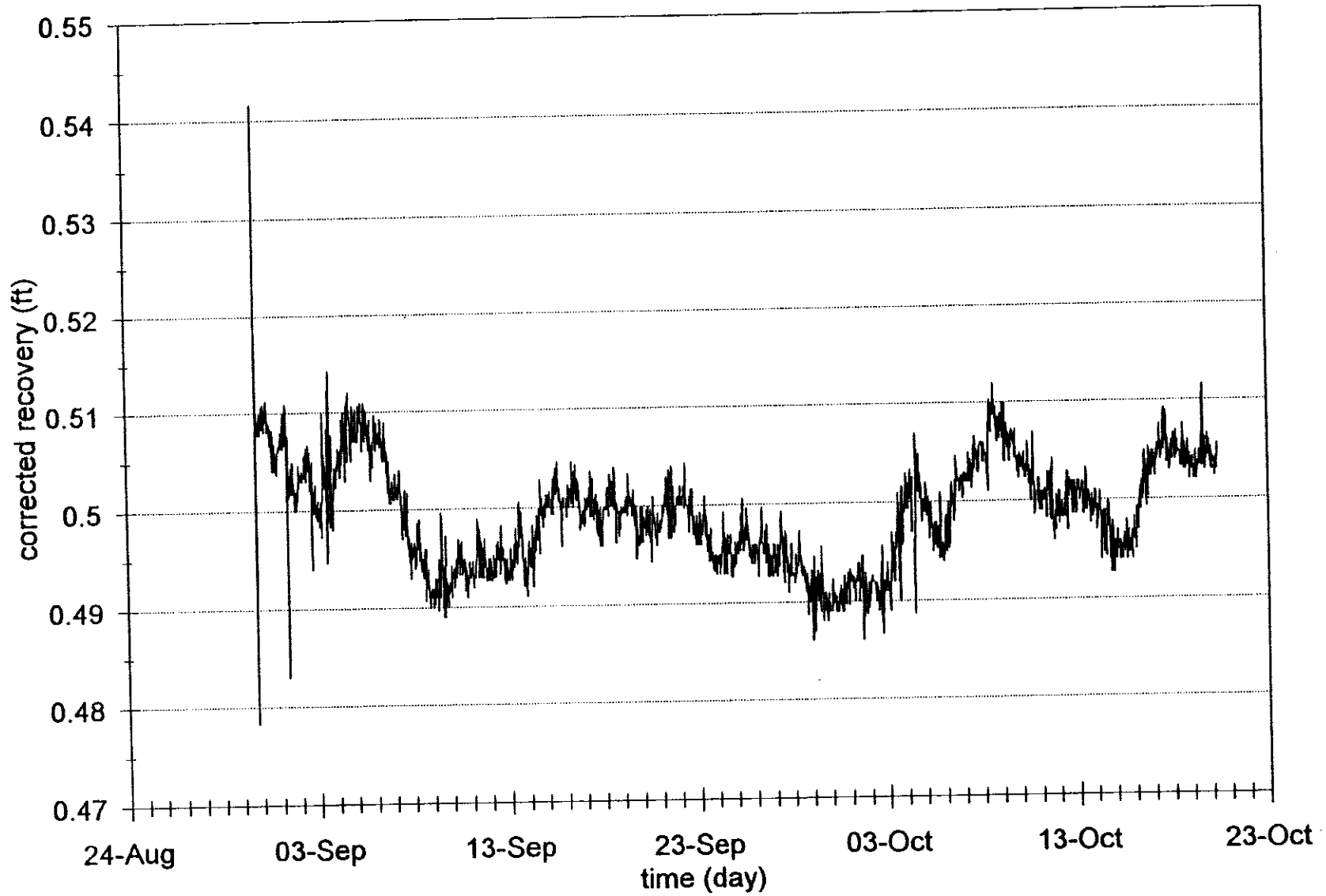
OW1 lower

filtered data



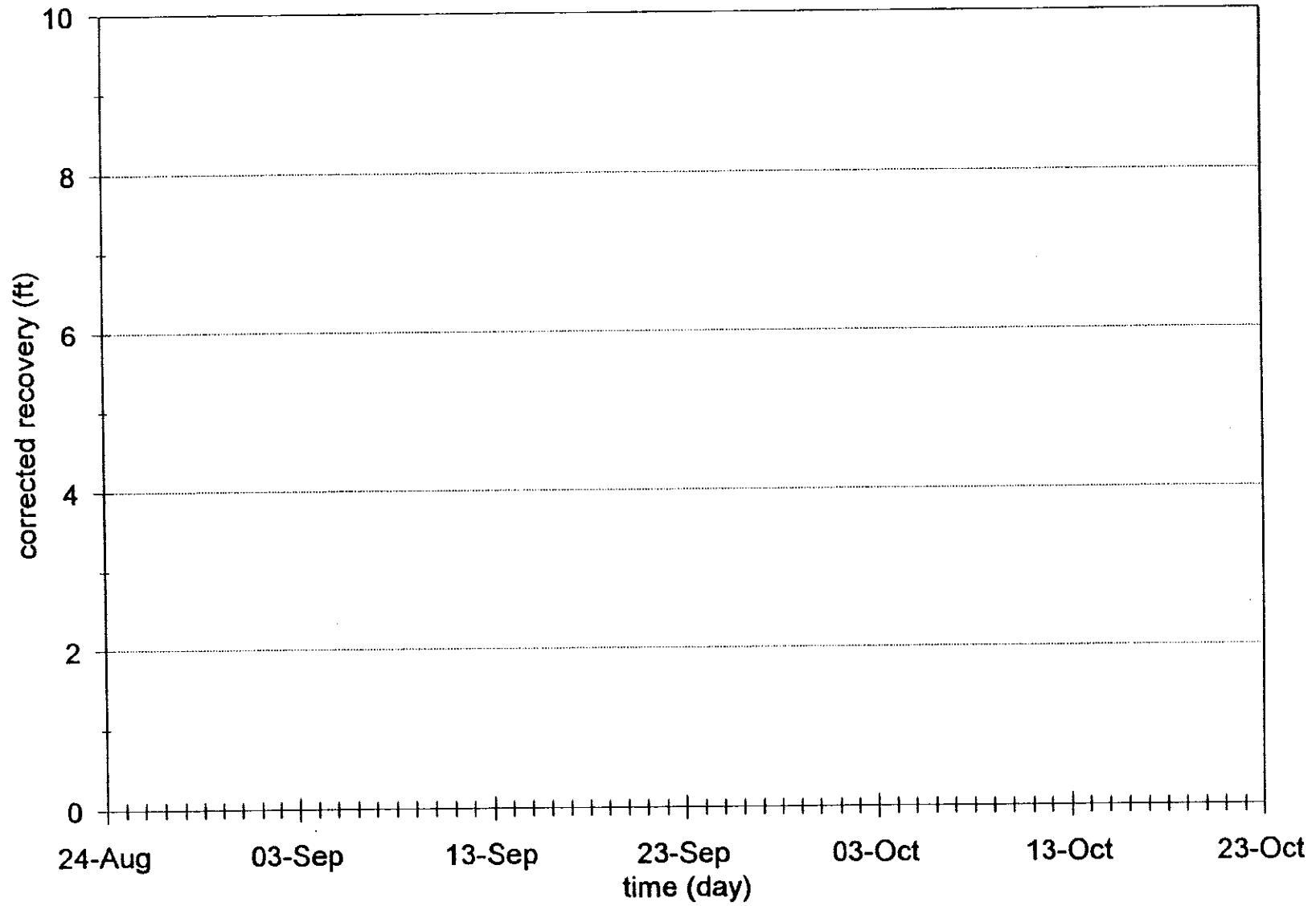
OW2 upper

filtered data



OW2 lower

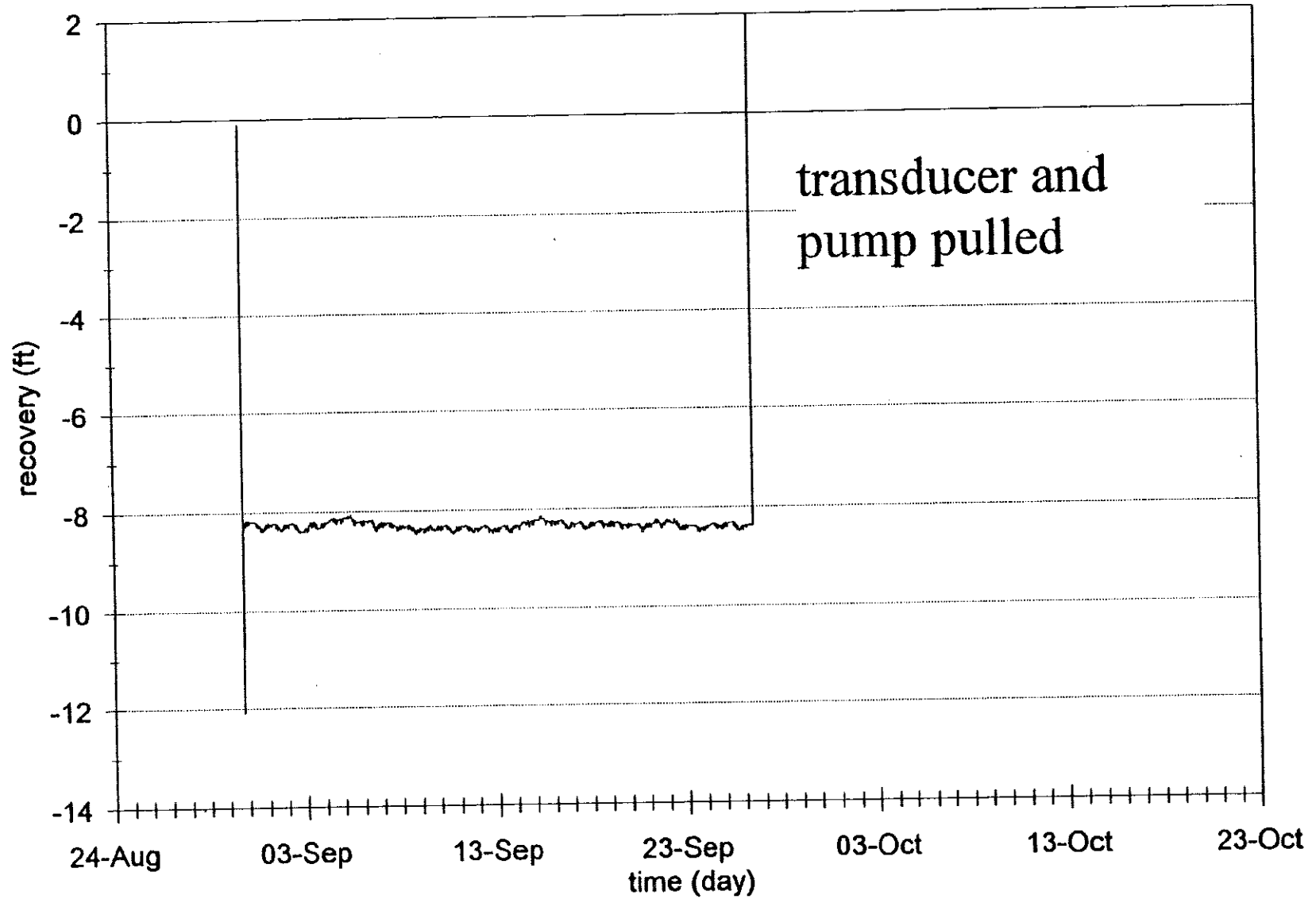
filtered data



Test Well

raw data

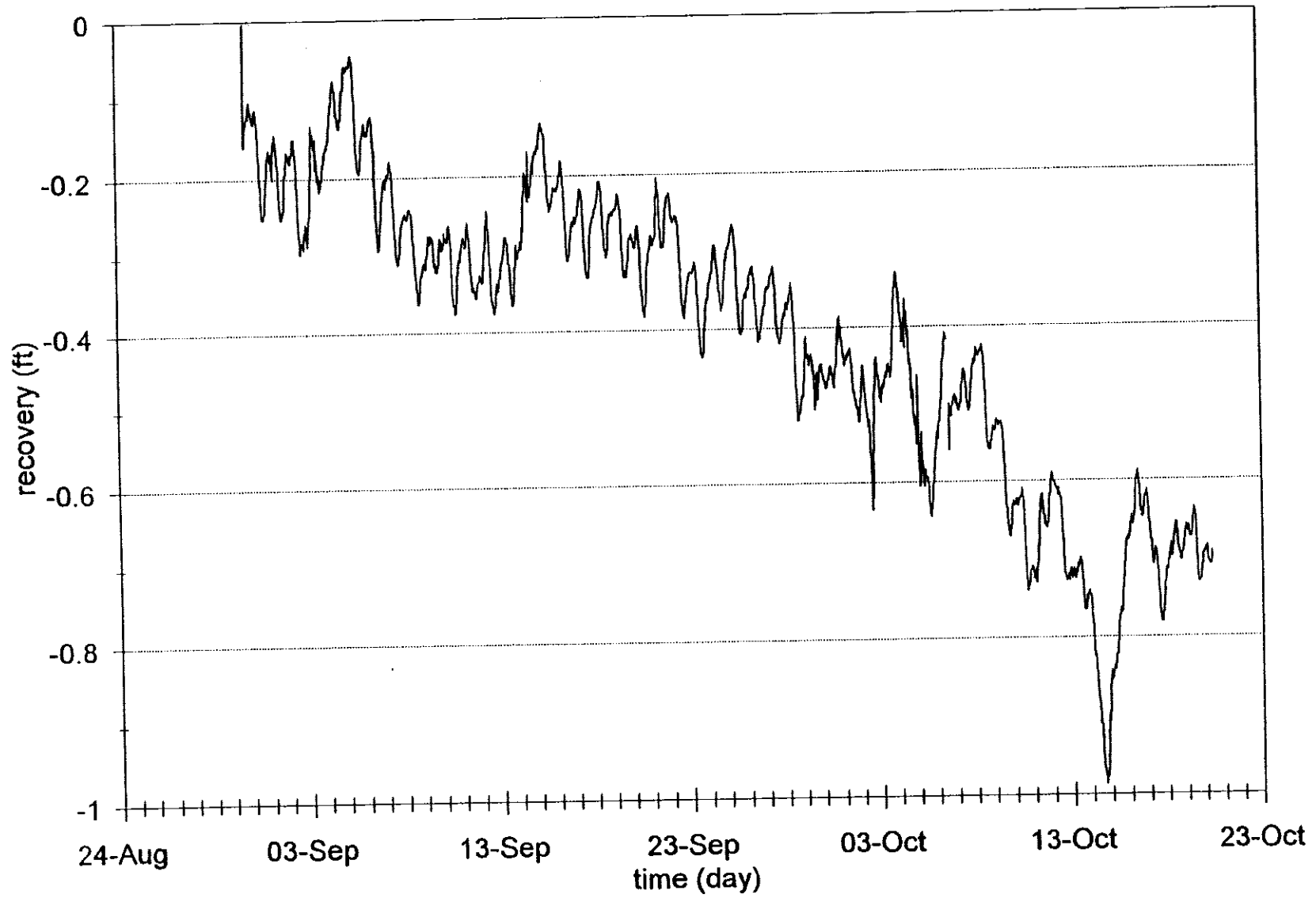
EG&G Idaho, Inc.
FORM EGG-2631#
(Rev. 01-92)



120

raw data

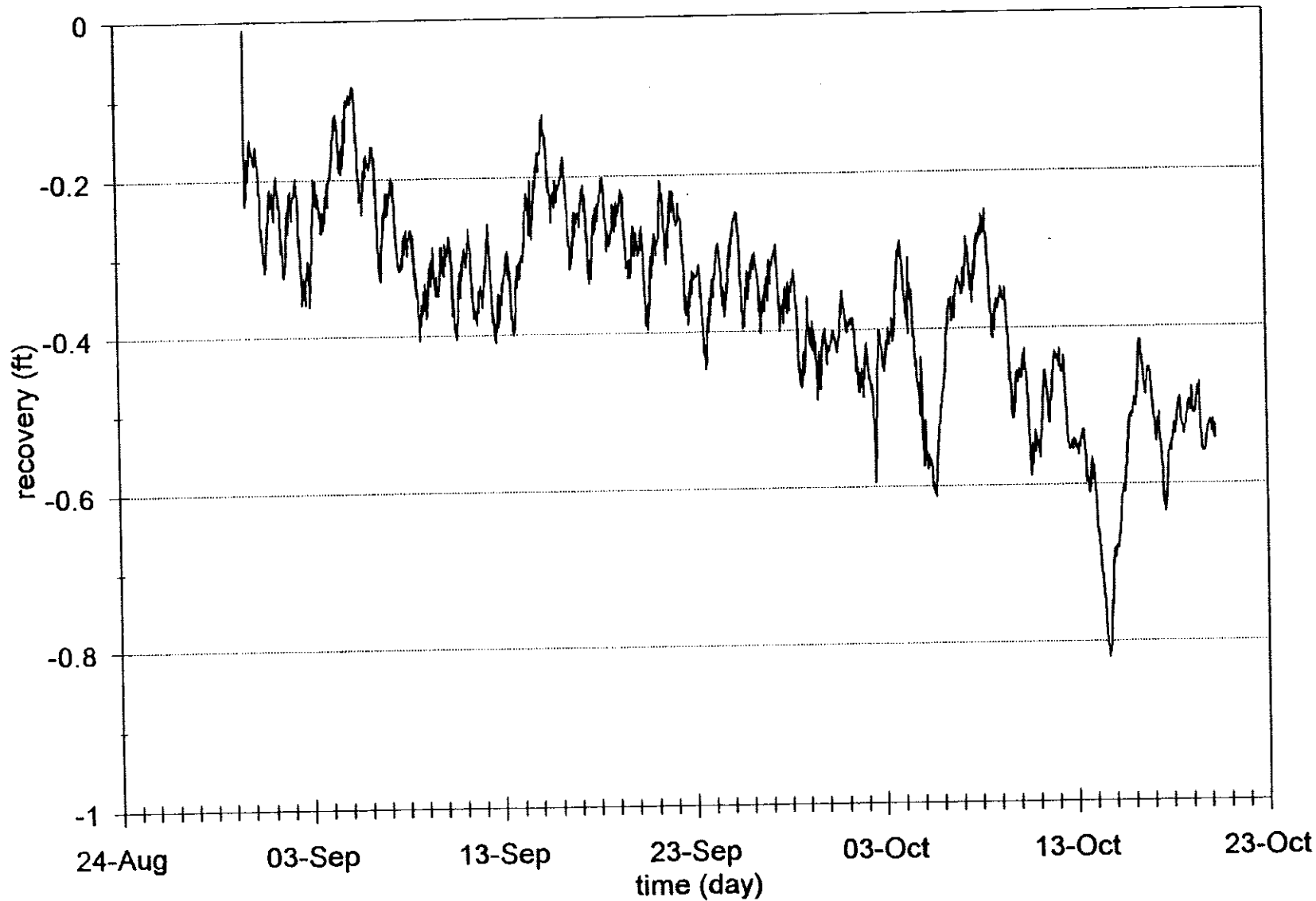
EG&G Idaho, Inc.
FORM EGG-2631#
(Rev. 01-92)



OW1 upper

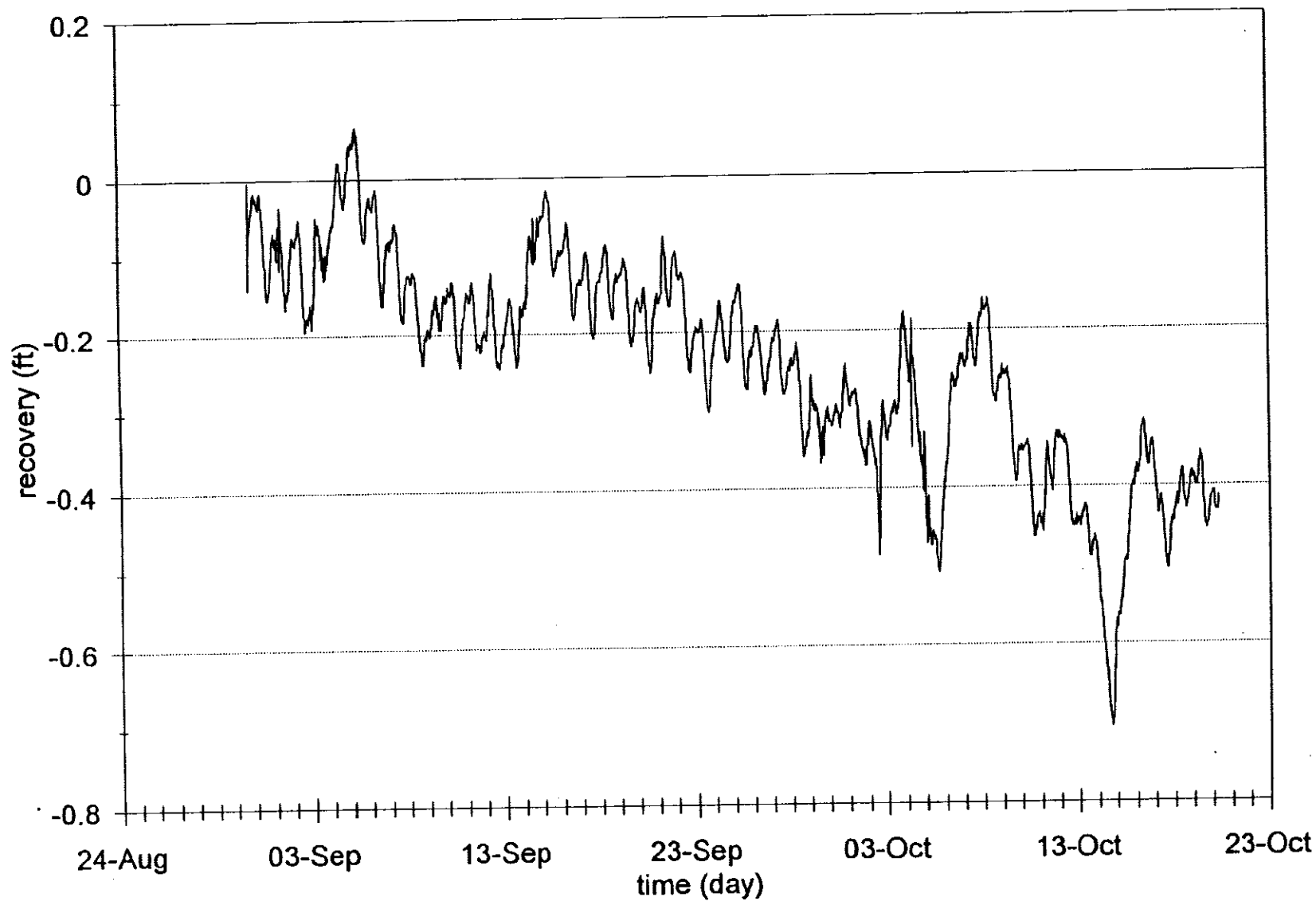
raw data

EG&G Idaho, Inc.
FORM EGG-2631#
(Rev. 01-92)



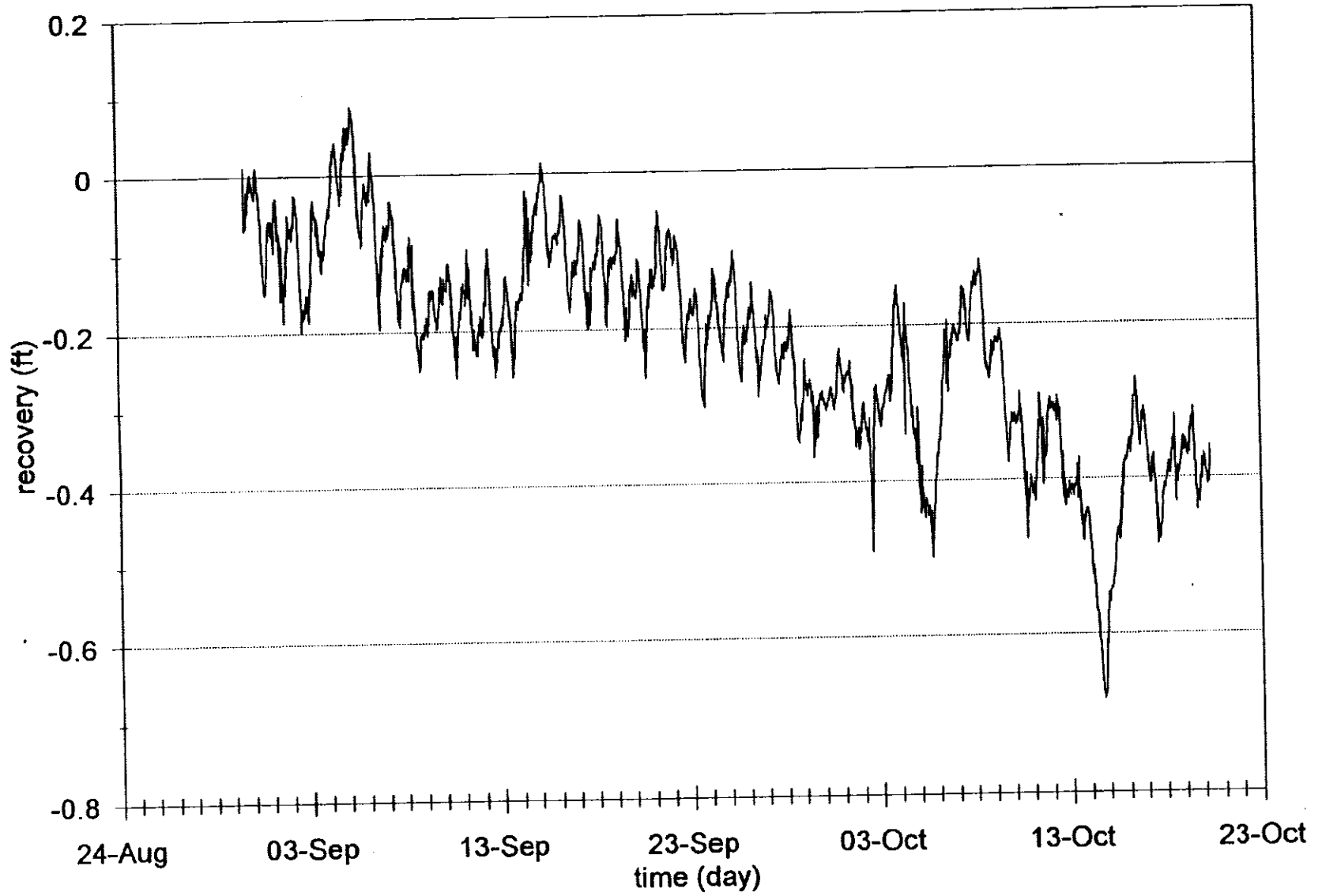
OW1 lower

raw data



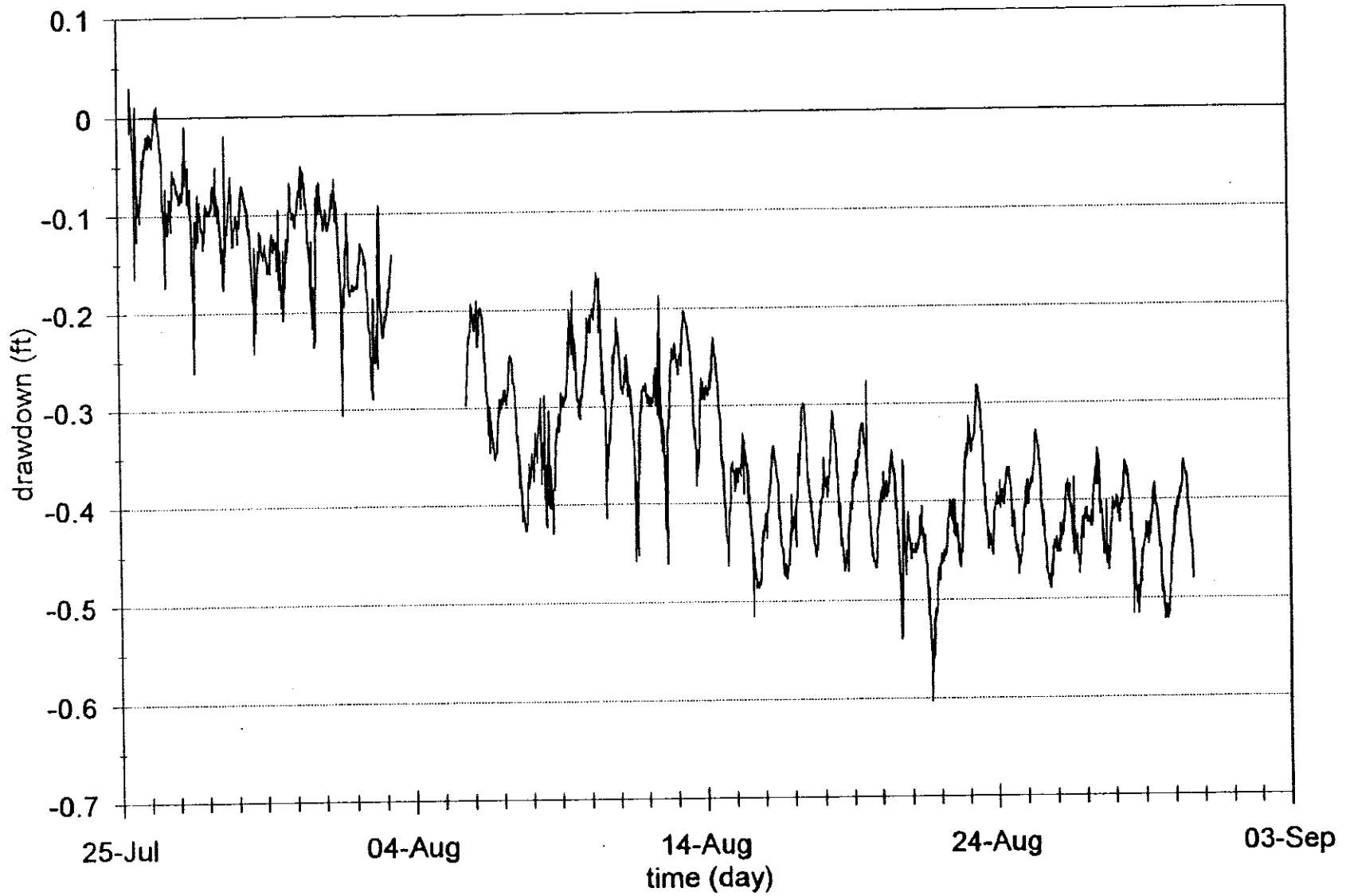
OW2 upper

raw data



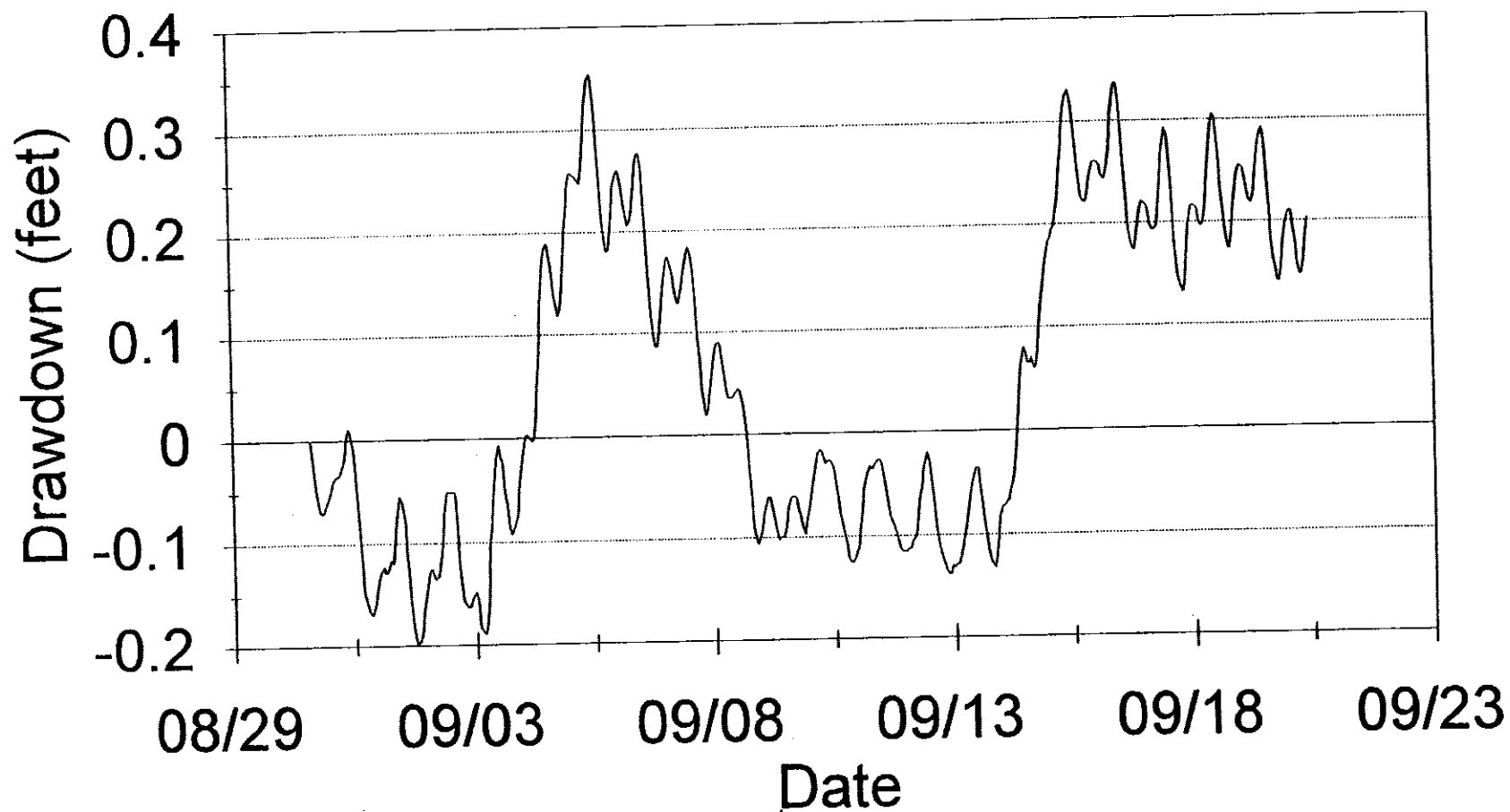
OW2 lower

raw data

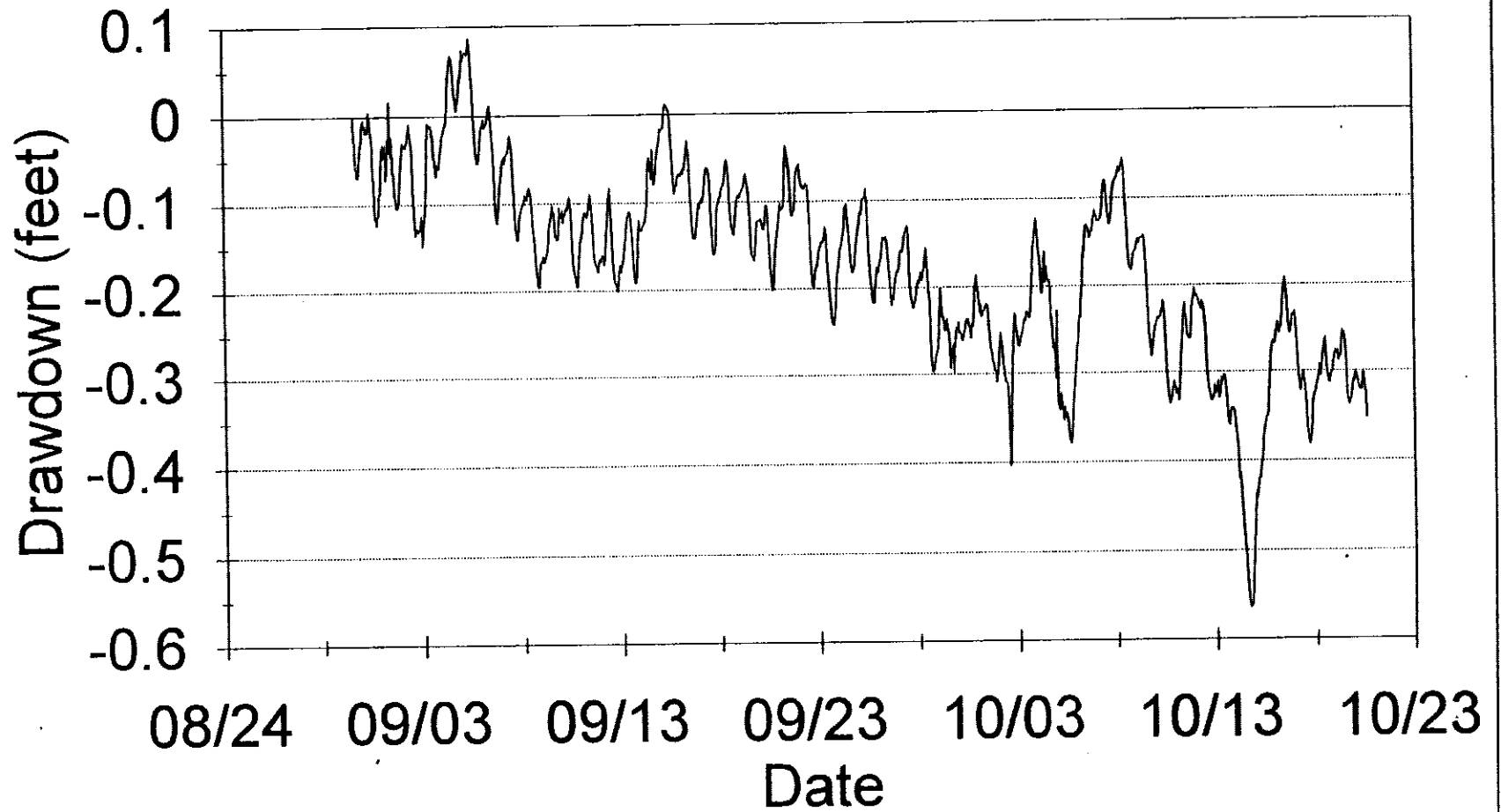


M4D

Post Test Trend Data

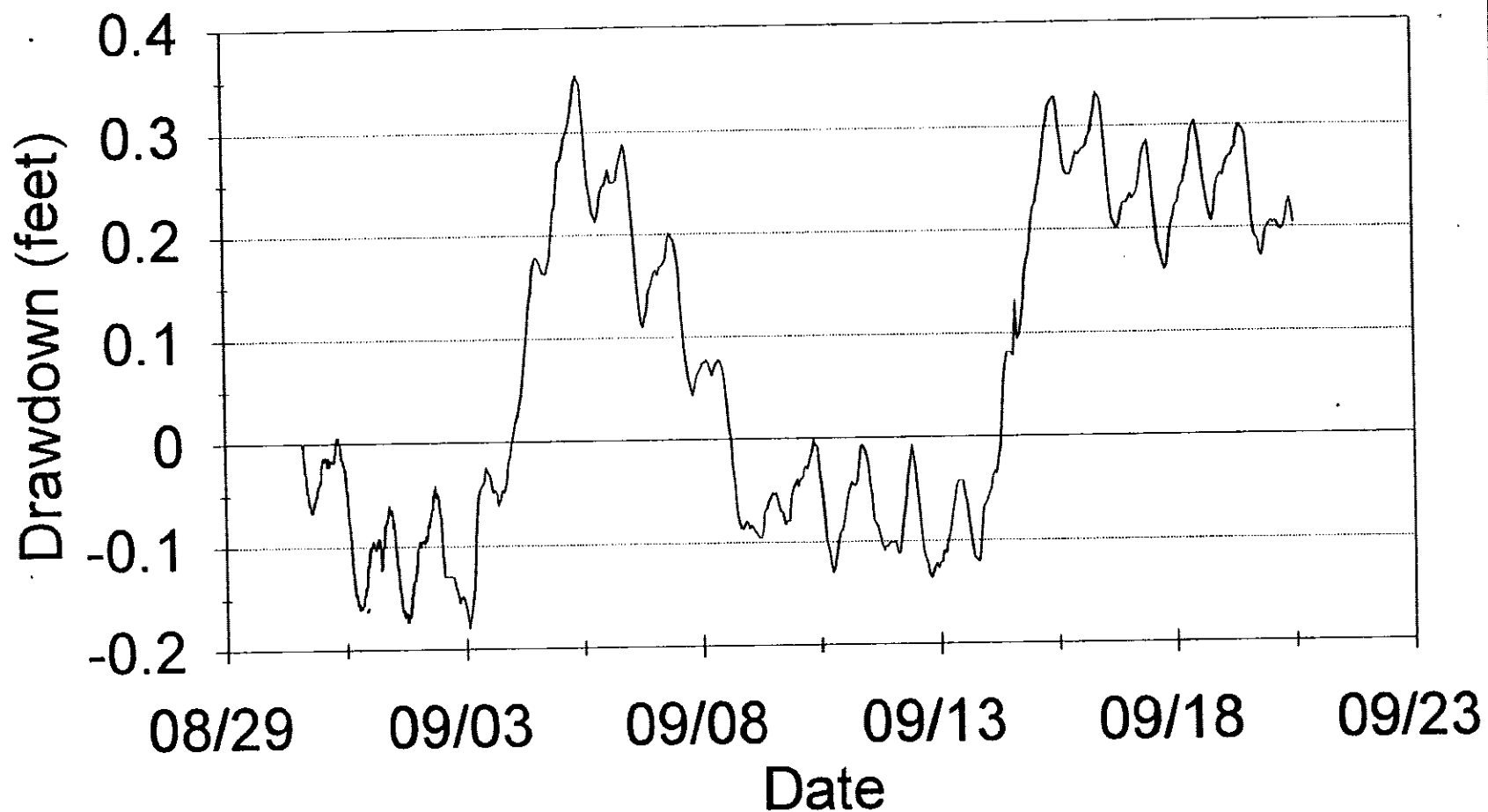


USGS 9 Post Test Trend Data



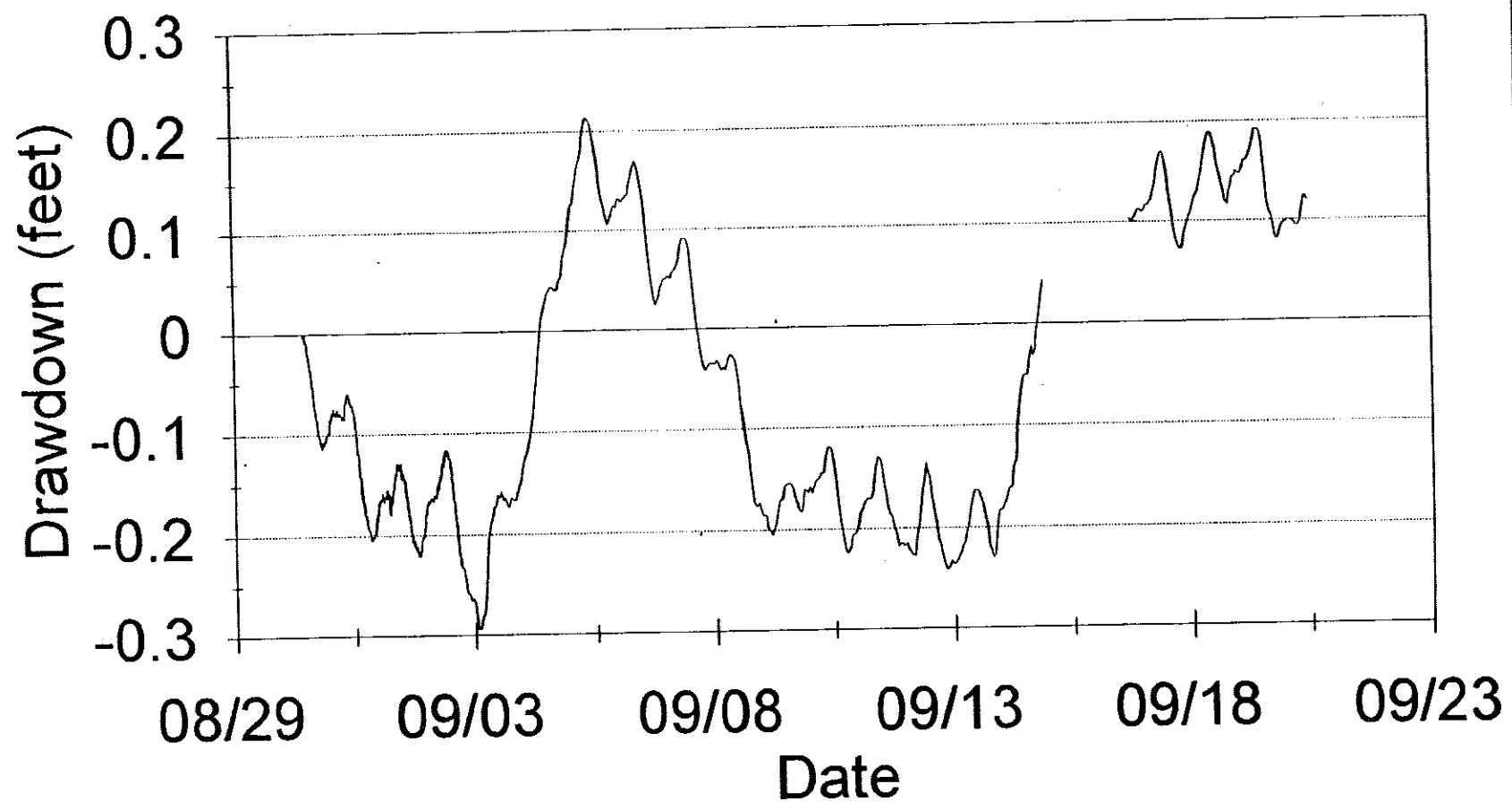
USGS 88

Post Test Trend Data



USGS 118

Post Test Trend Data



Appendix C

Analysis

Step 1
 1000 gpm

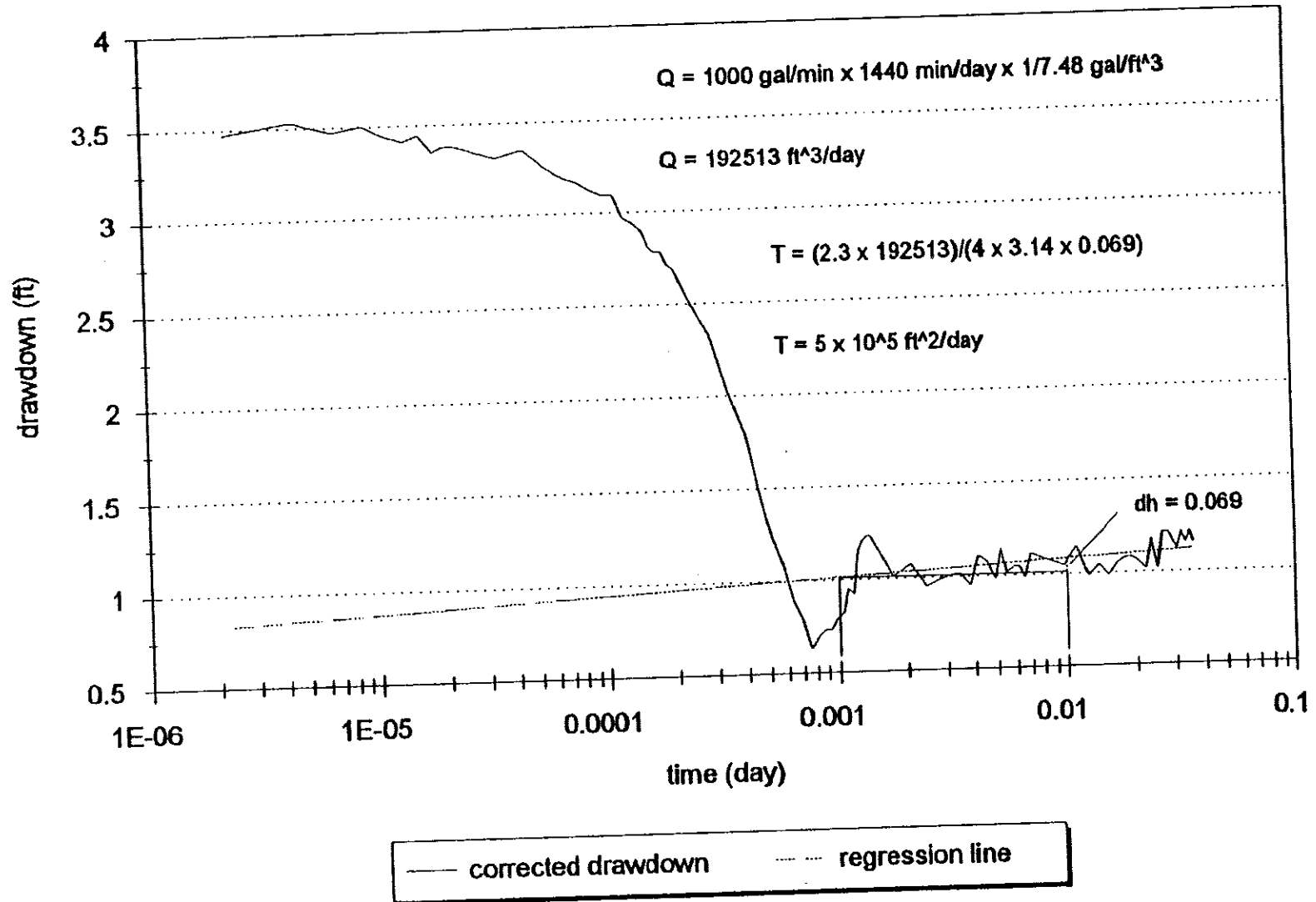


Figure 1: Cooper-Jacob plot and hand calculations.

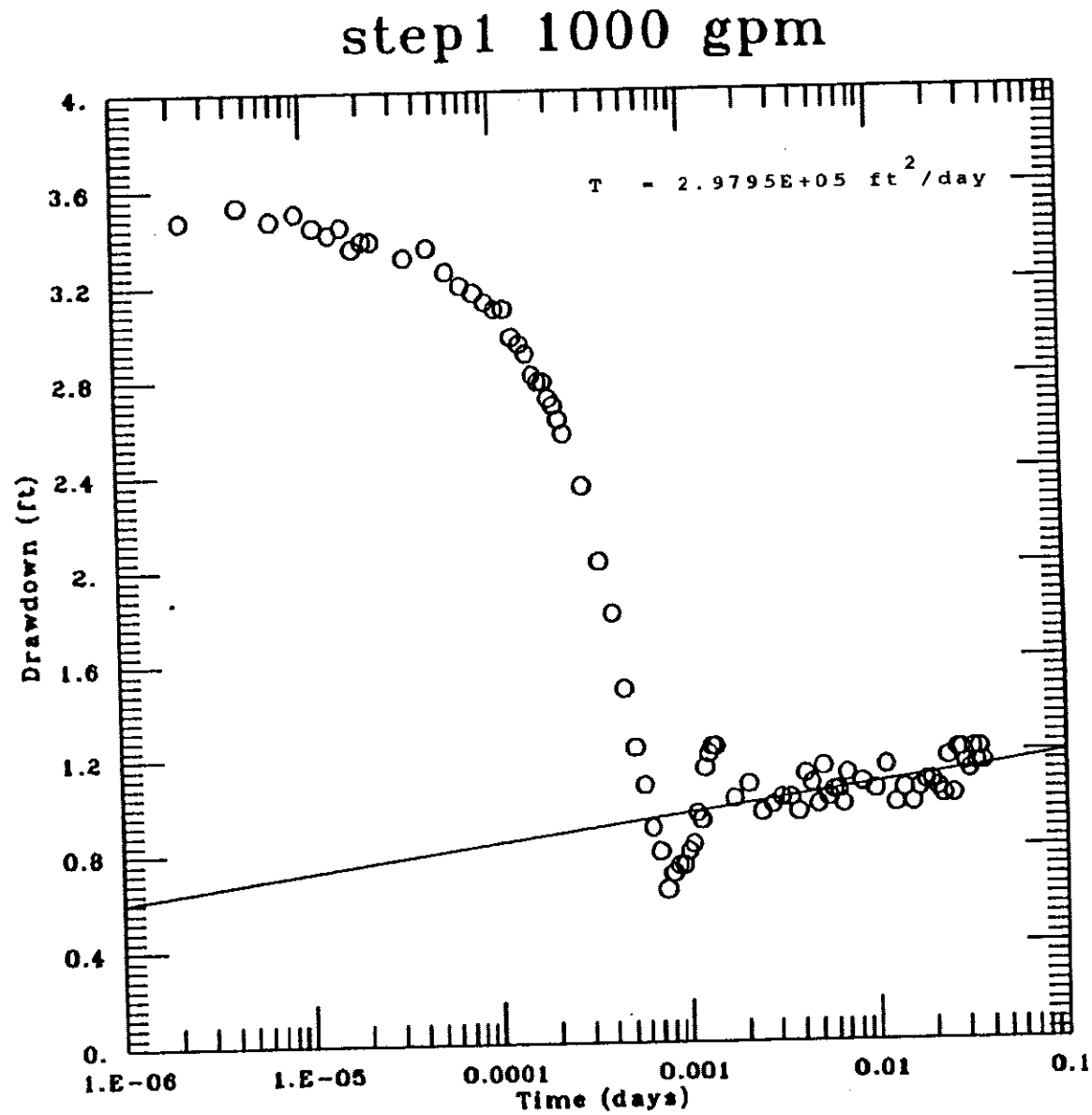


Figure 2: AQTESOLV generated Cooper-Jacob plot.

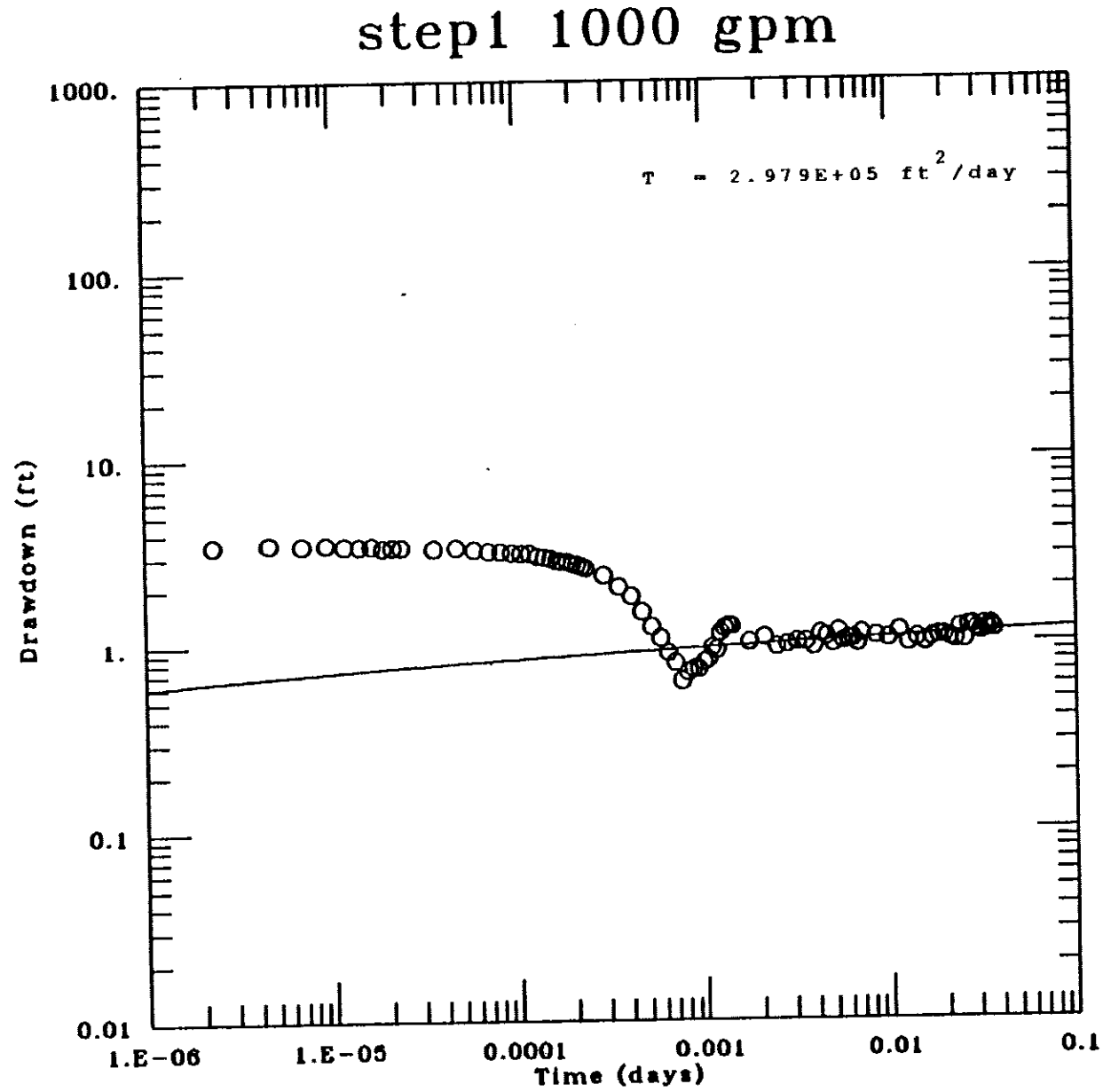


Figure 3: AQTESOLV generated Theis plot.

Step test analysis

Hantush-Bierschenk method

	sp cap gpm/ft	Tot Q gpm	drwdwn (sw) ft	d sw ft	sw/Q	reg Q s/Q
step1	877.19	1000	1.14	1.14	0.00114	0.001141
step2	697.67	1500	2.15	1.01	0.001433	0.001445
step3	560.22	2000	3.57	1.42	0.001785	0.001749
step4	522.62	2310	4.42	0.85	0.001913	0.001937
		3000				

Regression Output: Step test analysis

Constant	0.000534
Std Err of Y Est	3.2E-05
R Squared	0.994531
No. of Observations	4
Degrees of Freedom	2

X Coefficient(s)	6.072E-07
Std Err of Coef.	3.184E-08

C= 6.07E-07

B= 0.000534

$$s = BQ + CQ^2$$

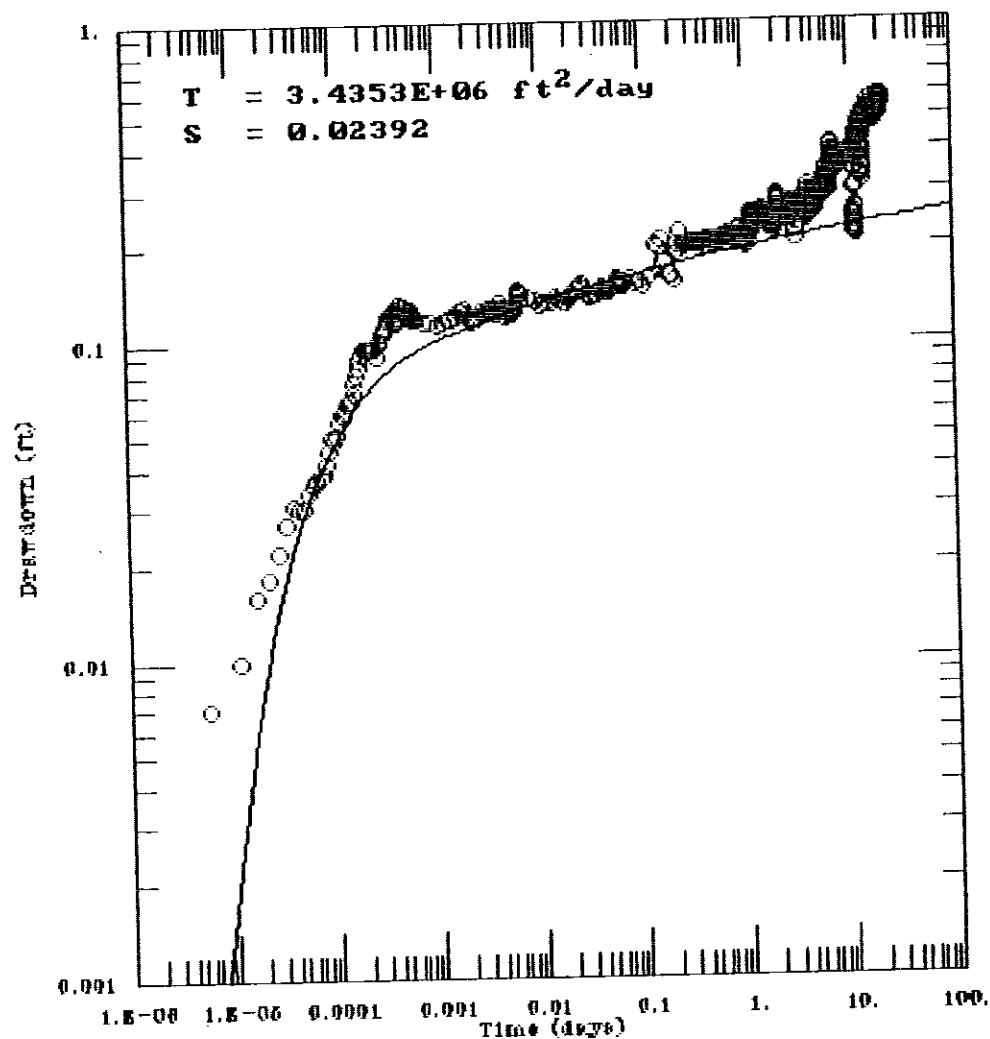
7.07

well eff @ 3000 gpm
29 %

well yield

	20% drawdown =	47.4
pmp rate	drawdown	
gpm	ft	root finding solution
1500	2.17	maximum yeild with 20% drawdown
2000	3.50	
3000	7.07	max pmp
6000	25.06	rate gpm equation
10000	66.06	8407 47.4-((SC\$23*E39)+(SC\$22*E39^2))
15000	144.62	
20000	253.55	

ow1 upper confined



AQTESOLV

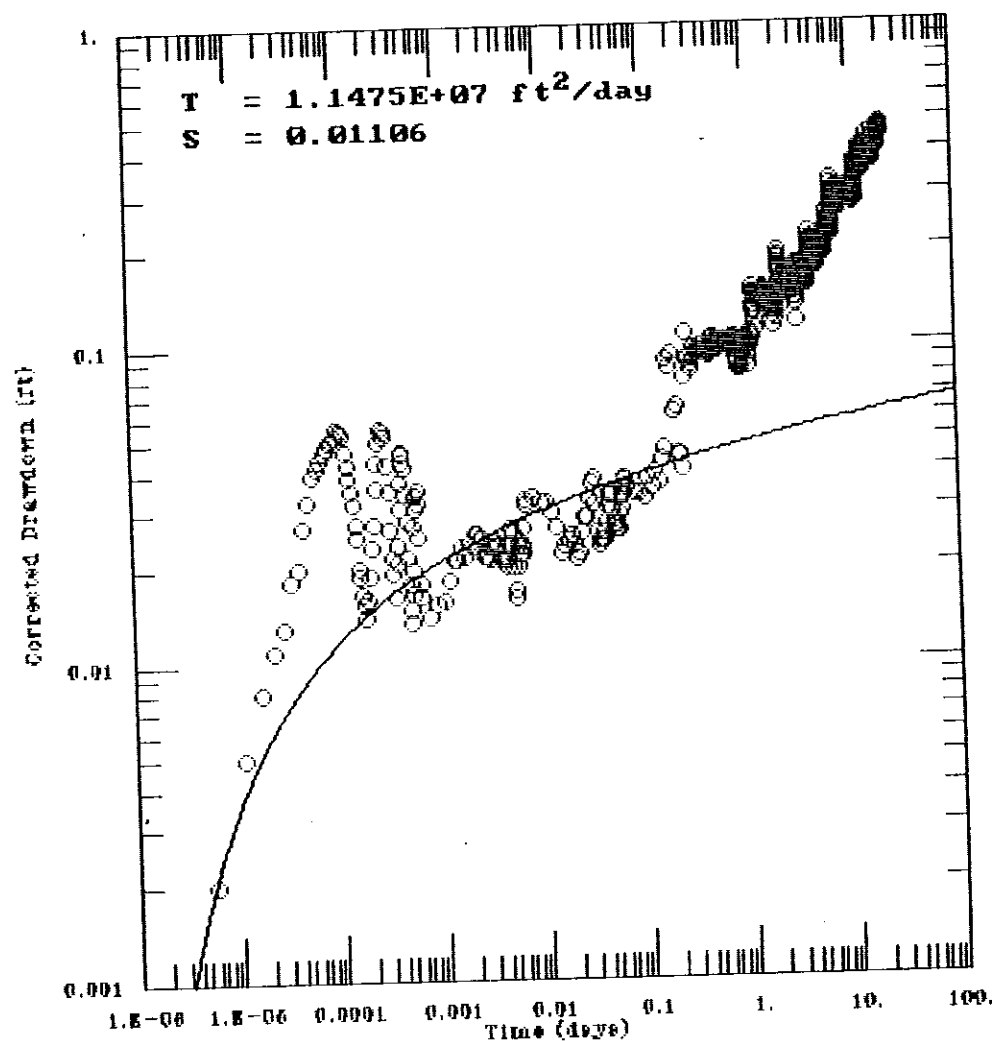


GERAGHTY
 & MILLER, INC.



Modeling Group

0W1L confined



AQTESOLV

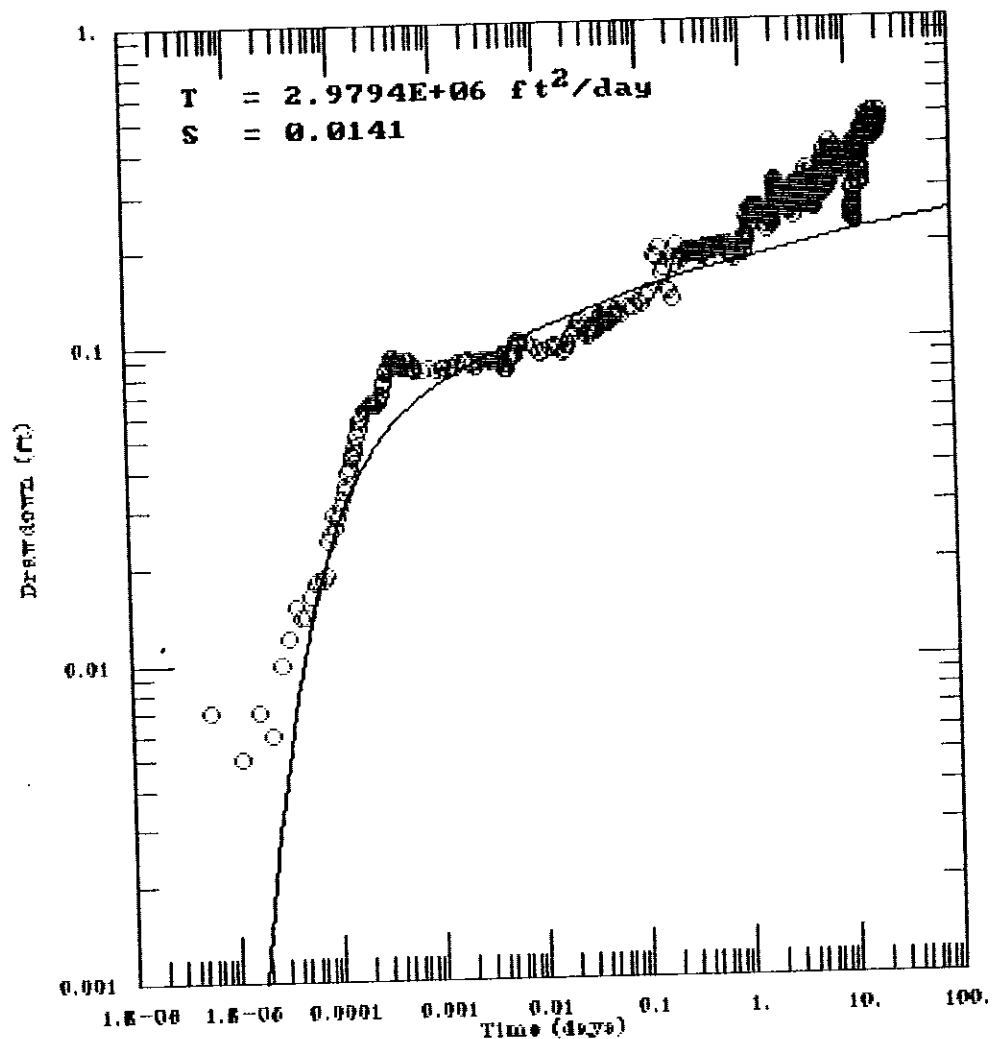


GERAGHTY
& MILLER, INC.



Modeling Group

120 confined



AQTESOLV

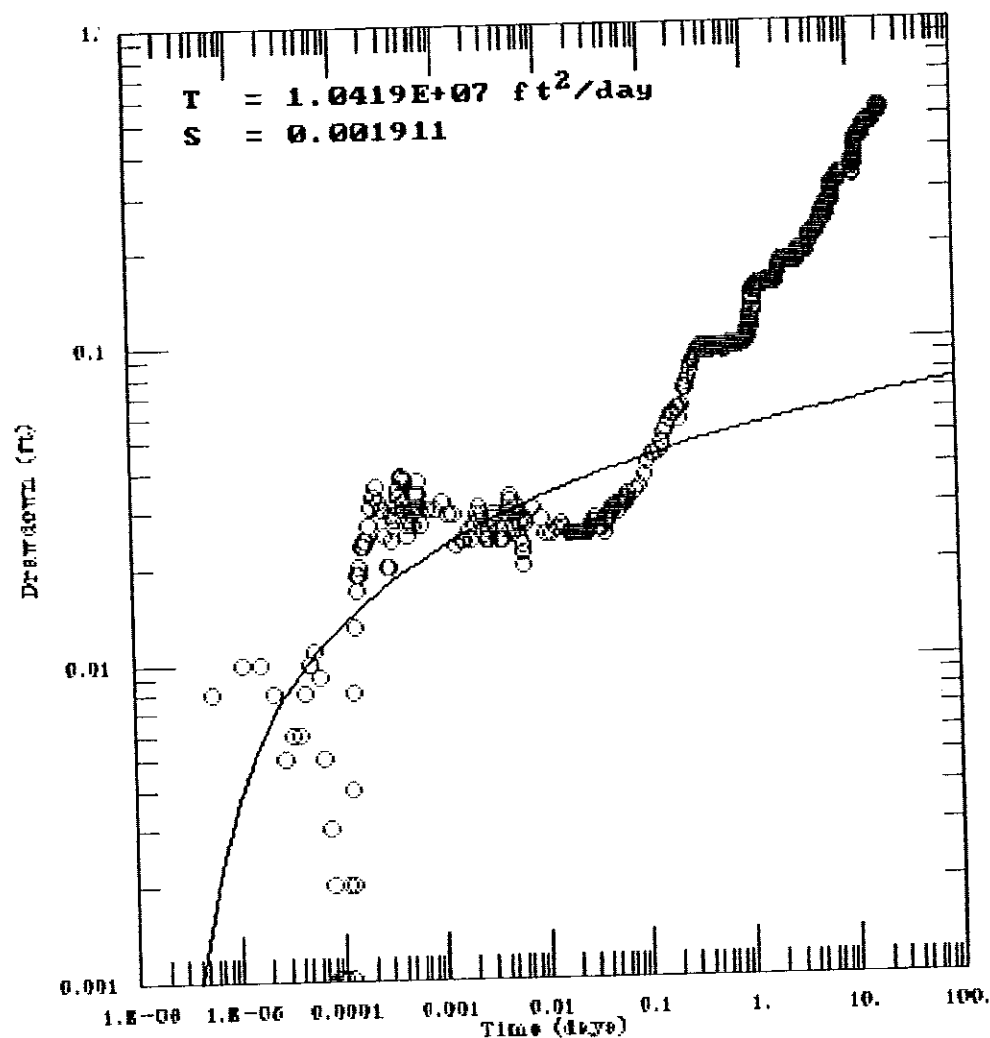


GERAGHTY
& MILLER, INC.



Modeling Group

ow2 upper confined



AQTESOLV



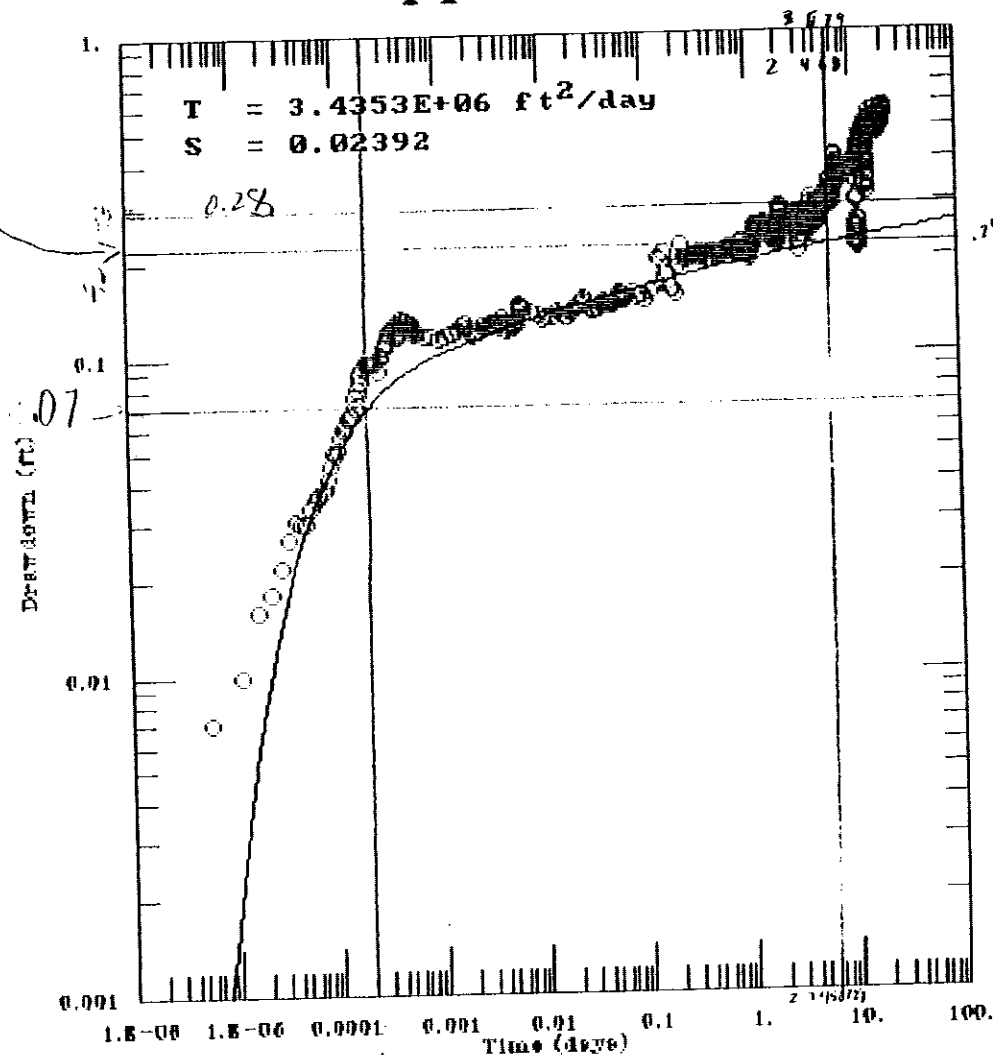
GERAGHTY
& MILLER, INC.



Modeling Group

ow1 upper confined

S_1 0.18 0.21 0.07



AQTESOLV



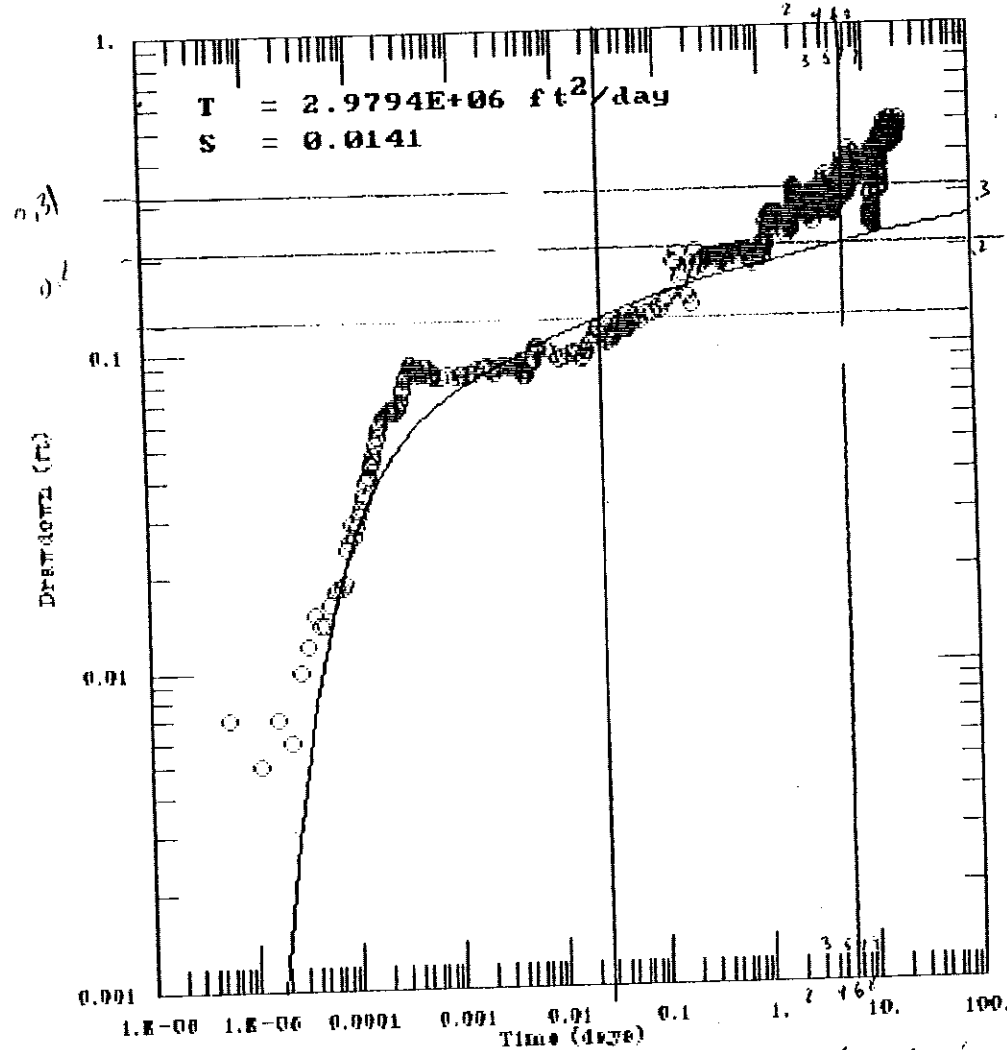
GERAGHTY
& MILLER, INC.



Modeling Group

120 confined

$S_0 = 0.2$ $0.2 = 0.1$



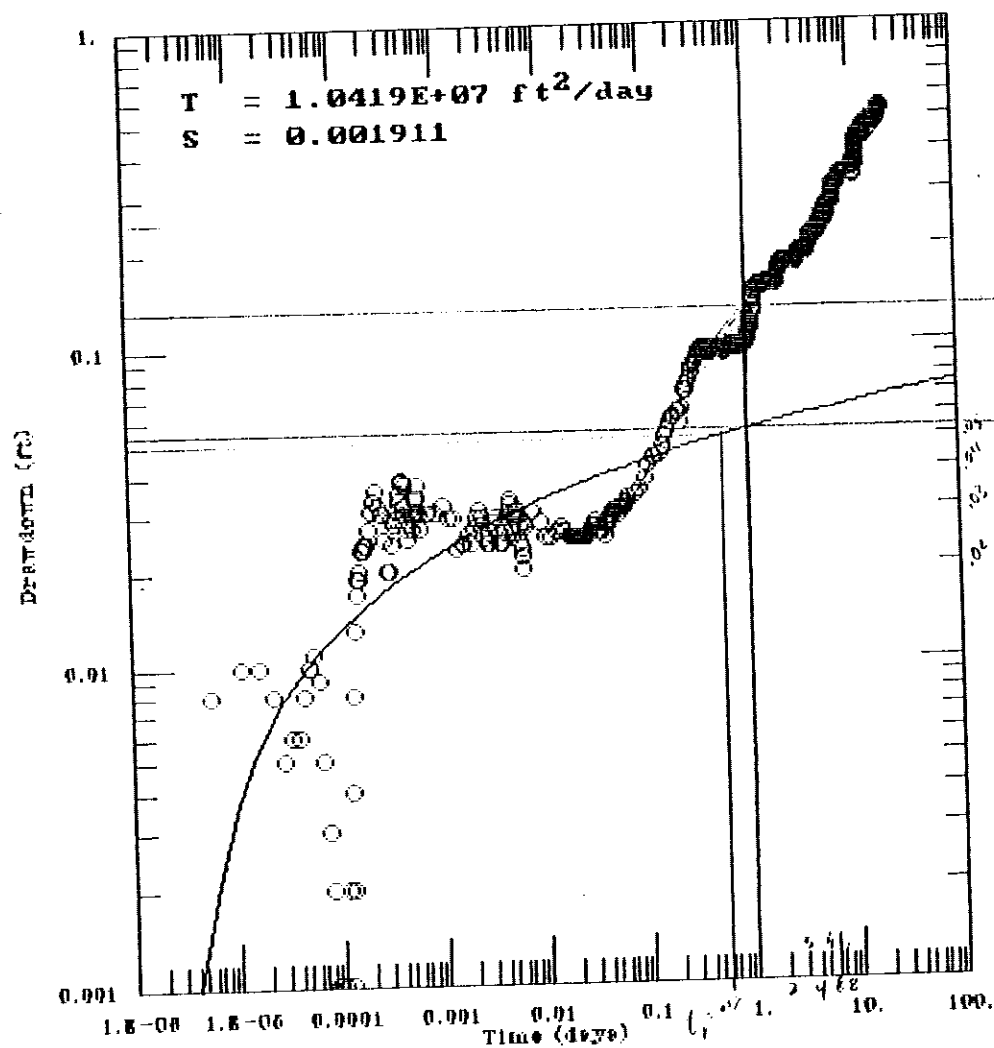
$t_0 = 0.014$

$t_0 = 6 \text{ days}$

AQTESOLV

GERAGHTY
& MILLER, INC.
Modeling Group

ow2 upper confined



AQTESOLV



GERAGHTY
& MILLER, INC.



Modeling Group

A program to calculate aquifer boundaries from
 aquifer test data
 given discharge (Q), drawdown (s), and time (t).

OW1 upper

$$r = 110.02 \cdot \text{ft}$$

$$t_i = 6 \cdot \text{day}$$

$$t_r = .0002 \cdot \text{day}$$

$$r_i = \sqrt{\frac{r^2 \cdot t_i}{t_r}}$$

$$r_i = 19056 \cdot \text{ft}$$

120

$$r = 199.89 \cdot \text{ft}$$

$$t_i = 6 \cdot \text{day}$$

$$t_r = .014 \cdot \text{day}$$

$$r_i = \sqrt{\frac{r^2 \cdot t_i}{t_r}}$$

$$r_i = 4138 \cdot \text{ft}$$

OW2 upper

$$r = 378.29 \cdot \text{ft}$$

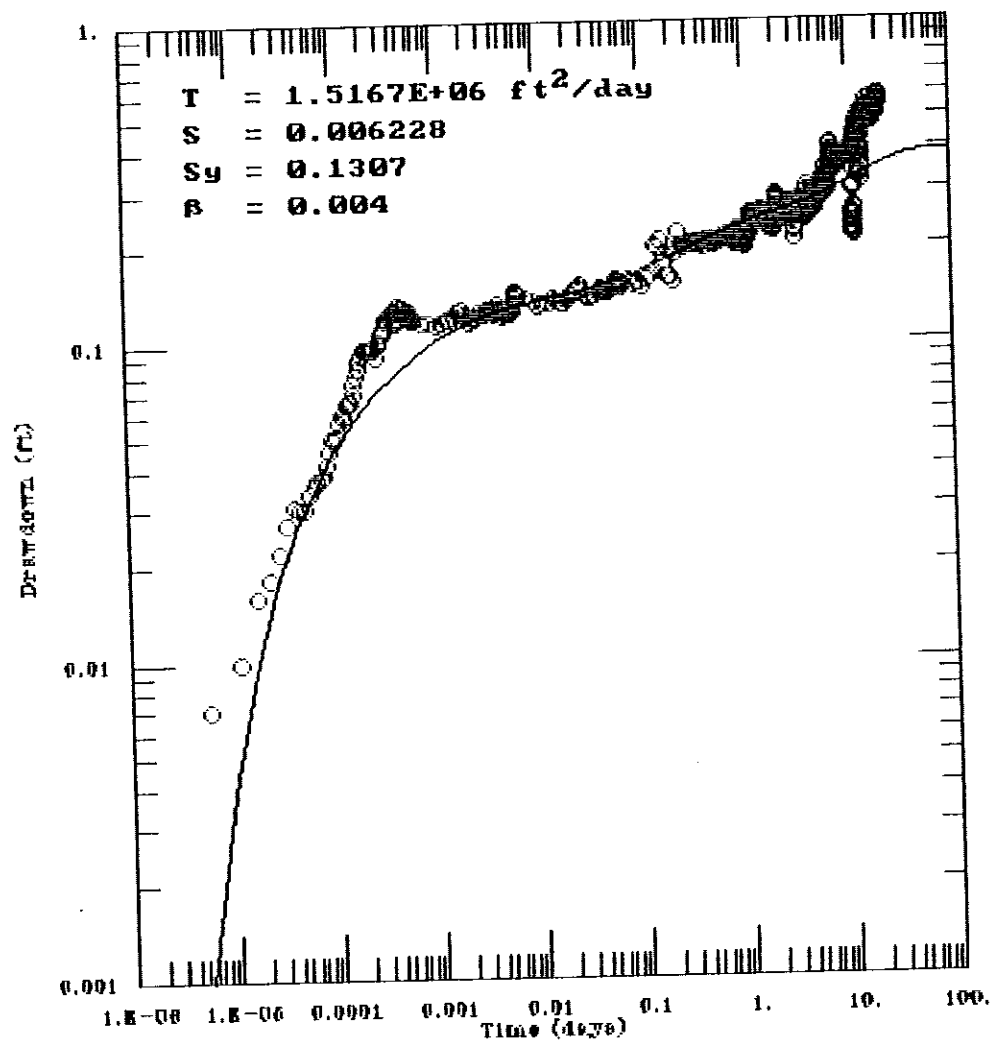
$$t_i = 1 \cdot \text{day}$$

$$t_r = .59 \cdot \text{day}$$

$$r_i = \sqrt{\frac{r^2 \cdot t_i}{t_r}}$$

$$r_i = 492 \cdot \text{ft}$$

ow1 upper unconfined



AQTESOLV

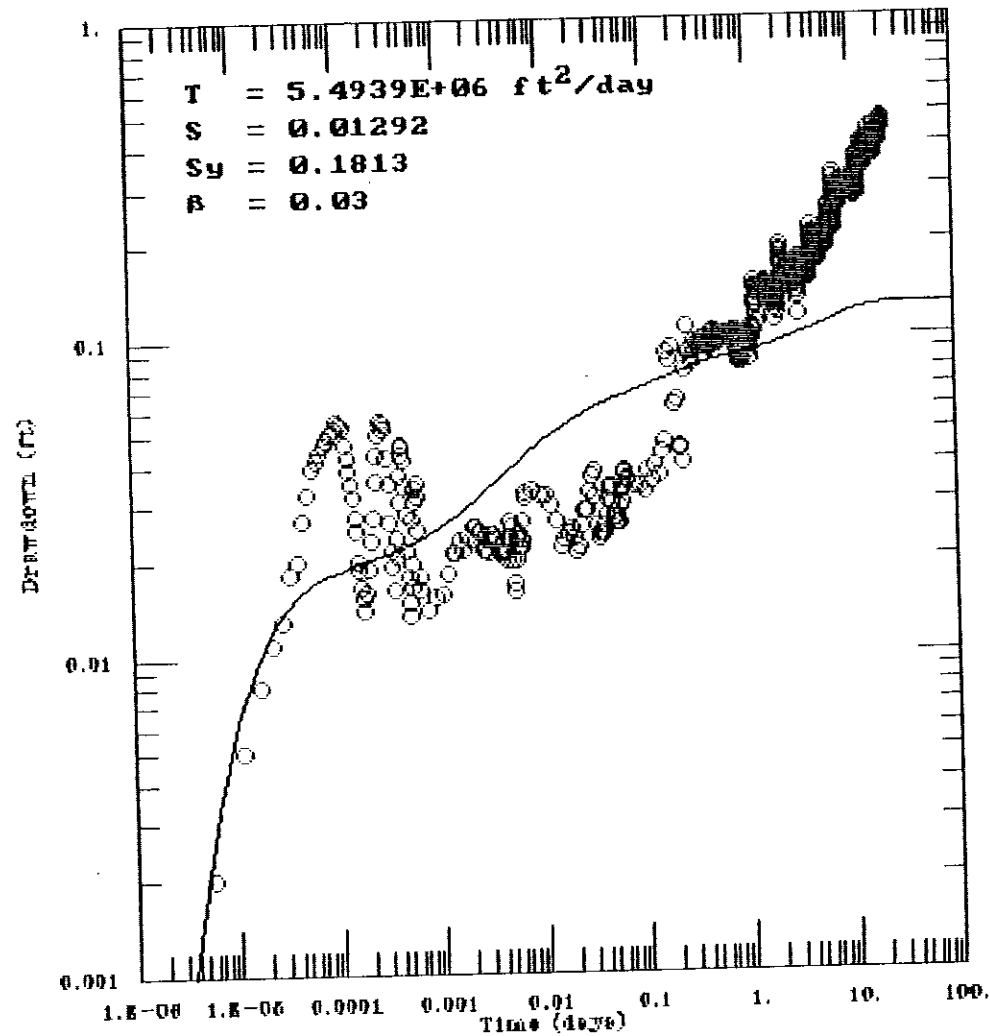


GERAGHTY
 & MILLER, INC.



Modeling Group

ow1 lower unconfined



AQTESOLV

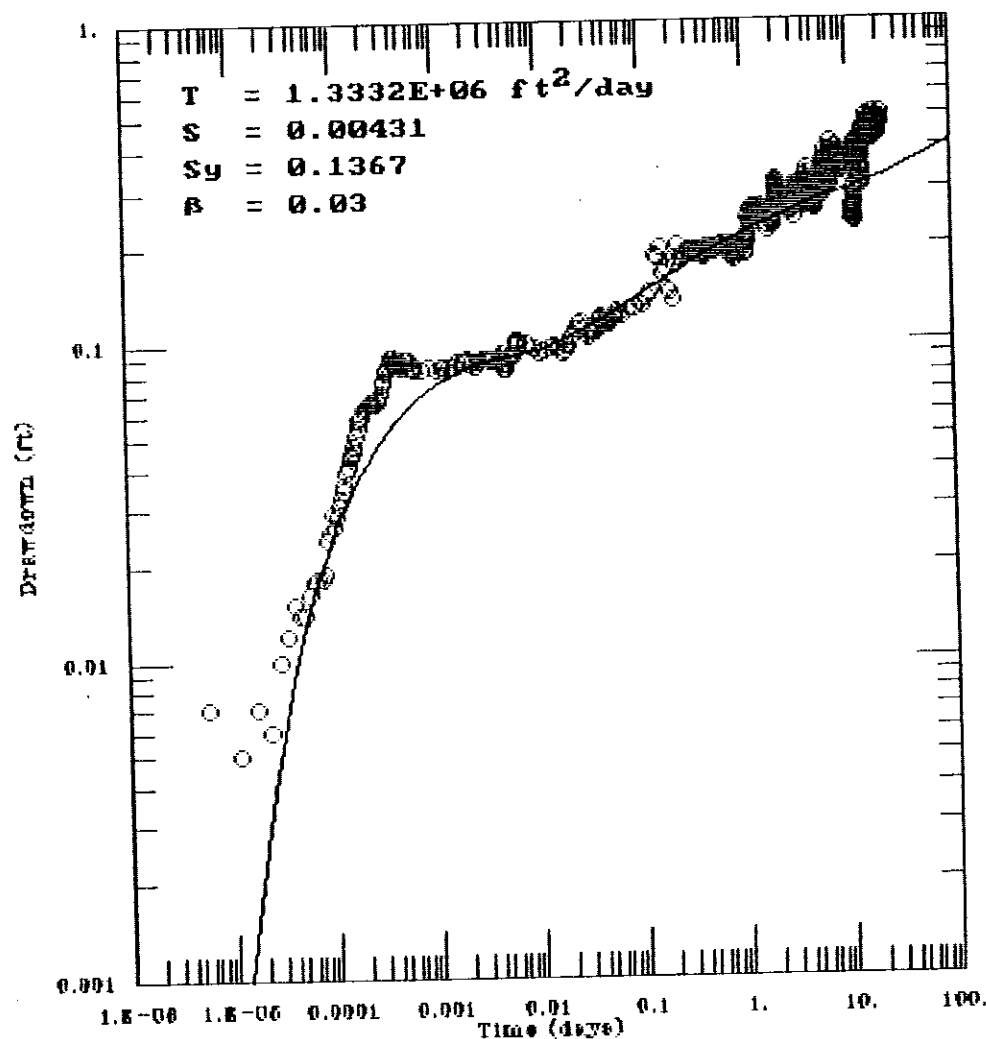


GERAGHTY
 & MILLER, INC.



Modeling Group

120 unconfined



AQTESOLV

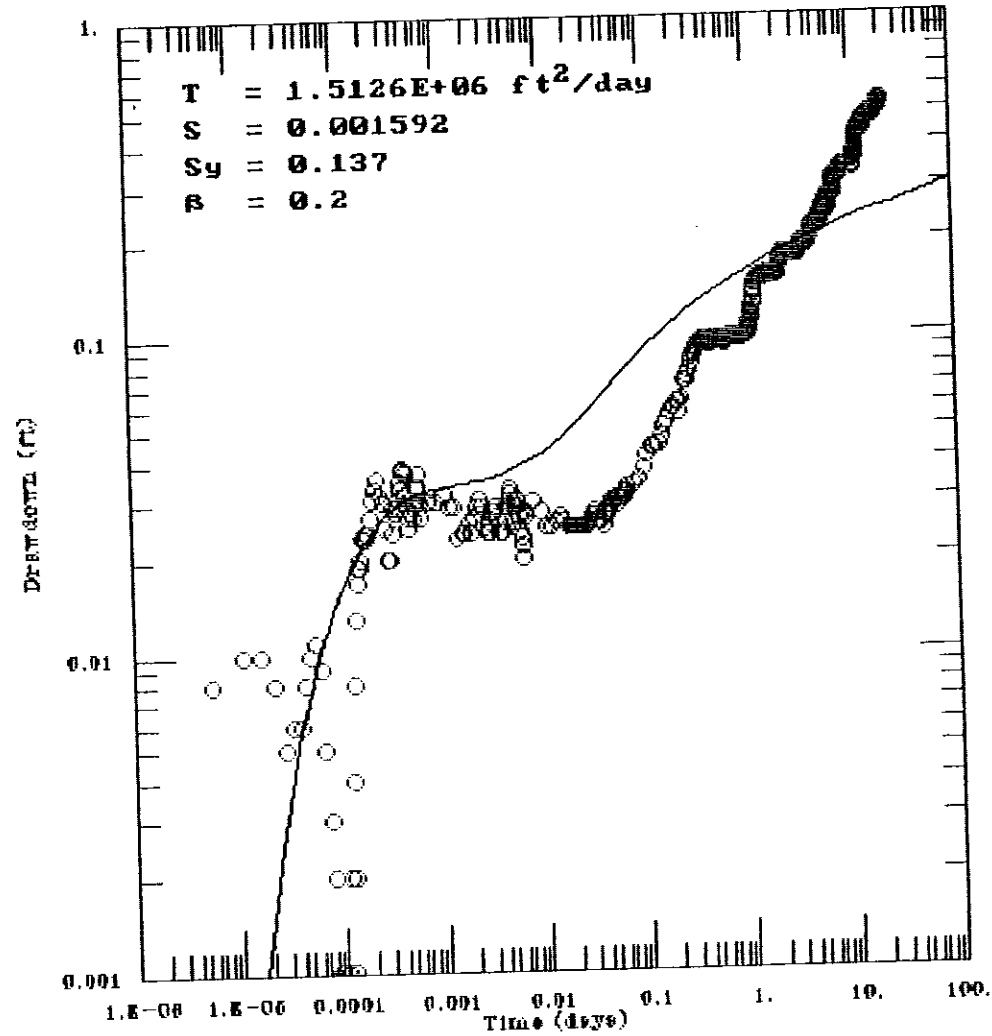


GERAGHTY
 & MILLER, INC.



Modeling Group

0W2 Unconfined



AQTESOLV



GERAGHTY
 & MILLER, INC.



Modeling Group

A program to calculate vertical hydraulic conductivity from curve match data using the Neuman
EG&G (1975) method.

FORM EGG-2631#

(Rev. 01-92)

OW1 Upper

$$b := 155 \cdot \text{ft}$$

$$\beta := 0.004$$

$$r := 110 \cdot \text{ft}$$

$$KhKv := \frac{r^2}{\beta \cdot b^2}$$

$$KhKv = 1 \cdot 10^2$$

120

$$\beta := 0.03$$

$$r := 200 \cdot \text{ft}$$

$$KhKv := \frac{r^2}{\beta \cdot b^2}$$

$$KhKv = 6 \cdot 10^1$$

OW2 Upper

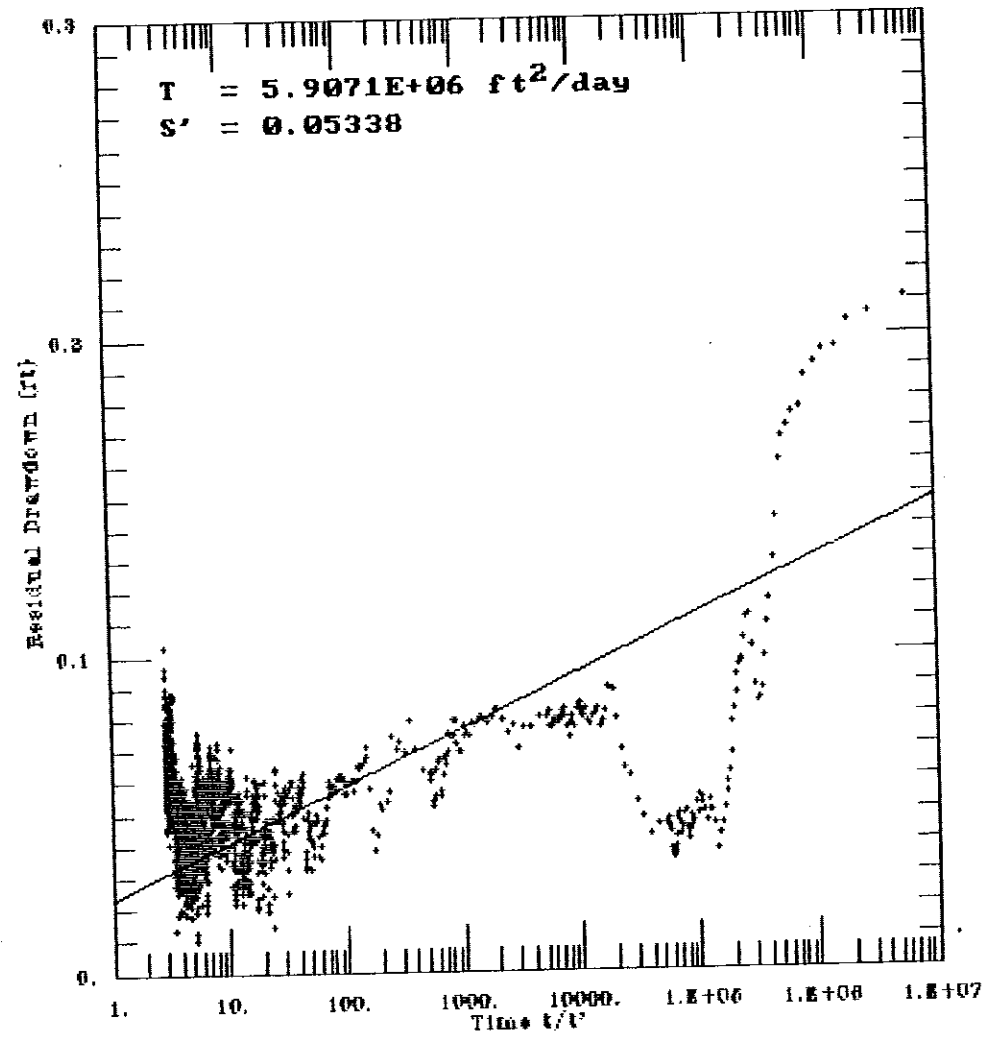
$$\beta := 0.2$$



$$r := 378 \cdot \text{ft}$$

$$KhKv := \frac{r^2}{\beta \cdot b^2}$$

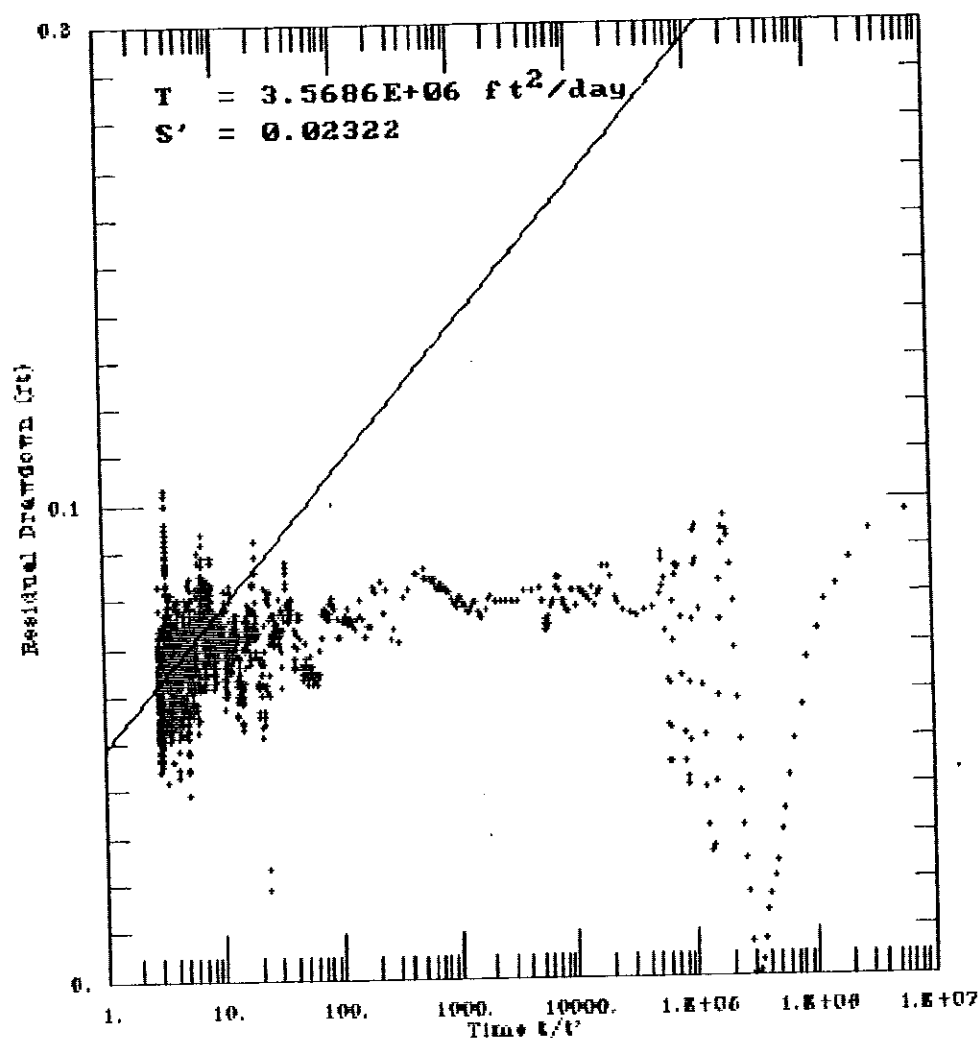
$$KhKv = 3 \cdot 10^1$$

0W1 upper, recovery



AQTESOLV
 GERAGHTY
 & MILLER, INC.
 Modeling Group

OW1 lower, recovery



AQTESOLV

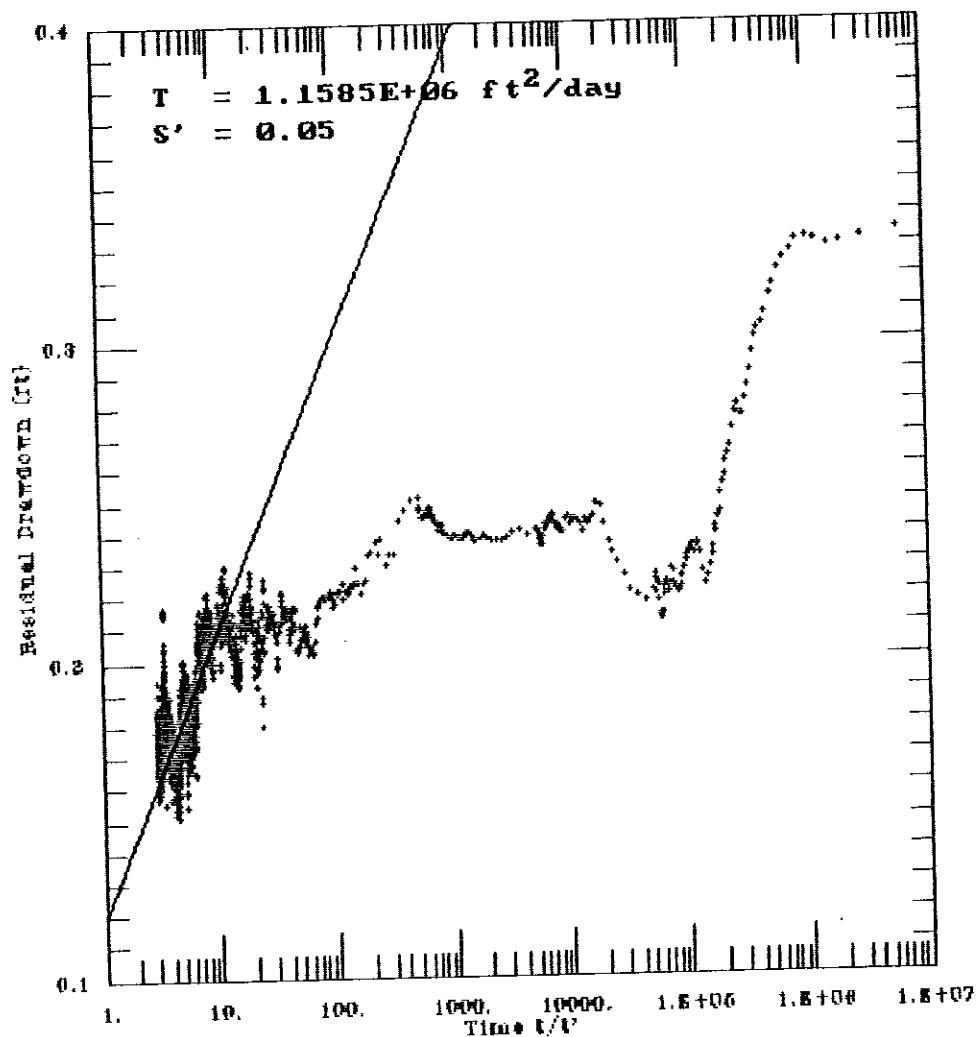


GERAGHTY
 & MILLER, INC.



Modeling Group

120, recovery



AQTESOLV

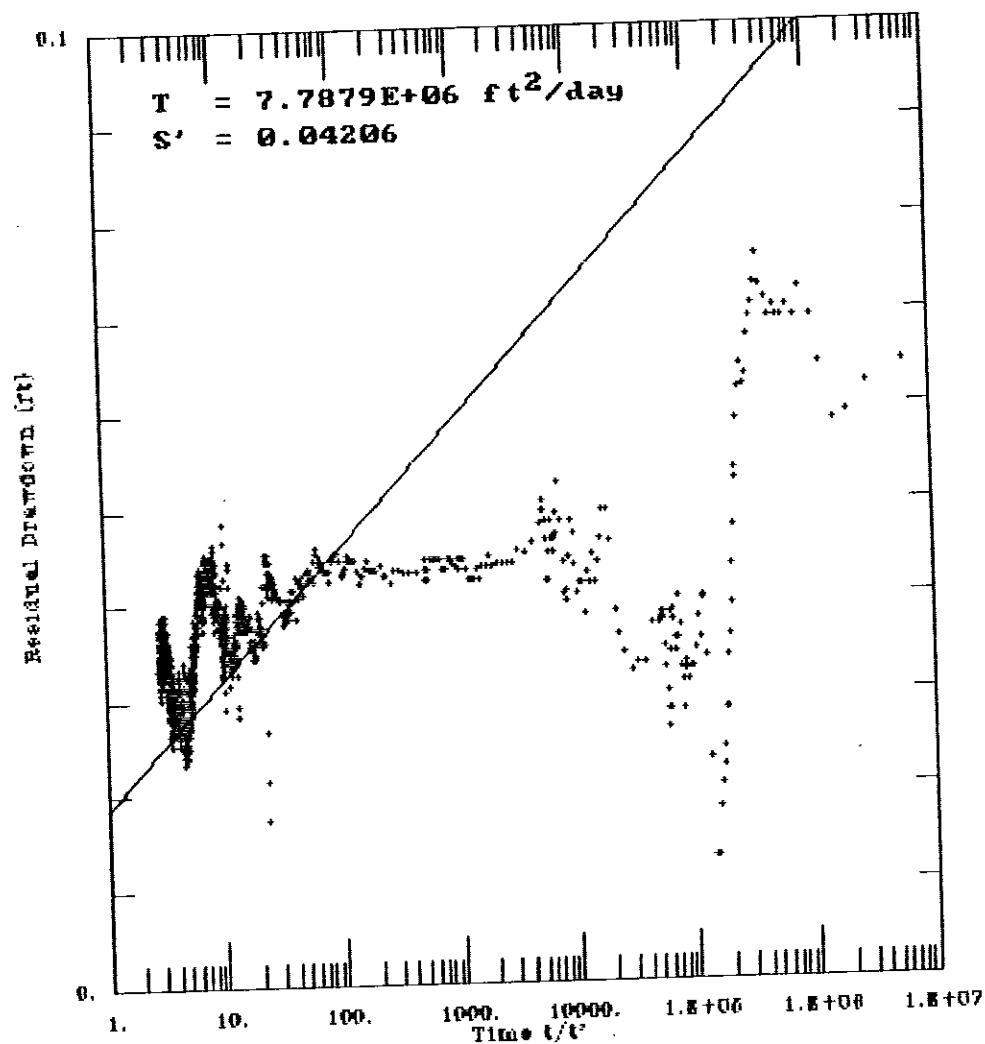


GERAGHTY
 & MILLER, INC.



Modeling Group

OW2 upper recovery



AQTESOLV



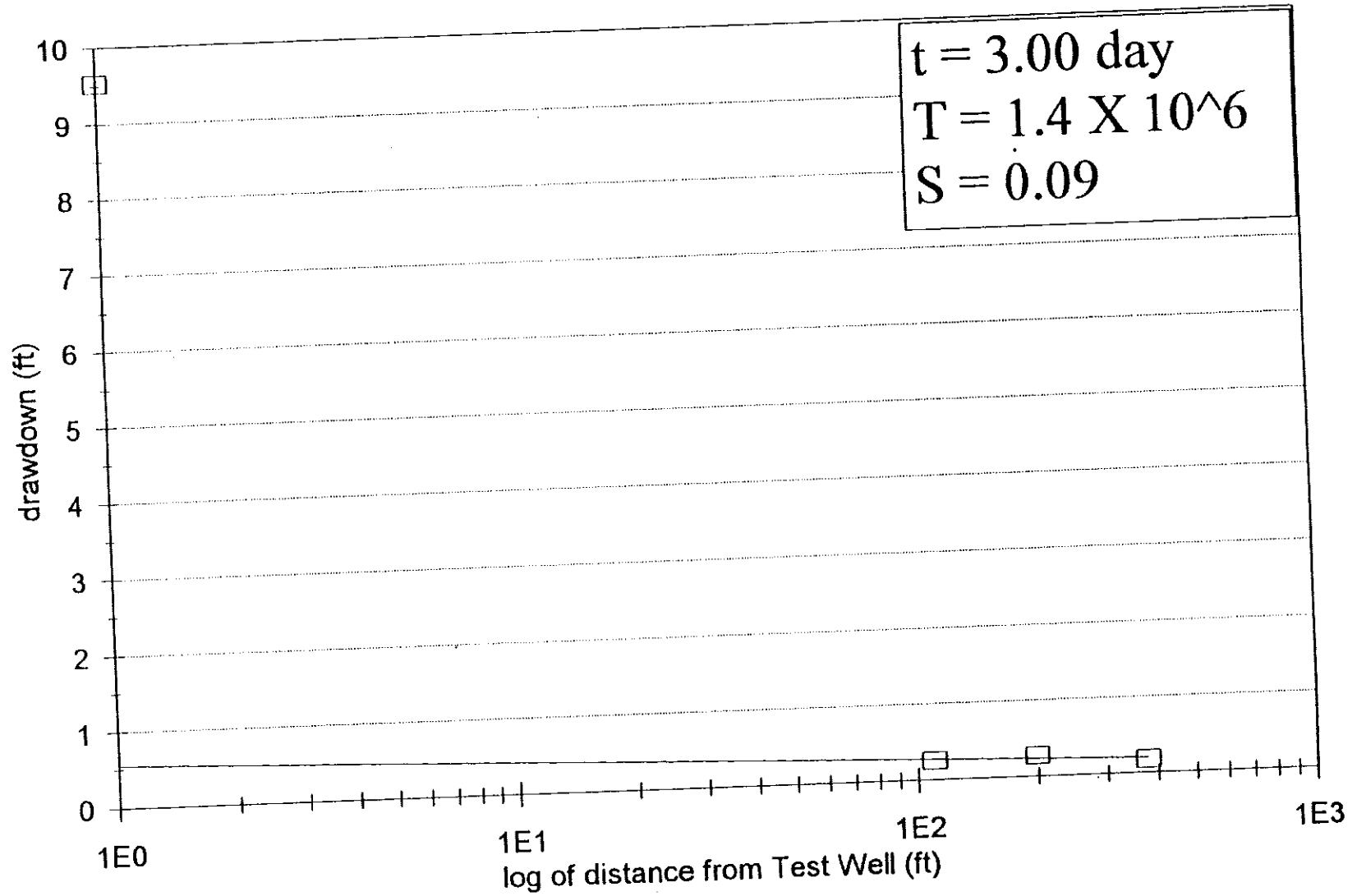
GERAGHTY
 & MILLER, INC.



Modeling Group

Large Scale Test

distance drawdown plot



EG&G Idaho, Inc.

FORM EGG-2631#

(Rev. 01-92)

t = 1 day

Q= 577540 ft³/day duration = 3.00 day

well	drawdown	distance	log dist	regression
Test Well	9.53	1	0.00	0.56
OW1U	0.25	110.02	2.04	0.27
120	0.27	199.89	2.30	0.24
OW2U	0.18	378.29	2.58	0.20

Well eff@ 3000 gpm
6 %

Regression Output:

Constant	0.556806
Std Err of Y Est	0.044535
R Squared	0.583866
No. of Observations	3
Degrees of Freedom	1

X Coefficient(s)	-0.13906
Std Err of Coef.	0.117401

ro= 10092 ft
dh= 1.39E-01 ft
T= 1.4E+06 ft²/day
S= 0.09
K= 9003 ft/day

P A P A D O P V2.1

Directional Permeability Analysis

IN-SITU INC. SOFTWARE SERIES

RWMC aquifer pumping test

Well #	X (ft)	Y (ft)	T (ft**2/d)	S
1	50.83	97.57	1.52E+06	1.31E-01
2	188.15	-328.18	1.51E+06	1.37E-01
3	-199.89	-1.31	1.33E+06	1.37E-01

SUMMARY OF RESULTS - 3 WELL COMBINATIONS

Well No.	T-major (ft**2/d)	T-minor (ft**2/d)	T-mean (ft**2/d)	Angle of T-major (degrees)	Storage Coeff.
1 2 3	1.61E+06	1.31E+06	1.45E+06	83.1	1.35E-01

PAPADOP COMPLETED

P A P A D O P V2.1

Directional Permeability Analysis

IN-SITU INC. SOFTWARE SERIES

RWMC aquifer pumping test

Well #	X (ft)	Y (ft)	T (ft**2/d)	S
1	50.83	97.57	5.90E+06	5.30E-02
2	188.15	-328.18	7.79E+06	4.20E-02
3	-199.89	-1.31	1.16E+06	5.00E-02

SUMMARY OF RESULTS - 3 WELL COMBINATIONS

Well No.	T-major (ft**2/d)	T-minor (ft**2/d)	T-mean (ft**2/d)	Angle of T-major (degrees)	Storage Coeff.
1 2 3	Probably heterogeneous media				

PAPADOP COMPLETED

APPENDIX D - Graphs of the Numerical Model Results

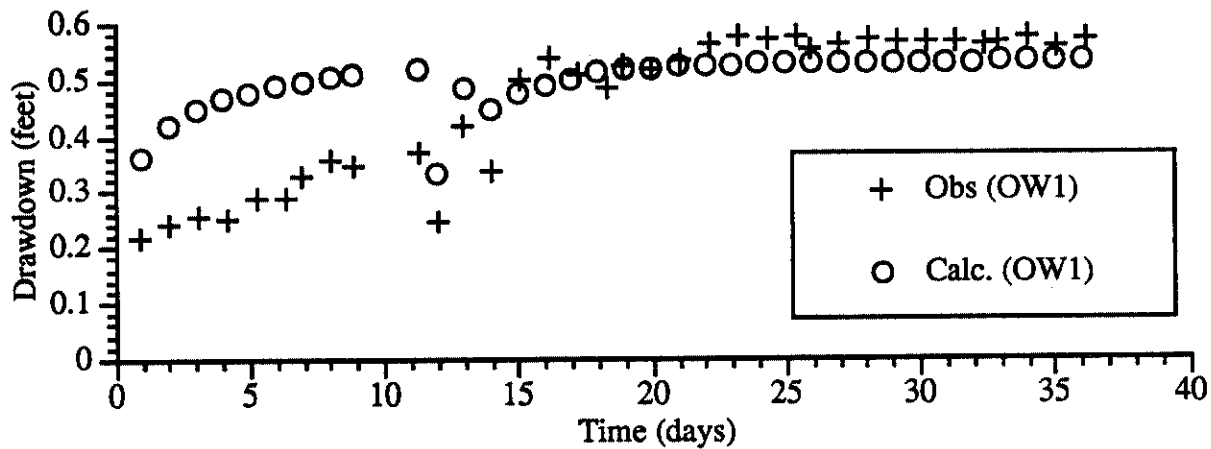


Figure D-1. Comparison of the well OW1 drawdown values used for the calibration and the simulated drawdowns for test run 1 (homogeneous T, $S_y=1.3$).

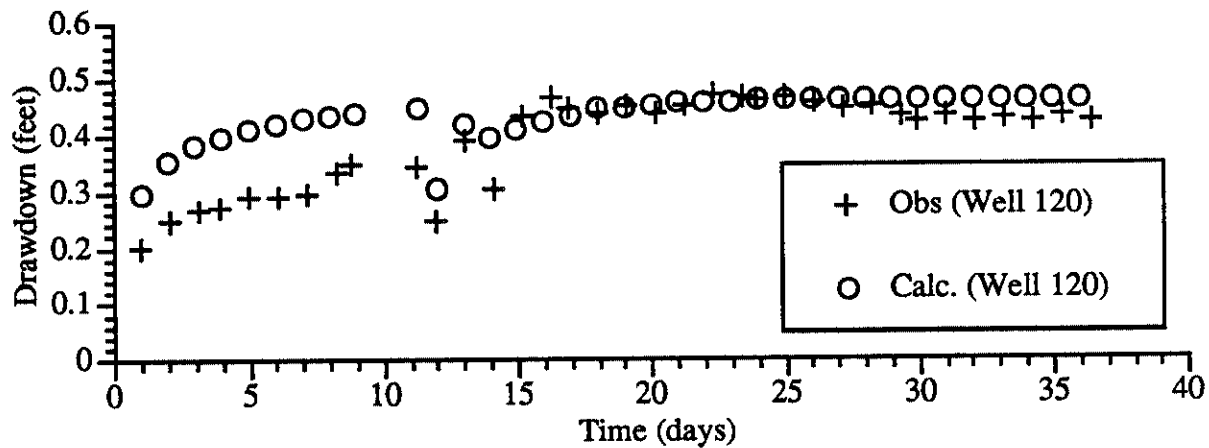


Figure D-2. Comparison of the well 120 drawdown values used for the calibration and the simulated drawdowns for test run 1 (homogeneous T, $S_y=1.3$).

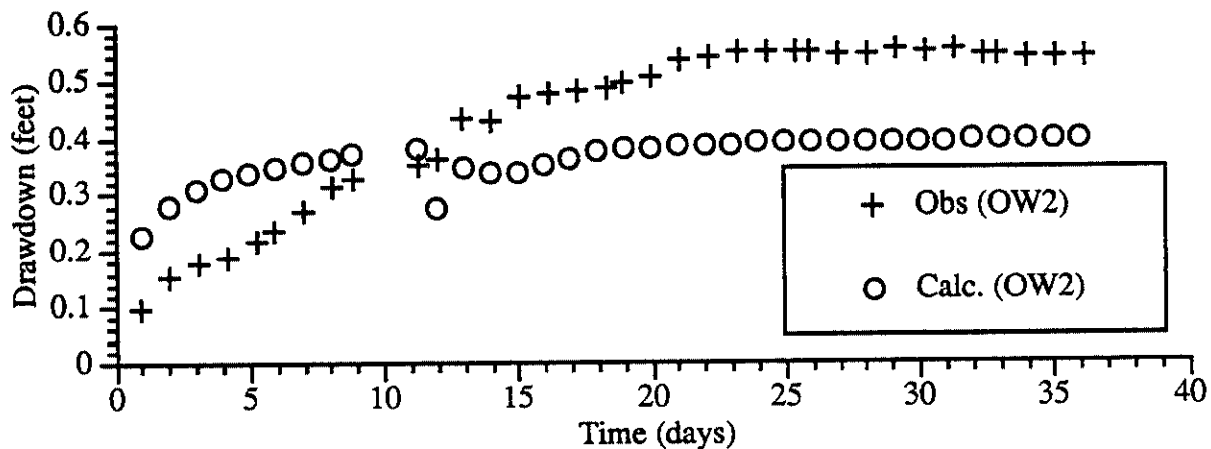


Figure D-3. Comparison of the well OW2 drawdown values used for the calibration and the simulated drawdowns for test run 1 (homogeneous T, $S_y=1.3$).

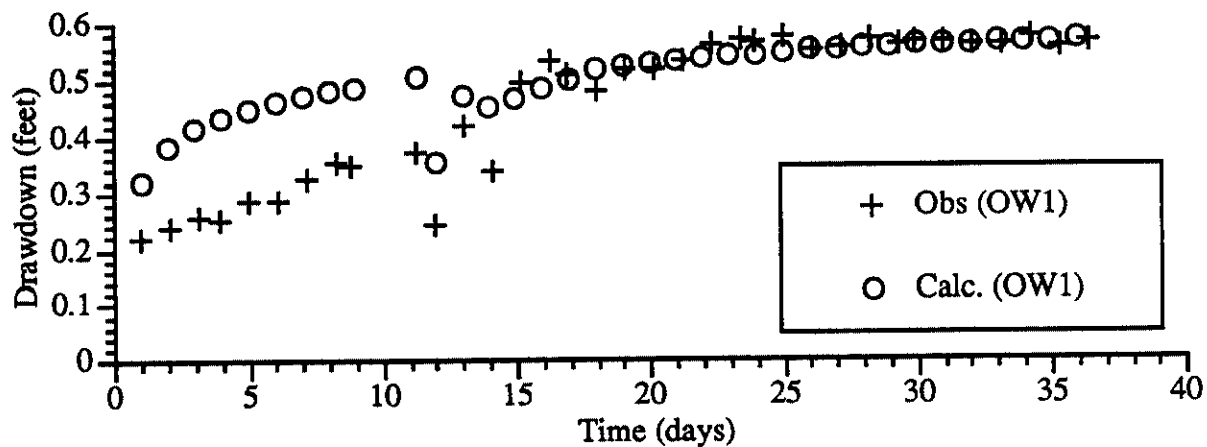


Figure D-4. Comparison of the well OW1 drawdown values used for the calibration and the simulated drawdowns for test run 2 (homogeneous T and Sy).

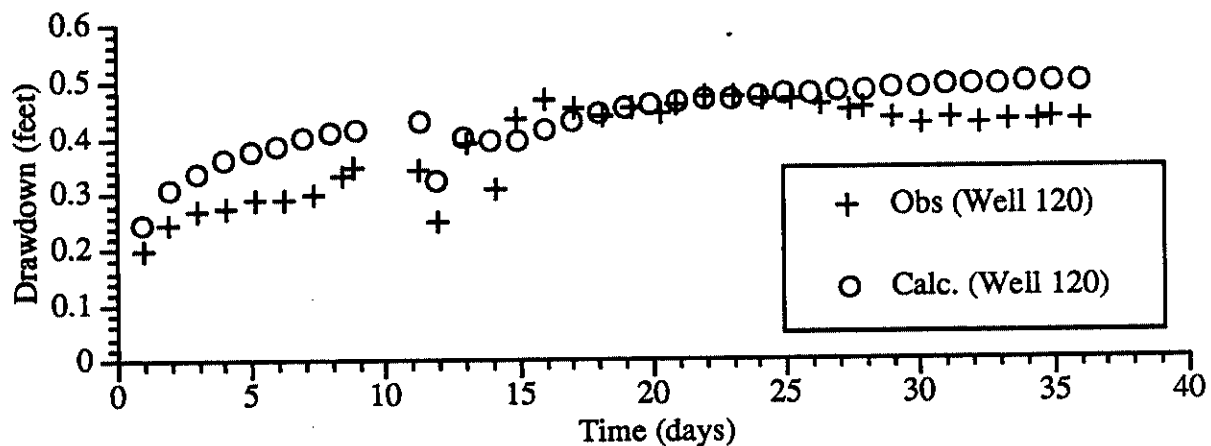


Figure D-5. Comparison of the well 120 drawdown values used for the calibration and the simulated drawdowns for test run 2 (homogeneous T and Sy).

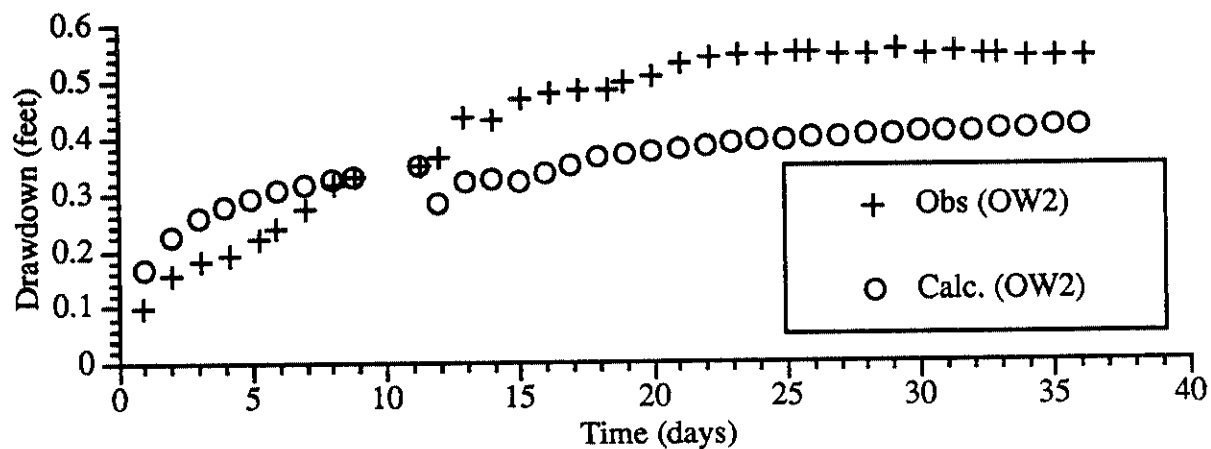


Figure D-6. Comparison of the well OW2 drawdown values used for the calibration and the simulated drawdowns for test run 2 (homogeneous T and Sy).

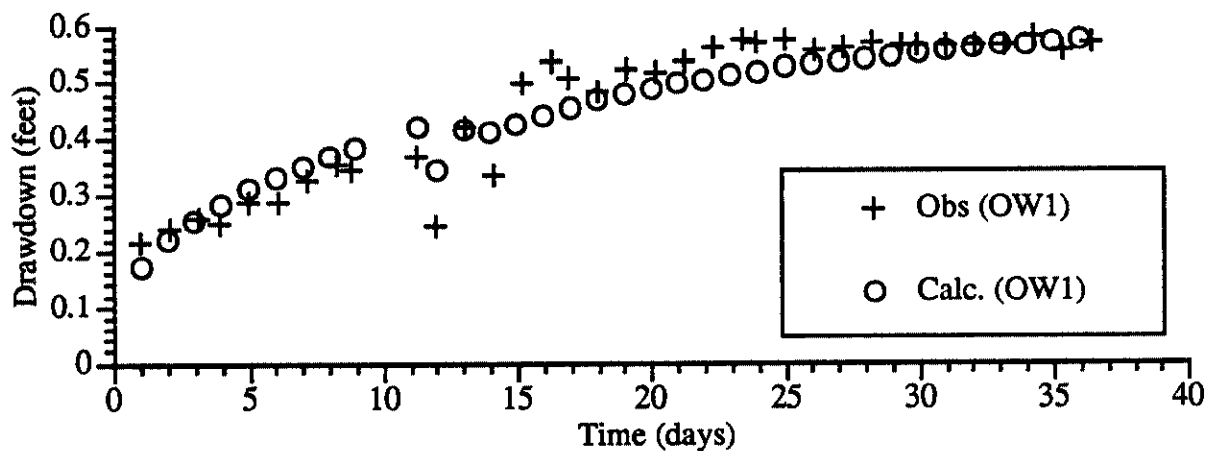


Figure D-7. Comparison of the well OW1 drawdown values used for the calibration and the simulated drawdowns for test run 4 (two T zones and $S_y=1.3$).

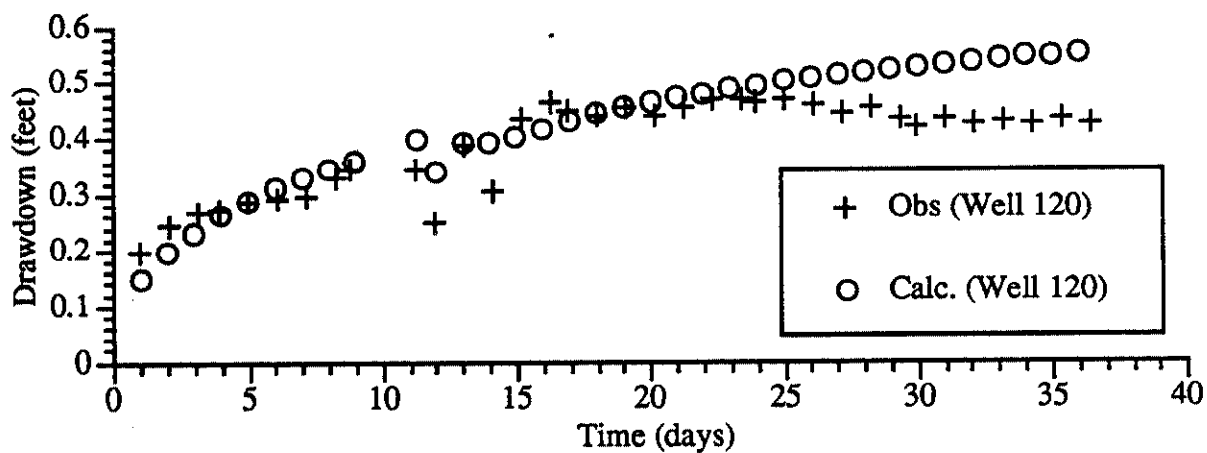


Figure D-8. Comparison of the well 120 drawdown values used for the calibration and the simulated drawdowns for test run 4 (two T zones and $S_y=1.3$).

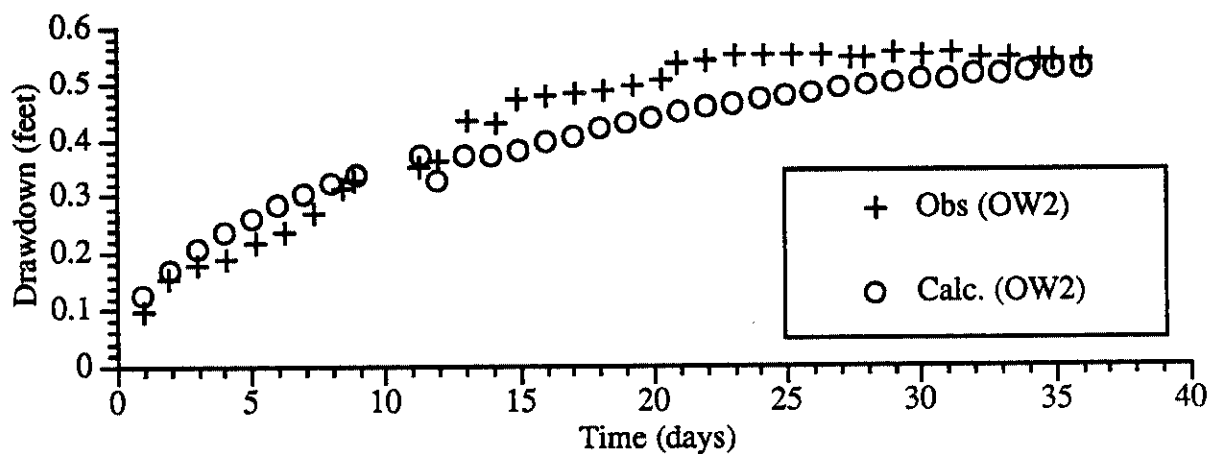


Figure D-9. Comparison of the well OW2 drawdown values used for the calibration and the simulated drawdowns for test run 4 (two T zones and $S_y=1.3$).

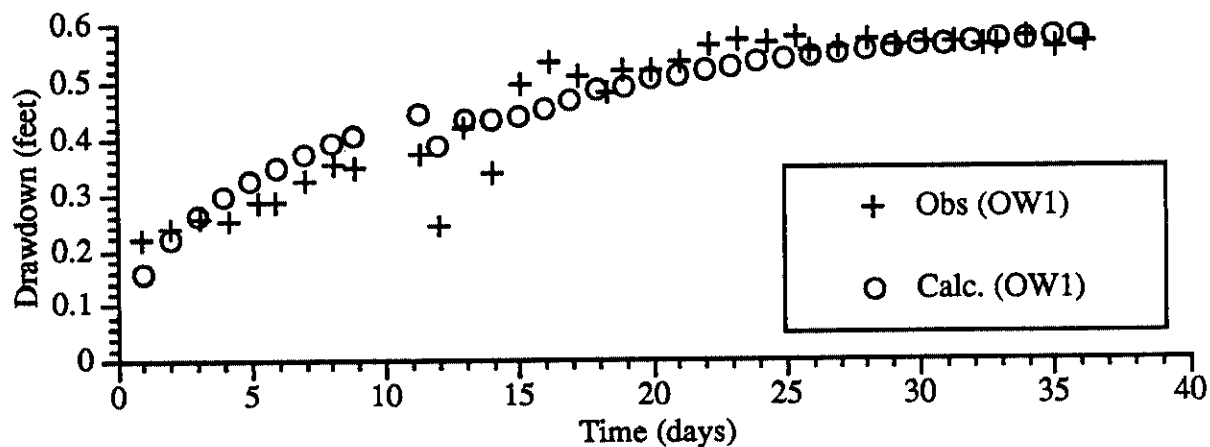


Figure D-10. Comparison of the well OW1 drawdown values used for the calibration and the simulated drawdowns for test run 7 (four T zones and homogeneous Sy).

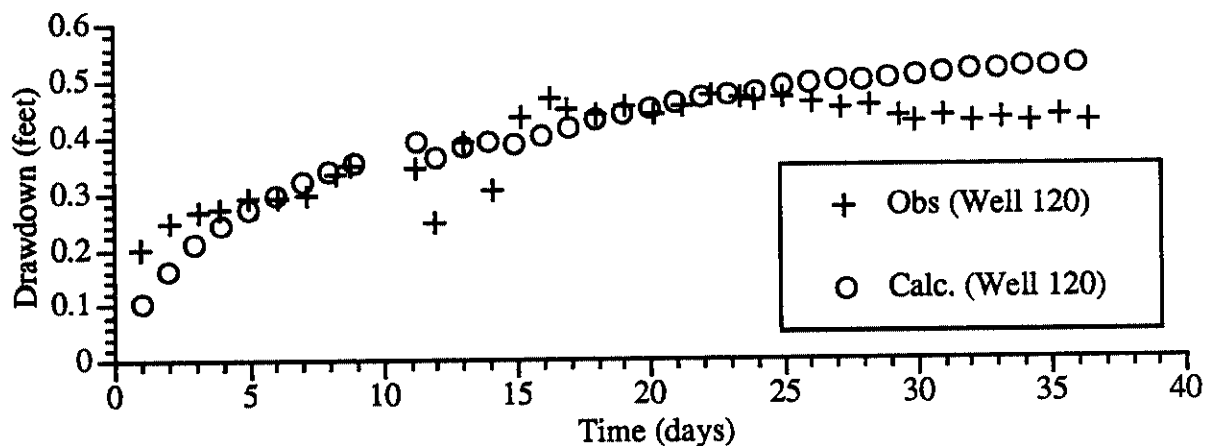


Figure D-11. Comparison of the well 120 drawdown values used for the calibration and the simulated drawdowns for test run 7 (four T zones and homogeneous Sy).

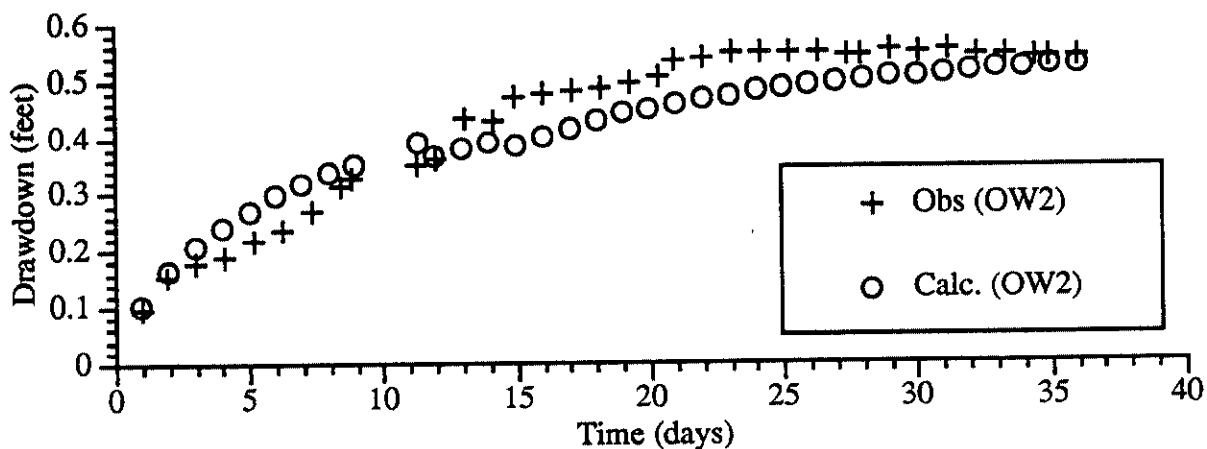


Figure D-12. Comparison of the well OW2 drawdown values used for the calibration and the simulated drawdowns for test run 7 (four T zones and homogeneous Sy).

APPENDIX E - MODFLOWP Input Files for Test Run Number 5

List of Input and Output Files and the Assigned Unit Numbers

out_2K_homoSy	2
bas.inp	1
bcf2.inp	11
wel.inp	12
oc.inp	22
pcg2.inp	23
pe.inp	25
ibound.inp	31
delta_row.inp	32
delta_col.inp	33
kzones_new.inp	34

Basic Package Input File

Large Scale Pumping Test - two dimensional transient simulation.

Prepared by James McCarthy, Jan. 1995.

1	201	201	34	4	NLAY,NROW,NCOL,NPER,ITMUNI
11 12 0 0 0 0 0 0 0 0 0 22 23 0 25 0 0 0					
0	1	IAPART,ISTRT			
31	1	(4012)			-1 LOCAT,ICONST,FMTIN,IPRN, IBOUND
999.					Inactive node value
0	0.0	(15X,F10.2)			-1 LOCAT,CNSTNT,FMTIN,IPRN, ic
0.0001	1	1.0	PERLEN,NSTP,TSMULT (modflowp adds one stress per. for ss)		
10.9999	11	1.0	PERLEN,NSTP,TSMULT		
0.7778	1	1.0	PERLEN,NSTP,TSMULT		
0.3750	1	1.0	PERLEN,NSTP,TSMULT		
0.8472	1	1.0	PERLEN,NSTP,TSMULT		
0.9340	1	1.0	PERLEN,NSTP,TSMULT		
0.3752	1	1.0	PERLEN,NSTP,TSMULT		
0.6908	1	1.0	PERLEN,NSTP,TSMULT		
21.000	7	1.0	PERLEN,NSTP,TSMULT		
0.2868	1	1.0	PERLEN,NSTP,TSMULT		
0.7132	1	1.0	PERLEN,NSTP,TSMULT		
14.000	7	1.0	PERLEN,NSTP,TSMULT		

[illegible][illegible][illegible]

-1

•

[illegible][illegible][illegible]

Row 201

Block Centered Flow Package Input File

	0	0	0.	0	0.5	2	0	
1		/						
	0	1.0			/			TRPY(NLAY) anisotropy level
	32	1.0	(15f5.0)		-1 /			DELR(NCOL) units feet
	33	1.0	(15f5.0)		-1 /			DELC(NROW) units feet
	0	0.13						sfl(ncol,nrow) storage coeff.
	0	5000.	(15X,G15.4)		-1			LOCAT,CNSTNT,FMTIN,IPRN K layer 1 (f/d)
	0	-155.	(15X,G15.4)		-1			LOCAT,CNSTNT,FMTIN,IPRN BOT layer 1 (f)

Cell Width Along Rows - Used With the Block Centered Flow Package Input File

400.	400.	400.	400.	400.	400.	400.	400.	400.	400.	300.	300.	300.	300.	300.
300.	300.	300.	300.	300.	200.	200.	200.	200.	200.	200.	200.	200.	200.	200.
200.	200.	200.	200.	200.	200.	200.	200.	200.	200.	50.	50.	50.	50.	50.
50.	50.	50.	50.	50.	50.	50.	50.	50.	50.	25.	25.	25.	25.	25.
10.	10.	10.	10.	10.	10.	10.	10.	10.	10.	10.	10.	10.	10.	10.
10.	10.	10.	10.	10.	10.	10.	10.	10.	10.	10.	10.	10.	10.	10.
10.	10.	10.	10.	10.	10.	10.	10.	10.	10.	10.	10.	10.	10.	10.
10.	10.	10.	10.	10.	10.	10.	10.	10.	10.	10.	10.	10.	10.	10.
10.	10.	10.	10.	10.	10.	10.	10.	10.	10.	10.	10.	10.	10.	10.
10.	10.	10.	10.	10.	10.	25.	25.	25.	25.	25.	50.	50.	50.	50.
50.	50.	50.	50.	50.	50.	50.	50.	50.	50.	50.	200.	200.	200.	200.
200.	200.	200.	200.	200.	200.	200.	200.	200.	200.	200.	200.	200.	200.	200.
200.	300.	300.	300.	300.	300.	300.	300.	300.	300.	300.	400.	400.	400.	400.
400.	400.	400.	400.	400.	400.									

Cell Width Along Columns - Used With the Block Centered Flow Package Input File

400.	400.	400.	400.	400.	400.	400.	400.	400.	400.	300.	300.	300.	300.	300.
300.	300.	300.	300.	300.	200.	200.	200.	200.	200.	200.	200.	200.	200.	200.
200.	200.	200.	200.	200.	200.	200.	200.	200.	200.	50.	50.	50.	50.	50.
50.	50.	50.	50.	50.	50.	50.	50.	50.	50.	25.	25.	25.	25.	25.
10.	10.	10.	10.	10.	10.	10.	10.	10.	10.	10.	10.	10.	10.	10.
10.	10.	10.	10.	10.	10.	10.	10.	10.	10.	10.	10.	10.	10.	10.
10.	10.	10.	10.	10.	10.	10.	10.	10.	10.	10.	10.	10.	10.	10.
10.	10.	10.	10.	10.	10.	10.	10.	10.	10.	10.	10.	10.	10.	10.
10.	10.	10.	10.	10.	10.	10.	10.	10.	10.	10.	10.	10.	10.	10.
10.	10.	10.	10.	10.	10.	10.	10.	10.	10.	10.	10.	10.	10.	10.
10.	10.	10.	10.	10.	10.	25.	25.	25.	25.	25.	50.	50.	50.	50.
50.	50.	50.	50.	50.	50.	50.	50.	50.	50.	50.	200.	200.	200.	200.
200.	200.	200.	200.	200.	200.	200.	200.	200.	200.	200.	200.	200.	200.	200.
200.	300.	300.	300.	300.	300.	300.	300.	300.	300.	300.	400.	400.	400.	400.
400.	400.	400.	400.	400.	400.									

Well Package Input File

1	0			
1				
1	101	101	0.00	when using pe need this ss pumping
1				
1	101	101	-5.775e+5	stress period 1
1				
1	101	101	-5.775e+5	stress period 2
1				
1	101	101	-5.775e+5	stress period 3
1				
1	101	101	0.0	stress period 4
1				
1	101	101	-5.775e+5	stress period 5
1				
1	101	101	-5.775e+5	stress period 6
1				
1	101	101	0.0	stress period 7
1				
1	101	101	-5.775e+5	stress period 8
1				
1	101	101	-5.775e+5	stress period 9
1				
1	101	101	-5.775e+5	stress period 10
1				
1	101	101	0.0	stress period 11
1				
1	101	101	0.0	stress period 12

Output Control Package Input File

-1	-1	91	92	IHEDFM, IDDNFM, IHEDUN, IDDNUN
0	0	2	1	INCODE, IHDDFL, IBUDFL, ICBCFL (ss time step)
1	0	3	0	Hdpr, Ddpr, Hdsv, Ddsv all layers
0	0	2	1	INCODE, IHDDFL, IBUDFL, ICBCFL (time step 1)
1	0	3	0	Hdpr, Ddpr, Hdsv, Ddsv all layers
-1	0	2	1	INCODE, IHDDFL, IBUDFL, ICBCFL (time step 2)
-1	0	2	1	INCODE, IHDDFL, IBUDFL, ICBCFL (time step 3)
-1	0	2	1	INCODE, IHDDFL, IBUDFL, ICBCFL (time step 4)
-1	0	2	1	INCODE, IHDDFL, IBUDFL, ICBCFL (time step 5)
-1	0	2	1	INCODE, IHDDFL, IBUDFL, ICBCFL (time step 6)
-1	0	2	1	INCODE, IHDDFL, IBUDFL, ICBCFL (time step 7)
-1	0	2	1	INCODE, IHDDFL, IBUDFL, ICBCFL (time step 8)
-1	0	2	1	INCODE, IHDDFL, IBUDFL, ICBCFL (time step 9)
-1	0	2	1	INCODE, IHDDFL, IBUDFL, ICBCFL (time step 10)
-1	0	2	1	INCODE, IHDDFL, IBUDFL, ICBCFL (time step 11)
-1	0	2	1	INCODE, IHDDFL, IBUDFL, ICBCFL (time step 12)
-1	0	2	1	INCODE, IHDDFL, IBUDFL, ICBCFL (time step 13)
-1	0	2	1	INCODE, IHDDFL, IBUDFL, ICBCFL (time step 14)
-1	0	2	1	INCODE, IHDDFL, IBUDFL, ICBCFL (time step 15)
-1	0	2	1	INCODE, IHDDFL, IBUDFL, ICBCFL (time step 16)
-1	0	2	1	INCODE, IHDDFL, IBUDFL, ICBCFL (time step 17)
-1	0	2	1	INCODE, IHDDFL, IBUDFL, ICBCFL (time step 18)
-1	0	2	1	INCODE, IHDDFL, IBUDFL, ICBCFL (time step 19)
-1	0	2	1	INCODE, IHDDFL, IBUDFL, ICBCFL (time step 20)
-1	0	2	1	INCODE, IHDDFL, IBUDFL, ICBCFL (time step 21)
-1	0	2	1	INCODE, IHDDFL, IBUDFL, ICBCFL (time step 22)
-1	0	2	1	INCODE, IHDDFL, IBUDFL, ICBCFL (time step 23)
-1	0	2	1	INCODE, IHDDFL, IBUDFL, ICBCFL (time step 24)
-1	0	2	1	INCODE, IHDDFL, IBUDFL, ICBCFL (time step 25)

Large Scale Pumping Test -

LINE 1
LINE 2
LINE 3
LINE 4
LINE 5
LINE 6
LINE 7
LINE 8

[illegible]

Data set 4, Zone array
DATA SET 5

	34	1	(4013)		-1				Data S	
	1.0	1.0	0	0	1.0				DATA S	
owlu	1	90	101	2	.0000	.0000	.0068	-.21500	1.00000	0
owlu	1	90	101	3	.0000	.0000	.0068	-.23800	1.00000	0
owlu	1	90	101	4	.0000	.0000	.0068	-.25600	1.00000	0
owlu	1	90	101	5	.0000	.0000	.0068	-.24933	1.00000	0
owlu	1	90	101	6	.0000	.0000	.0068	-.28633	1.00000	0
owlu	1	90	101	7	.0000	.0000	.0069	-.28633	1.00000	0
owlu	1	90	101	8	.0000	.0000	.0069	-.32367	1.00000	0
owlu	1	90	101	9	.0000	.0000	.0069	-.35400	1.00000	0
owlu	1	90	101	9	.0000	.0000	.8819	-.34500	1.00000	0
owlu	1	90	101	12	.0000	.0000	.4371	-.36933	1.00000	0
owlu	1	90	101	13	.0000	.0000	.6112	-.24333	1.00000	0
owlu	1	90	101	15	.0000	.0000	.0075	-.41867	1.00000	0
owlu	1	90	101	16	.0000	.0000	.1946	-.33533	1.00000	0
owlu	1	90	101	18	.0000	.0000	.0023	-.49733	1.00000	0
owlu	1	90	101	18	.0000	.0000	.3357	-.53500	1.00000	0
owlu	1	90	101	18	.0000	.0000	.6690	-.50800	1.00000	0
owlu	1	90	101	19	.0000	.0000	.0023	-.48333	1.00000	0
owlu	1	90	101	19	.0000	.0000	.3357	-.52233	1.00000	0
owlu	1	90	101	19	.0000	.0000	.6690	-.51900	1.00000	0
owlu	1	90	101	20	.0000	.0000	.0023	-.53367	1.00000	0
owlu	1	90	101	20	.0000	.0000	.3357	-.56100	1.00000	0
owlu	1	90	101	20	.0000	.0000	.6690	-.57367	1.00000	0
owlu	1	90	101	21	.0000	.0000	.0023	-.57033	1.00000	0
owlu	1	90	101	21	.0000	.0000	.3357	-.57467	1.00000	0
owlu	1	90	101	21	.0000	.0000	.6690	-.55333	1.00000	0
owlu	1	90	101	22	.0000	.0000	.0023	-.55967	1.00000	0
owlu	1	90	101	22	.0000	.0000	.3357	-.57133	1.00000	0
owlu	1	90	101	22	.0000	.0000	.6690	-.56433	1.00000	0
owlu	1	90	101	23	.0000	.0000	.0023	-.56700	1.00000	0
owlu	1	90	101	23	.0000	.0000	.3357	-.56733	1.00000	0
owlu	1	90	101	23	.0000	.0000	.6690	-.56267	1.00000	0
owlu	1	90	101	24	.0000	.0000	.0023	-.56400	1.00000	0
owlu	1	90	101	24	.0000	.0000	.3357	-.57833	1.00000	0
owlu	1	90	101	24	.0000	.0000	.6690	-.55733	1.00000	0
owlu	1	90	101	25	.0000	.0000	.0244	-.57000	1.00000	0
owlu	1	90	101	25	.0000	.0000	.6416	-.58483	1.00000	0
w120	1	111	84	2	.0000	-.3200	.0068	-.19567	1.00000	0
w120	1	111	84	3	.0000	-.3200	.0068	-.24367	1.00000	0
w120	1	111	84	4	.0000	-.3200	.0068	-.26667	1.00000	0
w120	1	111	84	5	.0000	-.3200	.0068	-.27233	1.00000	0
w120	1	111	84	6	.0000	-.3200	.0068	-.28700	1.00000	0
w120	1	111								

w120	1	111	84	12	.0000	-.3200	.4371	-.34200	1.00000	0
w120	1	111	84	13	.0000	-.3200	.6112	-.24733	1.00000	0
w120	1	111	84	15	.0000	-.3200	.0075	-.38867	1.00000	0
w120	1	111	84	16	.0000	-.3200	.1946	-.30533	1.00000	0
w120	1	111	84	18	.0000	-.3200	.0023	-.43367	1.00000	0
w120	1	111	84	18	.0000	-.3200	.3357	-.46533	1.00000	0
w120	1	111	84	18	.0000	-.3200	.6690	-.44967	1.00000	0
w120	1	111	84	19	.0000	-.3200	.0023	-.43767	1.00000	0
w120	1	111	84	19	.0000	-.3200	.3357	-.45167	1.00000	0
w120	1	111	84	19	.0000	-.3200	.6690	-.43933	1.00000	0
w120	1	111	84	20	.0000	-.3200	.0023	-.45367	1.00000	0
w120	1	111	84	20	.0000	-.3200	.3357	-.47067	1.00000	0
w120	1	111	84	20	.0000	-.3200	.6690	-.46767	1.00000	0
w120	1	111	84	21	.0000	-.3200	.0023	-.46433	1.00000	0
w120	1	111	84	21	.0000	-.3200	.3357	-.46733	1.00000	0
w120	1	111	84	21	.0000	-.3200	.6690	-.45667	1.00000	0
w120	1	111	84	22	.0000	-.3200	.0023	-.44633	1.00000	0
w120	1	111	84	22	.0000	-.3200	.3357	-.45267	1.00000	0
w120	1	111	84	22	.0000	-.3200	.6690	-.43333	1.00000	0
w120	1	111	84	23	.0000	-.3200	.0023	-.42167	1.00000	0
w120	1	111	84	23	.0000	-.3200	.3357	-.43367	1.00000	0
w120	1	111	84	23	.0000	-.3200	.6690	-.42367	1.00000	0
w120	1	111	84	24	.0000	-.3200	.0023	-.42800	1.00000	0
w120	1	111	84	24	.0000	-.3200	.3357	-.42533	1.00000	0
w120	1	111	84	24	.0000	-.3200	.6690	-.43300	1.00000	0
w120	1	111	84	25	.0000	-.3200	.0244	-.42567	1.00000	0
w120	1	111	84	25	.0000	-.3200	.6416	-.42300	1.00000	0
ow2u	1	120	134	2	.2500	.3400	.0068	-.09768	1.00000	0
ow2u	1	120	134	3	.2500	.3400	.0068	-.15368	1.00000	0
ow2u	1	120	134	4	.2500	.3400	.0068	-.17901	1.00000	0
ow2u	1	120	134	5	.2500	.3400	.0068	-.18934	1.00000	0
ow2u	1	120	134	6	.2500	.3400	.0068	-.21534	1.00000	0
ow2u	1	120	134	7	.2500	.3400	.0069	-.23734	1.00000	0
ow2u	1	120	134	8	.2500	.3400	.0069	-.26901	1.00000	0
ow2u	1	120	134	9	.2500	.3400	.0069	-.31101	1.00000	0
ow2u	1	120	134	9	.2500	.3400	.8819	-.32801	1.00000	0
ow2u	1	120	134	12	.2500	.3400	.4371	-.34901	1.00000	0
ow2u	1	120	134	13	.2500	.3400	.6112	-.36034	1.00000	0
ow2u	1	120	134	15	.2500	.3400	.0075	-.43401	1.00000	0
ow2u	1	120	134	16	.2500	.3400	.1946	-.42701	1.00000	0
ow2u	1	120	134	18	.2500	.3400	.0023	-.46801	1.00000	0
ow2u	1	120	134	18	.2500	.3400	.3357	-.47534	1.00000	0
ow2u	1	120	134	18	.2500	.3400	.6690	-.48101	1.00000	0
ow2u	1	120	134	19	.2500	.3400	.0023	-.48301	1.00000	0
ow2u	1	120	134	19	.2500	.3400	.3357	-.49534	1.00000	0
ow2u	1	120	134	19	.2500	.3400	.6690	-.50568	1.00000	0
ow2u	1	120	134	20	.2500	.3400	.0023	-.53101	1.00000	0
ow2u	1	120	134	20	.2500	.3400	.3357	-.53801	1.00000	0
ow2u	1	120	134	20	.2500	.3400	.6690	-.54468	1.00000	0
ow2u	1	120	134	21	.2500	.3400	.0023	-.54568	1.00000	0
ow2u	1	120	134	21	.2500	.3400	.3357	-.54734	1.00000	0
ow2u	1	120	134	21	.2500	.3400	.6690	-.54668	1.00000	0
ow2u	1	120	134	22	.2500	.3400	.0023	-.54301	1.00000	0
ow2u	1	120	134	22	.2500	.3400	.3357	-.54401	1.00000	0
ow2u	1	120	134	22	.2500	.3400	.6690	-.55101	1.00000	0
ow2u	1	120	134	23	.2500	.3400	.0023	-.54634	1.00000	0
ow2u	1	120	134	23	.2500	.3400	.3357	-.55001	1.00000	0
ow2u	1	120	134	23	.2500	.3400	.6690	-.54301	1.00000	0
ow2u	1	120	134	24	.2500	.3400	.0023	-.54334	1.00000	0
ow2u	1	120	134	24	.2500	.3400	.3357	-.53934	1.00000	0
ow2u	1	120	134	24	.2500	.3400	.6690	-.53801	1.00000	0
ow2u	1	120	134	25	.2500	.3400	.0244	-.53668	1.00000	0
ow2u	1	120	134	25	.2500	.3400	.6416	-.53301	1.00000	0

5000.0

5000.0

0.13

1.0

Data set 8

Data Set 9
Data Set 10
DATA SET 11
DATA SET 13
DATA SET 14

**Transmissivity (or Hydraulic Conductivity) Zone Flag File - Used
With the Parameter Estimation Package Input File**

This is a very long input file that assigns a transmissivity flag value for each of the finite difference grids based on the zones defined in Figure 20. The Domain is actually divided into 11 rather than the 4 zones shown in Figure 20 but zones 4 through 11 are all treated as one zone (zone 4).

Preconditioned Conjugate Gradient Package Input File

100	10	1				
1.e-03	1.e+01	1.00	2	0	0	0

Summary of MODFLOW Output File

PARAMETER ESTIMATION CONVERGED BECAUSE SUM OF SQUARED, WEIGHTED RESIDUALS HAS NOT CHANGED
1.0000 PERCENT IN 2 ITERATIONS

DATA AT HEAD LOCATIONS

WEIGHTED		TIME			ROW/COL/TIME			MEAS.	CALC.		
OBS#	ID	LAYER, ROW, COL	STEP	OFFSETS			HEAD	HEAD	RESIDUAL	WEIGHT**.	
RESIDUAL											
1	owlu	1 90 101	2	.00	.00	.01	-.215	-.155	-.601E-01	1.00	
2	owlu	1 90 101	3	.00	.00	.01	-.238	-.206	-.316E-01	1.00	
3	owlu	1 90 101	4	.00	.00	.01	-.256	-.246	-.104E-01	1.00	
4	owlu	1 90 101	5	.00	.00	.01	-.249	-.278	.285E-01	1.00	
5	owlu	1 90 101	6	.00	.00	.01	-.286	-.305	.191E-01	1.00	
6	owlu	1 90 101	7	.00	.00	.01	-.286	-.329	.431E-01	1.00	
7	owlu	1 90 101	8	.00	.00	.01	-.324	-.351	.271E-01	1.00	
8	owlu	1 90 101	9	.00	.00	.01	-.354	-.370	.159E-01	1.00	
9	owlu	1 90 101	9	.00	.00	.88	-.345	-.385	.401E-01	1.00	
10	owlu	1 90 101	12	.00	.00	.44	-.369	-.422	.525E-01	1.00	
11	owlu	1 90 101	13	.00	.00	.61	-.243	-.360	.117	1.00	
12	owlu	1 90 101	15	.00	.00	.01	-.419	-.418	-.388E-03	1.00	
13	owlu	1 90 101	16	.00	.00	.19	-.335	-.415	.792E-01	1.00	
14	owlu	1 90 101	18	.00	.00	.00	-.497	-.425	-.724E-01	1.00	
15	owlu	1 90 101	18	.00	.00	.34	-.535	-.439	-.960E-01	1.00	
16	owlu	1 90 101	18	.00	.00	.67	-.508	-.453	-.550E-01	1.00	
17	owlu	1 90 101	19	.00	.00	.00	-.483	-.467	-.164E-01	1.00	
18	owlu	1 90 101	19	.00	.00	.34	-.522	-.476	-.464E-01	1.00	
19	owlu	1 90 101	19	.00	.00	.67	-.519	-.485	-.341E-01	1.00	
20	owlu	1 90 101	20	.00	.00	.00	-.534	-.494	-.399E-01	1.00	
21	owlu	1 90 101	20	.00	.00	.34	-.561	-.501	-.605E-01	1.00	
22	owlu	1 90 101	20	.00	.00	.67	-.574	-.507	-.664E-01	1.00	
23	owlu	1 90 101	21	.00	.00	.00	-.570	-.514	-.564E-01	1.00	
24	owlu	1 90 101	21	.00	.00	.34	-.575	-.519	-.555E-01	1.00	
25	owlu	1 90 101	21	.00	.00	.67	-.553	-.524	-.289E-01	1.00	
26	owlu	1 90 101	22	.00	.00	.00	-.560	-.530	-.301E-01	1.00	
27	owlu	1 90 101	22	.00	.00	.34	-.571	-.534	-.376E-01	1.00	
28	owlu	1 90 101	22	.00	.00	.67	-.564	-.538	-.264E-01	1.00	
29	owlu	1 90 101	23	.00	.00	.00	-.567	-.542	-.249E-01	1.00	
30	owlu	1 90 101	23	.00	.00	.34	-.567	-.545	-.219E-01	1.00	
31	owlu	1 90 101	23	.00	.00	.67	-.563	-.549	-.139E-01	1.00	
32	owlu	1 90 101	24	.00	.00	.00	-.564	-.552	-.119E-01	1.00	

33	ow1u	1	90	101	24	.00	.00	.34	-.578	-.555	-.236E-01	1.00
34	ow1u	1	90	101	24	.00	.00	.67	-.557	-.557	.884E-04	1.00
35	ow1u	1	90	101	25	.00	.00	.02	-.570	-.560	-.992E-02	1.00
36	ow1u	1	90	101	25	.00	.00	.64	-.585	-.560	-.247E-01	1.00
37	w120	1	111	84	2	.00	-.32	.01	-.196	-.138	-.581E-01	1.00
38	w120	1	111	84	3	.00	-.32	.01	-.244	-.189	-.546E-01	1.00
39	w120	1	111	84	4	.00	-.32	.01	-.267	-.228	-.385E-01	1.00
40	w120	1	111	84	5	.00	-.32	.01	-.272	-.260	-.119E-01	1.00
41	w120	1	111	84	6	.00	-.32	.01	-.287	-.288	.101E-02	1.00
42	w120	1	111	84	7	.00	-.32	.01	-.290	-.312	.221E-01	1.00
43	w120	1	111	84	8	.00	-.32	.01	-.296	-.333	.374E-01	1.00
44	w120	1	111	84	9	.00	-.32	.01	-.331	-.353	.215E-01	1.00
45	w120	1	111	84	9	.00	-.32	.88	-.345	-.368	.227E-01	1.00
46	w120	1	111	84	12	.00	-.32	.44	-.342	-.404	.625E-01	1.00
47	w120	1	111	84	13	.00	-.32	.61	-.247	-.353	.106	1.00
48	w120	1	111	84	15	.00	-.32	.01	-.389	-.401	.122E-01	1.00
49	w120	1	111	84	16	.00	-.32	.19	-.305	-.400	.951E-01	1.00
50	w120	1	111	84	18	.00	-.32	.00	-.434	-.408	-.261E-01	1.00
51	w120	1	111	84	18	.00	-.32	.34	-.465	-.422	-.438E-01	1.00
52	w120	1	111	84	18	.00	-.32	.67	-.450	-.436	-.141E-01	1.00
53	w120	1	111	84	19	.00	-.32	.00	-.438	-.450	.118E-01	1.00
54	w120	1	111	84	19	.00	-.32	.34	-.452	-.458	.681E-02	1.00
55	w120	1	111	84	19	.00	-.32	.67	-.439	-.467	.281E-01	1.00
56	w120	1	111	84	20	.00	-.32	.00	-.454	-.476	.227E-01	1.00
57	w120	1	111	84	20	.00	-.32	.34	-.471	-.483	.124E-01	1.00
58	w120	1	111	84	20	.00	-.32	.67	-.468	-.490	.221E-01	1.00
59	w120	1	111	84	21	.00	-.32	.00	-.464	-.497	.322E-01	1.00
60	w120	1	111	84	21	.00	-.32	.34	-.467	-.502	.344E-01	1.00
61	w120	1	111	84	21	.00	-.32	.67	-.457	-.507	.503E-01	1.00
62	w120	1	111	84	22	.00	-.32	.00	-.446	-.512	.659E-01	1.00
63	w120	1	111	84	22	.00	-.32	.34	-.453	-.516	.637E-01	1.00
64	w120	1	111	84	22	.00	-.32	.67	-.433	-.520	.872E-01	1.00
65	w120	1	111	84	23	.00	-.32	.00	-.422	-.525	.103	1.00
66	w120	1	111	84	23	.00	-.32	.34	-.434	-.528	.943E-01	1.00
67	w120	1	111	84	23	.00	-.32	.67	-.424	-.531	.108	1.00
68	w120	1	111	84	24	.00	-.32	.00	-.428	-.535	.107	1.00
69	w120	1	111	84	24	.00	-.32	.34	-.425	-.537	.112	1.00
70	w120	1	111	84	24	.00	-.32	.67	-.433	-.540	.107	1.00
71	w120	1	111	84	25	.00	-.32	.02	-.426	-.543	.117	1.00
72	w120	1	111	84	25	.00	-.32	.64	-.423	-.543	.120	1.00
73	ow2u	1	120	134	2	.25	.34	.01	-.098	-.119	.210E-01	1.00
74	ow2u	1	120	134	3	.25	.34	.01	-.154	-.170	.164E-01	1.00
75	ow2u	1	120	134	4	.25	.34	.01	-.179	-.209	.302E-01	1.00
76	ow2u	1	120	134	5	.25	.34	.01	-.189	-.241	.521E-01	1.00
77	ow2u	1	120	134	6	.25	.34	.01	-.215	-.269	.536E-01	1.00
78	ow2u	1	120	134	7	.25	.34	.01	-.237	-.293	.557E-01	1.00
79	ow2u	1	120	134	8	.25	.34	.01	-.269	-.314	.453E-01	1.00
80	ow2u	1	120	134	9	.25	.34	.01	-.311	-.333	.225E-01	1.00
81	ow2u	1	120	134	9	.25	.34	.88	-.328	-.349	.206E-01	1.00
82	ow2u	1	120	134	12	.25	.34	.44	-.349	-.385	.364E-01	1.00
83	ow2u	1	120	134	13	.25	.34	.61	-.360	-.346	-.145E-01	1.00
84	ow2u	1	120	134	15	.25	.34	.01	-.434	-.382	-.521E-01	1.00
85	ow2u	1	120	134	16	.25	.34	.19	-.427	-.385	-.419E-01	1.00
86	ow2u	1	120	134	18	.25	.34	.00	-.468	-.389	-.794E-01	1.00
87	ow2u	1	120	134	18	.25	.34	.34	-.475	-.403	-.727E-01	1.00
88	ow2u	1	120	134	18	.25	.34	.67	-.481	-.417	-.645E-01	1.00
89	ow2u	1	120	134	19	.25	.34	.00	-.483	-.430	-.526E-01	1.00
90	ow2u	1	120	134	19	.25	.34	.34	-.495	-.439	-.559E-01	1.00
91	ow2u	1	120	134	19	.25	.34	.67	-.506	-.448	-.573E-01	1.00
92	ow2u	1	120	134	20	.25	.34	.00	-.531	-.457	-.737E-01	1.00
93	ow2u	1	120	134	20	.25	.34	.34	-.538	-.464	-.740E-01	1.00
94	ow2u	1	120	134	20	.25	.34	.67	-.545	-.471	-.739E-01	1.00
95	ow2u	1	120	134	21	.25	.34	.00	-.546	-.477	-.682E-01	1.00
96	ow2u	1	120	134	21	.25	.34	.34	-.547	-.483	-.647E-01	1.00

97	ow2u	1	120	134	21	.25	.34	.67	-.547	-.488	-.588E-01	1.00
98	ow2u	1	120	134	22	.25	.34	.00	-.543	-.493	-.499E-01	1.00
99	ow2u	1	120	134	22	.25	.34	.34	-.544	-.497	-.467E-01	1.00
100	ow2u	1	120	134	22	.25	.34	.67	-.551	-.501	-.496E-01	1.00
101	ow2u	1	120	134	23	.25	.34	.00	-.546	-.506	-.408E-01	1.00
102	ow2u	1	120	134	23	.25	.34	.34	-.550	-.509	-.411E-01	1.00
103	ow2u	1	120	134	23	.25	.34	.67	-.543	-.512	-.308E-01	1.00
104	ow2u	1	120	134	24	.25	.34	.00	-.543	-.516	-.278E-01	1.00
105	ow2u	1	120	134	24	.25	.34	.34	-.539	-.518	-.211E-01	1.00
106	ow2u	1	120	134	24	.25	.34	.67	-.538	-.521	-.171E-01	1.00
107	ow2u	1	120	134	25	.25	.34	.02	-.537	-.524	-.131E-01	1.00
108	ow2u	1	120	134	25	.25	.34	.64	-.533	-.524	-.943E-02	1.00

STATISTICS FOR THESE RESIDUALS :

MAXIMUM WEIGHTED RESIDUAL : .120E+00 OBS# 72

MINIMUM WEIGHTED RESIDUAL : -.960E-01 OBS# 15

AVERAGE WEIGHTED RESIDUAL : .721E-04

RESIDUALS >= 0. : 49

RESIDUALS < 0. : 59

NUMBER OF RUNS : 11 IN 108 OBSERVATIONS

SUM OF SQUARED WEIGHTED RESIDUALS (HEADS) .31796

SUM OF SQUARED WEIGHTED RESIDUALS (ALL DEP. VAR.) .31796

STATISTICS FOR ALL RESIDUALS :

AVERAGE WEIGHTED RESIDUAL : .721E-04

RESIDUALS >= 0. : 49

RESIDUALS < 0. : 59

NUMBER OF RUNS : 11 IN 109 OBSERVATIONS

RUNS STATISTIC (TOO FEW RUNS): -8.39

(IF #NEG>10 AND #POS>10, P(STAT < -1.28) = 0.10,

P(STAT < -1.645) = 0.05,

P(STAT < -1.96) = 0.025)

RUNS STATISTIC (TOO MANY RUNS): -8.59

(IF #NEG>10 AND #POS>10, P(STAT > 1.28) = 0.10,

P(STAT > 1.645) = 0.05,

P(STAT > 1.96) = 0.025)

SCALED SENSITIVITIES (SCALED BY B*(WT**.5))

PARAMETER # :	1	2	3
PARAMETER ID :	T	T	S1
OBS# & ID			
1 owlu	.867	.116	.518E-01
2 owlu	.927	.253	.785E-01
3 owlu	.951	.387	.969E-01
4 owlu	.967	.513	.110
5 owlu	.979	.633	.120
6 owlu	.988	.746	.128
7 owlu	.995	.853	.134
8 owlu	1.00	.956	.139
9 owlu	1.01	1.04	.141
10 owlu	1.01	1.27	.146
11 owlu	.527	1.31	.127
12 owlu	.976	1.37	.132
13 owlu	.854	1.45	.130
14 owlu	.967	1.50	.123
15 owlu	.984	1.58	.124
16 owlu	1.00	1.66	.125
17 owlu	1.02	1.74	.127
18 owlu	1.02	1.82	.125
19 owlu	1.03	1.89	.123
20 owlu	1.03	1.97	.121
21 owlu	1.03	2.04	.118
22 owlu	1.03	2.10	.116

23	owlu	1.04	2.17	.113
24	owlu	1.04	2.23	.110
25	owlu	1.04	2.29	.106
26	owlu	1.04	2.35	.103
27	owlu	1.04	2.41	.998E-01
28	owlu	1.04	2.46	.964E-01
29	owlu	1.04	2.52	.931E-01
30	owlu	1.04	2.57	.897E-01
31	owlu	1.05	2.61	.864E-01
32	owlu	1.05	2.66	.831E-01
33	owlu	1.05	2.70	.800E-01
34	owlu	1.05	2.75	.768E-01
35	owlu	1.05	2.79	.736E-01
36	owlu	1.05	2.79	.736E-01
37	w120	.694	.116	.517E-01
38	w120	.754	.253	.785E-01
39	w120	.779	.387	.969E-01
40	w120	.795	.513	.110
41	w120	.806	.633	.120
42	w120	.815	.746	.128
43	w120	.822	.853	.134
44	w120	.828	.956	.139
45	w120	.832	1.04	.141
46	w120	.842	1.27	.146
47	w120	.459	1.31	.127
48	w120	.803	1.37	.132
49	w120	.714	1.45	.130
50	w120	.795	1.50	.123
51	w120	.812	1.58	.124
52	w120	.829	1.66	.125
53	w120	.846	1.74	.126
54	w120	.850	1.82	.125
55	w120	.853	1.89	.123
56	w120	.857	1.97	.121
57	w120	.859	2.04	.118
58	w120	.861	2.10	.116
59	w120	.863	2.17	.113
60	w120	.865	2.23	.110
61	w120	.866	2.29	.106
62	w120	.867	2.35	.103
63	w120	.868	2.41	.998E-01
64	w120	.869	2.46	.964E-01
65	w120	.870	2.52	.930E-01
66	w120	.871	2.56	.897E-01
67	w120	.872	2.61	.864E-01
68	w120	.873	2.66	.831E-01
69	w120	.874	2.70	.799E-01
70	w120	.874	2.75	.768E-01
71	w120	.875	2.79	.736E-01
72	w120	.875	2.79	.736E-01
73	ow2u	.507	.116	.516E-01
74	ow2u	.566	.253	.785E-01
75	ow2u	.590	.387	.969E-01
76	ow2u	.606	.514	.110
77	ow2u	.617	.633	.120
78	ow2u	.626	.746	.128
79	ow2u	.633	.853	.134
80	ow2u	.639	.956	.138
81	ow2u	.643	1.04	.141
82	ow2u	.653	1.27	.146
83	ow2u	.383	1.31	.127
84	ow2u	.616	1.37	.132
85	ow2u	.561	1.45	.130
86	ow2u	.607	1.49	.123

87	ow2u	.624	1.58	.124
88	ow2u	.641	1.66	.125
89	ow2u	.657	1.74	.126
90	ow2u	.661	1.82	.125
91	ow2u	.664	1.89	.123
92	ow2u	.668	1.97	.121
93	ow2u	.670	2.04	.118
94	ow2u	.672	2.10	.116
95	ow2u	.674	2.17	.113
96	ow2u	.675	2.23	.110
97	ow2u	.677	2.29	.106
98	ow2u	.678	2.35	.103
99	ow2u	.679	2.41	.997E-01
100	ow2u	.680	2.46	.964E-01
101	ow2u	.681	2.52	.930E-01
102	ow2u	.682	2.56	.897E-01
103	ow2u	.683	2.61	.864E-01
104	ow2u	.684	2.66	.831E-01
105	ow2u	.684	2.70	.799E-01
106	ow2u	.685	2.75	.768E-01
107	ow2u	.686	2.79	.736E-01
108	ow2u	.686	2.79	.736E-01

((SUM OF THE SQUARED VALUES)**.5)/ND
.804E-01 .183E+00 .107E-01

PARAMETER VALUES AND STATISTICS FOR ALL ITERATIONS

PAR. ID.:		S1		SUM OF SQUARED WEIGHTED RESIDUALS					
AMP OR ITER	T	T	S1	HEADS	W/FLOWS	W/PARAMS	DMX	PAR#	AGMX
	.500E+04	.500E+04	.130E+00						
1	.111E+05	.622E+03	.126E+00	1.22	1.22	1.22	1.22	1	.000E+00
2	.187E+05	.152E+04	.998E-01	7.49	7.49	7.49	1.45	2	.000E+00
3	.203E+05	.148E+04	.101E+00	.319	.319	.319	.827E-01	1	.000E+00
4	.204E+05	.148E+04	.100E+00	.318	.318	.318	.882E-02	1	.000E+00
5				.318	.318	.318			

COVARIANCE MAT.

	1	2	3
1	7.318339E-02	-7.983190E-03	-3.690599E-03
2	-7.983190E-03	2.497985E-03	7.186210E-05
3	-3.690599E-03	7.186210E-05	2.760706E-04

PARAMETER SUMMARY

PARAMETER # :	1	2	3
PARAMETER ID :	T	T	S1
FINAL VALUES	.992E+01	.730E+01	.100E+00

EXPONENTIAL OF LN PARAMETERS

(0.0 FOR UNTRANSFORMED PARAMETERS)
 .204E+05 .148E+04 .000E+00
 STD. DEV.
 .271E+00 .500E-01 .166E-01
 COEF. OF VAR.
 .273E-01 .684E-02 .166E+00
 + 2 STD. DEV.
 .105E+02 .740E+01 .133E+00
 EXPONENTIAL OF LN PARAMETERS
 (0.0 FOR UNTRANSFORMED PARAMETERS)
 .351E+05 .164E+04 .000E+00
 - 2 STD. DEV.
 .938E+01 .720E+01 .669E-01
 EXPONENTIAL OF LN PARAMETERS
 (0.0 FOR UNTRANSFORMED PARAMETERS)
 .119E+05 .134E+04 .000E+00

CORRELATION MAT.

	1	2	3
1	1.000000	-.590439	-.821071
2	-.590439	1.000000	8.653563E-02
3	-.821071	8.653563E-02	1.000000

THE CORRELATION OF THE FOLLOWING PARAMETER PAIRS >= .95
 PARAMETER # ID # ID CORRELATION

THE CORRELATION OF THE FOLLOWING PARAMETER PAIRS IS BETWEEN .90 AND .95
 PARAMETER # ID # ID CORRELATION

THE CORRELATION OF THE FOLLOWING PARAMETER PAIRS IS BETWEEN .85 AND .90
 PARAMETER # ID # ID CORRELATION

RSQ (DEP.VAR. ONLY)----- = .31796
 RSQ (W/PARAMETERS)----- = .31796
 CALCULATED ERROR VARIANCE = .30282E-02
 CORRELATION COEFFICIENT-- = .89416
 W/PARAMETERS----- = .89416
 ITERATIONS----- = 5

MAX LIKE OBJ FUNC = 198.81
 AIC STATISTIC---- = 204.81
 BIC STATISTIC---- = 212.86

ORDERED DEPENDENT-VARIABLE WEIGHTED RESIDUALS NUMBER OF RESIDUALS INCLUDED: 108

-.960E-01 -.794E-01 -.740E-01 -.739E-01 -.737E-01 -.727E-01 -.724E-01 -.682E-01
 -.664E-01 -.647E-01 -.645E-01 -.605E-01 -.601E-01 -.588E-01 -.581E-01 -.573E-01
 -.564E-01 -.559E-01 -.555E-01 -.550E-01 -.546E-01 -.526E-01 -.521E-01 -.499E-01
 -.496E-01 -.467E-01 -.464E-01 -.438E-01 -.419E-01 -.411E-01 -.408E-01 -.399E-01
 -.385E-01 -.376E-01 -.341E-01 -.316E-01 -.308E-01 -.301E-01 -.289E-01 -.278E-01
 -.264E-01 -.261E-01 -.249E-01 -.247E-01 -.236E-01 -.219E-01 -.211E-01 -.171E-01
 -.164E-01 -.145E-01 -.141E-01 -.139E-01 -.131E-01 -.119E-01 -.119E-01 -.104E-01
 -.992E-02 -.943E-02 -.388E-03 .884E-04 .101E-02 .681E-02 .118E-01 .122E-01
 .124E-01 .159E-01 .164E-01 .191E-01 .206E-01 .210E-01 .215E-01 .221E-01

.221E-01	.225E-01	.227E-01	.227E-01	.271E-01	.281E-01	.285E-01	.302E-01
.322E-01	.344E-01	.364E-01	.374E-01	.401E-01	.431E-01	.453E-01	.503E-01
.521E-01	.525E-01	.536E-01	.557E-01	.625E-01	.637E-01	.659E-01	.792E-01
.872E-01	.943E-01	.951E-01	.103	.106	.107	.107	.108
.112	.117	.117	.120				

CORRELATION BETWEEN ORDERED WEIGHTED RESIDUALS AND
INDEPENDENT NORMAL DEVIATES (EQ.38 OF TEXT) = .927